PHYSICAL REVIEW B **94**, 165142 (2016)

Coupled wire model of symmetric Majorana surfaces of topological superconductors

Sharmistha Sahoo, Zhao Zhang, and Jeffrey C. Y. Teo*
Department of Physics, University of Virginia, Virginia 22904, USA
(Received 15 July 2016; revised manuscript received 28 September 2016; published 19 October 2016)

Time-reversal-symmetric topological superconductors in three spatial dimensions carry gapless surface Majorana fermions. They are robust against any time-reversal-symmetric single-body perturbation weaker than the bulk energy gap. We mimic the massless surface Majoranas by coupled wire models in two spatial dimensions. We introduce explicit many-body interwire interactions that preserve time-reversal symmetry and give energy gaps to all low-energy degrees of freedom. We show the gapped models generically carry nontrivial topological order and support anyonic excitations.

DOI: 10.1103/PhysRevB.94.165142

I. INTRODUCTION

Topological superconductors (TSC) are electronic phases of matter with finite excitation energy gaps that are not continuously connected to a conventional BCS s-wave superconductor. In particular, BCS superconductors in three dimensions can have nontrivial topologies protected by time-reversal symmetry [1–3]. There is a bulk integral quantity N of the mean-field system, known as chirality, that cannot change upon any adiabatic evolution unless the energy gap is closed or time-reversal symmetry (TRS) is broken. TSC also exhibits unique physical signature along its surface. Despite there is a bulk energy gap, the surface of a TSC hosts N gapless Majorana (real) fermion modes that are robust, in the single-body mean-field framework, to all symmetry and bulk gap preserving perturbations. The superfluid ^{3}He -B [4–7] and perhaps superconducting $Cu_xBi_2Se_3$ [8,9] are candidates of TSC.

The $\mathbb{Z}$ classification of TSC, or class DIII band theories according to the Altland-Zirnbauer classification [10], relies heavily on the single-body BCS description of the electronic structure. It has recently been shown that under strong many-body interaction, the surface state of 16 copies of a TSC can be gapped without breaking time-reversal symmetry or introducing surface topological order. This reduces the integer classification of TSC into $\mathbb{Z}_{16}$ [11–17]. This suggests the many-body extension allows a continuous path that connects 16 copies of a TSC to a trivial s-wave superconductor in three dimensions without breaking symmetry or closing the bulk gap. In fact, the surface Majorana modes of *any* TSC can be gapped without breaking symmetries. However, there would generically be a residue topological order, unless N is a multiple of 16, that allows nontrivial anyonic excitations to live on the surface [11,12]. As a result, these three-dimensional (3D) bulk systems are still topologically distinct from a trivial state.

Similar phenomena were also seen in topological insulators [18–21] in three dimensions and topological superconductors [22] in one dimension. Many-body interactions allow the surface Dirac mode of a topological insulator to acquire an energy gap without breaking time-reversal or charge conservation symmetries. However, a nontrivial surface topological order would be left behind [23–26]. This indicates the bulk insulator still carries a nontrivial $\mathbb{Z}_2$ symmetry-protected topology (SPT) even in the many-body framework. On the other hand, the $\mathbb{Z}$ classification of time-reversal-symmetric BDI superconductors in one dimension breaks down to $\mathbb{Z}_8$ in the presence of strong interaction [27–30].

The topological order of a gapped symmetric surface of a topological insulator or superconductor was deduced mainly using vortex condensation or other topological field theory techniques. They do not specify the microscopic many-body surface gapping interactions that give rise to these exotic surface states. A pioneer work that addressed this issue was done by Fidkowski and Kitaev in Ref. [27] where they constructed explicit time-reversal-symmetric four-fermion interactions that give an energy gap to eight boundary Majorana zero modes of a one-dimensional (1D) TSC. Another insightful work was published by Mross, Essin, and Alicea in Ref. [31] where they mimicked the surface Dirac mode of a topological insulator using a coupled wire model and wrote explicit symmetric gapping interactions that lead to different gapped or gapless surface states.

Sliding Luttinger liquids [32–36] and coupled wire constructions [37] are immensely powerful in building two-dimensional (2D) topological phases. They model 2D systems by arrays of coupled 1D chains, where interaction effects are more controlled and better understood. This theoretical technique has been frequently used in the study of fractional quantum Hall states [37–41], anyon models [42,43], spin liquids [44–46], (fractional) topological insulators [47–53], and superconductors [54,55].

In this paper, we imitate the surface Majorana modes of a 3D topological superconductor using a coupled Majorana wire model, construct explicit four-fermion interactions that lead to a finite excitation energy gap, and study the residue surface topological order.

A. Summary of results

We consider a 2D array of chiral Majorana wires, each of which carries N Majorana fermion channels that propagate in a single direction. The chiralities of wires alternate so that adjacent wires counterpropagate and Majoranas can backscatter to their neighbors through electron tunneling (see Fig. 1). When the interwire backscattering is uniform, the 2D system is gapless. In the long-wavelength continuum limit, the

*jteo@virginia.edu

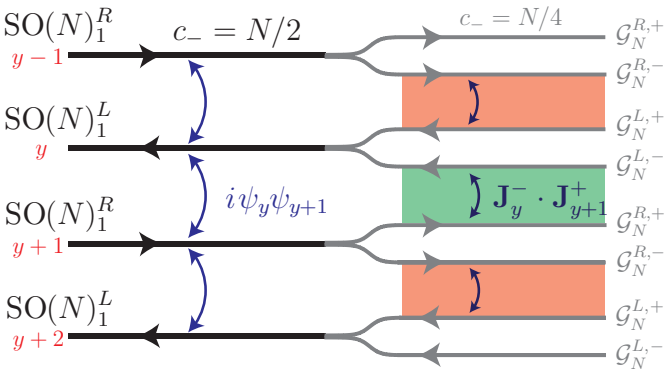

FIG. 1. (Left) Coupled wire model (2.4) of N gapless surface Majorana cones. (Right) Fractionalization (3.4) and coupled wire construction (3.8) of gapped anomalous and topological surface state.

energy spectrum is linear in both k_x and k_y directions and the model gives N Majorana cones.

If the N massless Majorana species decouple, each of them is protected by a nonlocal "antiferromagnetic" time-reversal symmetry (TRS) that translates all Majoranas to the next wire while reversing the propagating direction. This symmetry requires uniform interwire backscattering and forbids a fermion mass. However, this TRS is qualitatively different from the conventional one, which is local. For instance, a gap can be introduced when N is even by interspecies single-body backscatterings which preserves symmetry [31]. Thus, the surface classification becomes $\mathbb{Z}_2$ instead of $\mathbb{Z}$ even in the single-body framework. Despite the discrepancy, the coupled wire model does bear resemblance to the original problem of topological superconductor surfaces, especially when the number of chiral species N is odd.

A major result of this work is to construct many-body gapping potentials that freeze-out all low-energy degrees of freedom while preserving the nonlocal time-reversal symmetry. This is achieved by *fractionalizing* or *bipartitioning* the Majorana channels on each wire into a pair of independent sectors without interfering each other. They can then be backscattered to adjacent wires in opposite directions. When there are even Majorana species, the decomposition is obvious as $N = 2r = r + r$ and one can simply separate the first r Majoranas from the remaining r. The fractionalization in the odd case is more involved but is well worth known in the conformal field theory (CFT) community. First, the emergent rotation symmetry $\psi^a \to O_b^a \psi^b$ among the fermion species corresponds to a chiral $\mathrm{SO}(N)$ current algebra at level 1, also known as an affine Kac-Moody algebra or Wess-Zumino-Witten (WZW) theory, along each wire [56]. Low-energy excitations along the chiral wires, referred as primary fields, are irreducible representations of the $\mathrm{SO}(N)_1$ algebra. Fractionalization of the WZW CFT is also known as level-rank duality [56–58] or conformal embedding [56,59–61]:

$$\mathrm{SO}(N)_1 \supseteq \mathcal{G}_N^+ \times \mathcal{G}_N^-, \tag{1.1}$$

where the two $\mathcal{G}_N$'s are mutually commuting subalgebras of $\mathrm{SO}(N)$. For example, $\mathrm{SO}(9)_1$ can be decomposed into the tensor product $\mathrm{SO}(3)_3 \otimes \mathrm{SO}(3)_3$ as $9 = 3 \times 3$. The embedding (1.1) allows us to split the original free-fermionic degrees of freedom, referred as a $\mathrm{SO}(N)_1$ WZW current, into a pair of mutually decoupled fractional channels, denoted by $\mathcal{G}_N^\pm$ (see Fig. 1). For instance, the chiral central charge $c_- = N/2$, which loosely speaking counts the degrees of freedom and characterizes the heat current [62–65] running along each wire, also decomposes so that each $\mathcal{G}_N$ channel carries $c_- = N/4$.

The many-body gapping interaction is given by interwire current-current backscattering (see also Fig. 1)

$$\mathcal{H}_{\mathrm{int}} = u \sum_y \mathbf{J}^y_{\mathcal{G}_N^-} \cdot \mathbf{J}^{y+1}_{\mathcal{G}_N^+}, \tag{1.2}$$

where $\mathbf{J}^y_{\mathcal{G}_N^\pm}$ are the $\mathcal{G}_N^\pm$ currents operators along wire y. All current operators are certain combinations of fermion bilinears, and the backscattering interaction therefore consists of four-fermion terms. This Hamiltonian is exactly solvable. It preserves the "antiferromagnetic" time-reversal symmetry and opens up an excitation energy gap.

In the main body of the paper, we adopt one particular conformal embedding to implement the symmetric surface energy gap. In Sec. V B, we discuss alternative embeddings that lead to different surface topological orders. In the simplest case, the symmetric gapped surface generically carries a nontrivial G_N topological order

$$G_N = \begin{cases} \mathrm{SO}(r)_1 & \text{for } N = 2r, \\ \mathrm{SO}(3)_3 \boxtimes_b \mathrm{SO}(r)_1 & \text{for } N = 9 + 2r, \end{cases} \tag{1.3}$$

where both N and r can be extended to negative integers. The G_N topological order refers to the long-range entangled quantum surface state that supports fractional quasiparticle excitations, called anyons [64,66–68]. These anyons follow a set of fusion rules and braiding statistics. The anyon structure for G_N can be inferred, using the bulk-boundary correspondence [64,69–71], from the $(1+1)$D $\mathcal{G}_N$ WZW CFT living along the interface that separates the TR-symmetric topological gapped domain and a TR-breaking trivial gapped domain. This is listed in Tables II and III of Sec. IV A. This anyon structure follows a 32-fold periodicity in the sense that $G_N \cong G_{N+32}$. Moreover, these 32 topological states exhibit a natural $\mathbb{Z}_{32}$ *relative* tensor product structure $G_{N_1} \boxtimes_b G_{N_2} \cong G_{N_1+N_2}$, where certain set b of nontrivial bosons are condensed [72] under the tensor product.

It is important to clarify at this point that the coupled wire construction is a $(2+1)$D model where the interaction (1.2) is built out of local bosonic current operators $\mathbf{J}$. Under this interpretation, the coupled $\mathrm{SO}(N)_1$ wire model is bosonic and Majorana fermions are treated as anyonic excitations that carry a quasiparticle string. There is a $\mathbb{Z}_2$ gauge degree of freedom that couples to the fermions, $\psi^a \to -\psi^a$, and there are deconfined π fluxes (or $hc/2e$ fluxes), which are anyonic excitations that are nonlocal with fermions.

When N is a multiple of four, the G_N topological order is Abelian with four distinct anyon types 1, ψ, s_+, s_-, where $s_\pm$ are π fluxes with opposite fermion parities. When N is 2 mod 4, the G_N state resembles an Ising topological order with anyons 1, ψ, σ. When N is odd, the topological state has seven anyon types 1, $\alpha_\pm$, $\gamma_\pm$, β, f, and has a structure similar to $\mathrm{SO}(3)_3$ [or equivalently $\mathrm{SU}(2)_6$]. All these anyon theories contain π fluxes, which should be absent on the surface of a

fermionic topological superconductor. In Ref. [11], the surface topological order of a $N = 1$ fermionic TSC only contains four quasiparticles 1, $\gamma_\pm$, f instead of seven. The additional π fluxes in our coupled wire model could become confined by reintroducing single-body interwire fermion backscattering. In this case, the 32 bosonic topological states reduce down to 2 fermionic ones: (1) a trivial state containing $1, \psi$ similar to copies of $p_x + ip_y$ superconductors when N is even, or (2) a nontrivial fermionic $SO(3)_3$ state with anyons 1, $\gamma_\pm$, f when N is odd. This $\mathbb{Z}_2$ classification, instead of $\mathbb{Z}_{16}$, is a natural consequence of the antiferromagnetic time-reversal symmetry. In particular, there is no reason to expect the result would match that of Refs. [11,12] when N is even.

We will introduce the single-body coupled Majorana wire model at the beginning of Sec. II. A review on the $SO(N)_1$ WZW CFT will be given in Secs. II A and II B as well as in Appendixes A–C. In Sec. III, we will construct time-reversal-symmetry four-fermion interactions that will open up an excitation energy gap. The discussion will be decomposed into the even and odd N cases in Secs. III A and III B, respectively. In the even case, the gapping Hamiltonian will match the $O(r)$ Gross-Neveu model [73–76] and we will show an energy gap in Sec. III A 1 by (partially) bosonizing the problem. The gapping potential for the odd case will rely on a conformal embedding and relate to the Zamolodchikov and Fateev $\mathbb{Z}_6$ parafermion CFT [77,78]. This will be discussed and reviewed in Secs. III B 1 and III B 2 as well as in Appendix D. The symmetric gapping interactions will correspond to nontrivial surface topological orders. This will be discussed in Sec. IV where we will present the class of 32-fold periodic topological G_N states. In Sec. V, we will describe alternative gapping interactions that would lead to even more possibilities. Lastly, we will conclude the article in Sec. VI where we will also discuss some possible future exploration.

II. COUPLED WIRE CONSTRUCTION OF SURFACE MAJORANA CONES

A time-reversal-symmetric BCS superconductor is described by a Bogoliubov–de Gennes (BdG) Hamiltonian $H_{\mathrm{BdG}}(\mathbf{k})$. Symmetries require $T H_{\mathrm{BdG}}(\mathbf{k}) T^{-1} = H_{\mathrm{BdG}}(-\mathbf{k})$ and $C H_{\mathrm{BdG}}(\mathbf{k}) C^{-1} = -H_{\mathrm{BdG}}(-\mathbf{k})$ where T and C are the antiunitary time-reversal and particle-hole operators. When the symmetries square to $C^2 = -T^2 = 1$, the BdG theory belongs to the symmetry class DIII according to the Altland-Zirnbauer classification [10] and theories in three dimensions with finite excitation energy gaps are topologically classified by integers [1–3]. Superconducting ^{3}He in the B-phase [4–7] and certain doped topological insulators [8,9] were suggested to carry nontrivial topologies.

Topological superconductors host protected gapless surface Majorana modes. The simplest version is a single Majorana cone, which is the spectrum of a massless two-component real fermion $\mathcal{H}_\pm = iv\boldsymbol{\psi}^T \partial_\pm \boldsymbol{\psi}$, where $\partial_\pm = \partial_y \tau_x \pm \partial_x \tau_z$ and the Pauli matrices τ_x, τ_y, τ_z act on the surface real fermion $\boldsymbol{\psi} = (\psi_R, \psi_L)$. Majorana fermions are Hermitian $\psi_j^\dagger = \psi_j$ and obey the anticommutation relation $\{\psi_j(\mathbf{r}), \psi_{j'}(\mathbf{r}')\} = 2\delta_{jj'}\delta(\mathbf{r} - \mathbf{r}')$. Time reversal switches the components $\mathcal{T}(\alpha_1 \psi_L + \alpha_2 \psi_R)\mathcal{T}^{-1} = \alpha_2^* \psi_L - \alpha_1^* \psi_R$ so that $\mathcal{T}^2 = -1$. The sign in the Hamiltonian $\mathcal{H}_\pm$ determines its *chirality*. A general surface state could consist of multiple copies of Majorana cones with different chiralities:

$$\mathcal{H}_c = \sum_{a=1}^{N_R} i v_a \boldsymbol{\psi}_a^T \partial_+ \boldsymbol{\psi}_a + \sum_{b=1}^{N_L} i v_b \boldsymbol{\psi}_b^T \partial_- \boldsymbol{\psi}_b. \tag{2.1}$$

Fermions $\boldsymbol{\psi}_a$ and $\boldsymbol{\psi}_b$ with opposite chiralities can annihilate each other by the time-reversal-symmetric mass term $im\boldsymbol{\psi}_a^T \tau_z \boldsymbol{\psi}_b$. Quadratic terms among fermions of the same chirality would, however, either break time reversal or only move the gapless Majorana cones away from zero momentum without destroying them. The net surface chirality $N = N_R - N_L$ is thus a robust topological signature that distinguishes and characterizes 3D bulk topological superconductors. It cannot be altered by any time-reversal-symmetric two-body perturbations that are not strong enough to close the bulk excitation energy gap.

Recent theoretical studies suggest many-body interactions can remove these gapless surface degrees of freedom. To construct explicit gapping terms, we turn to an anisotropic description of surface Majorana fermions using an array of coupled fermion wires (see Fig. 1). The horizontal wires are labeled according to their vertical position $y = \cdots, -2, -1, 0, 1, 2, \ldots$ and each carries N chiral (real) Majorana fermions $\boldsymbol{\psi}_y = (\psi_y^1, \ldots, \psi_y^N)$ which propagate only to the right (or left) if y is even (resp. odd). The number of flavors N here is going to be identified with the net chirality of the surface Majorana cone. Time-reversal symmetry is nonlocal in this model as it relates fermions on adjacent wires that propagate in opposite directions:

$$\mathcal{T}\left(\sum_{a=1}^{N} \alpha_a \psi_y^a\right)\mathcal{T}^{-1} = (-1)^y \sum_{a=1}^{N} \alpha_a^* \psi_{y+1}^a. \tag{2.2}$$

Similar to the symmetry of an antiferromagnet, here time reversal on the single-fermion Hilbert space squares to a primitive translation up to a sign $\mathcal{T}^2 = -\hat{t}_y$ for $\hat{t}_y$ the vertical lattice translation $y \to y + 2$ that relates nearest copropagating wires. In the many-body Hilbert space,

$$\mathcal{T}^2 = (-1)^F \hat{t}_y, \tag{2.3}$$

where $(-1)^F$ is the fermion parity operator whose sign depends on the evenness or oddness of fermion number.

We mimic N copies of surface Majorana cones by the coupled wire Hamiltonian

$$\mathcal{H}_0 = \sum_{y=-\infty}^{\infty} i v_{\mathrm{x}} (-1)^y \boldsymbol{\psi}_y^T \partial_x \boldsymbol{\psi}_y + i v_{\mathrm{y}} \boldsymbol{\psi}_y^T \boldsymbol{\psi}_{y+1}, \tag{2.4}$$

where the N-component Majorana fermion $\boldsymbol{\psi}$ disperses linearly (for small k_y) with velocities $v_{\mathrm{x}}, v_{\mathrm{y}}$ along the horizontal and vertical axes (see Fig. 2). By applying (2.2), we see $\mathcal{T}\mathcal{H}_0\mathcal{T}^{-1} = \mathcal{H}_0$ and the coupled wire model is therefore time-reversal symmetric. Moreover, $\mathcal{H}_0$ has continuous translation symmetry along x and discrete translation along $y \to y + 2$. The alternating sign in the first term of (2.4) specifies the propagating directions of the wires. Projecting to the $k_x = 0$ zero modes along the wires, the second term in Eq. (2.4) effectively becomes a 1D Kitaev Majorana

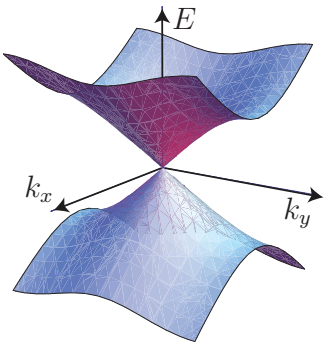

FIG. 2. The energy spectrum of the coupled Majorana wire model (2.4).

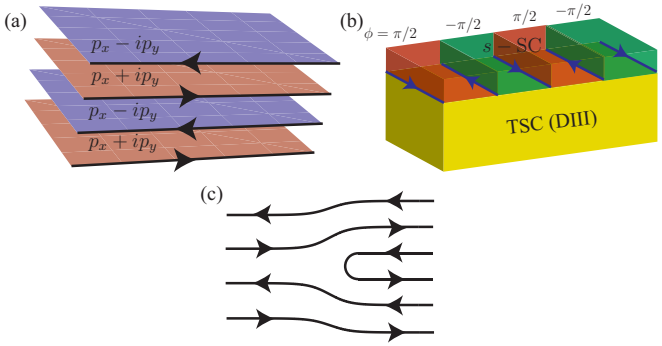

FIG. 3. Coupled Majorana wire model on the surface of (a) a stack of alternating $p_x \pm ip_y$ superconductors, and (b) a class DIII topological superconductor (TSC) with alternating TR-breaking surface domains. (c) A dislocation.

chain [22] which has a linear spectrum for small k_y. More explicitly, by using the Nambu basis $\boldsymbol{\xi}_{\mathbf{k}} = (c^a_{\mathbf{k}}, {c^a_{-\mathbf{k}}}^\dagger)^T$ for $c^a_{\mathbf{k}} = \sum_{xy} e^{i(k_x x + k_y y)} c^a_y(x)$ the Fourier transform of the Dirac fermion $c^a_y(x) = [\psi^a_{2y-1}(x) + i\psi^a_{2y}(x)]/2$, the coupled wire Hamiltonian (2.4) can be expressed as $\mathcal{H}_0 = \sum_{\mathbf{k}} \boldsymbol{\xi}^\dagger_{\mathbf{k}} H^0_{\mathrm{BdG}}(\mathbf{k}) \boldsymbol{\xi}_{\mathbf{k}}$, where the BdG Hamiltonian is given by

$$H^0_{\mathrm{BdG}}(\mathbf{k}) = 2v_{\mathbf{x}} k_x \tau_x + v_{\mathbf{y}}[-\sin k_y \tau_y + (1 - \cos k_y)\tau_z] \quad (2.5)$$

for $-\infty < k_x < \infty$ and $-\pi \leqslant k_y \leqslant \pi$. It has a linear spectrum near zero energy and momentum as shown in Fig. 2.

We notice in passing that if the time-reversal operation in Eq. (2.2) was defined without the alternating sign $(-1)^y$, it would square to a different sign $\mathcal{T}^2 = +\hat{t}_y$ in the single-fermion Hilbert space and the vertical term in Eq. (2.4) would need to be modified into $\sum_y i v_{\mathbf{y}} (-1)^y \boldsymbol{\psi}^T_y \boldsymbol{\psi}_{y+1}$ in order to preserve the symmetry. This would correspond to an alternating Majorana chain in the y direction, where the gapless Majorana cone would be positioned at $k_y = \pi$ instead of 0 and would still be protected by Kramers theorem as $T^2_{k_y=\pi} = e^{ik_y} = -1$. This scenario is actually equivalent and related to the original by a gauge transformation $(\psi_{4y}, \psi_{4y+1}, \psi_{4y+2}, \psi_{4y+1+3}) \to (\psi_{4y}, \psi_{4y+1}, -\psi_{4y+2}, -\psi_{4y+1+3})$, and therefore the sign of $\mathcal{T}^2$ is unimportant in this problem. Nevertheless, we will stick with previous convention defined in Eq. (2.2) in the following discussions.

The chirality N of the coupled Majorana wire model (2.4) is set by the *chiral central charge* $c_- = N/2$ along each wire. This quantity is defined by the difference of central charges [56] between right- and left-moving modes, and determines the energy (thermal) current $I_T \approx c_- \frac{\pi^2 k_B^2}{6h} T^2$ flowing along the wire in low temperature [62–65]. In general, a Majorana wire carrying N_R right-moving fermions and N_L left-moving ones has the kinetic Hamiltonian $\mathcal{H} = i v_{\mathbf{x}} \boldsymbol{\psi}^T \partial_x \boldsymbol{\psi}$, where $\partial_x = [\mathbb{1}_{N_R} \oplus (-\mathbb{1}_{N_L})]\partial_x$ acts on the $(N_R + N_L)$-component real fermion $\boldsymbol{\psi}$. In Eq. (2.4), we consider the simplest case when $(N_R, N_L) = (N, 0)$ for y even or $(0, N)$ for y odd.

A chiral 1D system violates fermion doubling [79] and can only be realized as an anomalous edge of a gapped 2D bulk [64,80,81]. The coupled Majorana wire model [(2.4) or Fig. 1] must therefore also be holographic and living on the surface of a 3D bulk superconductor. This can be modeled by a stack of alternating layers of spinless $p_x \pm ip_y$ superconductors [see Fig. 3(a)]. The interwire backscattering in Eq. (2.4) can be generated by bulk interlayer electron tunneling and pairing that are not competing with the intralayer $p + ip$ pairing. Time reversal (2.2) extends to the three-dimensional bulk by relating fermions on adjacent layers. The coupled Majorana wire model can also live on the surface of a 3D class DIII topological superconductor where each chiral Majorana mode is bound between adjacent domains with opposite time-reversal-breaking phases $\phi = \pm\pi/2$ [see Fig. 3(b)] [16,82]. The discrete translation order along the y axis perpendicular to the wire direction can be melted by proliferating dislocations [see Fig. 3(c)]. With continuous translation symmetry restored, time-reversal symmetry becomes local with $T^2 = -1$ and the coupled Majorana wire model (2.4) recovers the surface Majorana cone (2.1) in the continuum limit for small k_y.

The nonlocal time-reversal symmetry (2.2) actually provides a weaker topological protection to gapless surface Majorana's than a conventional local one. For instance in Sec. III, we will show that the $N = 2$ coupled Majorana wire model can be gapped by single-body backscattering terms without breaking time reversal, leaving behind a surface with trivial topological order. This reduced robustness stems from the half-translation component in the antiferromagnetic time reversal. In the BdG description (2.5), the time-reversal operator takes the momentum-dependent form

$$T_{\mathbf{k}} = \left(\frac{1 + e^{ik_y}}{2}\tau_y + i\frac{1 - e^{ik_y}}{2}\tau_z\right)\mathcal{K} \quad (2.6)$$

for $\mathcal{K}$ the complex-conjugation operator. It commutes with the BdG Hamiltonian $T_{\mathbf{k}} H^0_{\mathrm{BdG}}(\mathbf{k}) = H^0_{\mathrm{BdG}}(-\mathbf{k}) T_{\mathbf{k}}$ as well as the particle-hole (PH) $C T_{\mathbf{k}} = T_{-\mathbf{k}} C$, for $C = \tau_x \mathcal{K}$ the PH operator. In the continuum limit or for small k_y, $T \simeq \tau_y \mathcal{K}$ agrees with the conventional local time-reversal operator and protects a zero-energy Majorana Kramers doublet. The BdG Hamiltonian has a chiral symmetry $\Pi_{\mathbf{k}} H^0_{\mathrm{BdG}}(\mathbf{k}) = -H^0_{\mathrm{BdG}}(\mathbf{k}) \Pi_{\mathbf{k}}$, for $\Pi_{\mathbf{k}} = i C T_{\mathbf{k}}$ the chiral operator. It can be used to assign the chirality of a Majorana cone by an integral winding number

$$n = \frac{1}{2\pi i} \oint_{\mathcal{C}_\varepsilon(\mathbf{k}_0)} \mathrm{Tr}[h(\mathbf{k})^{-1} \nabla_{\mathbf{k}} h(\mathbf{k})] \cdot d\mathbf{l} \quad (2.7)$$

locally around a loop $\mathcal{C}_\varepsilon(\mathbf{k}_0)$ ε away from the zero mode at $\mathbf{k}_0$. Here, $h(\mathbf{k})$ is the elliptic operator

$$h(\mathbf{k}) = P^+_{\mathbf{k}} H^0_{\mathrm{BdG}}(\mathbf{k}) P^-_{\mathbf{k}} \tag{2.8}$$

for $P^\pm_{\mathbf{k}} = (P^\pm_{\mathbf{k}})^2$ the two *local* projectors diagonalizing the chiral operator $\Pi_{\mathbf{k}} = e^{-ik_y/2}(P^+_{\mathbf{k}} - P^-_{\mathbf{k}})$. However, as time reversal squares to $T_{\mathbf{k}} T_{-\mathbf{k}} = -e^{ik_y}$, which is the eigenvalue of the primitive translation $-\hat{t}_y$ at momentum $\mathbf{k}$, so does the *nonsymmorphic* chiral operator $\Pi^2_{\mathbf{k}} = e^{-ik_y}$. The two chiral branches $\Pi_{\mathbf{k}} = \pm e^{-ik_y/2}$ switch across the Brillouin zone when $k_y \to k_y + 2\pi$. As a result, a *global* winding number can only be defined modulo 2.

A. SO(N)$_1$ current algebra

We notice the coupled Majorana wire model (2.4) has a SO(N) symmetry that rotates the N-component Majorana fermion $\psi^a_y \to O^a_b \psi^b_y$. Consequently, there is a chiral SO(N) Wess-Zumino-Witten (WZW) theory [83,84] or affine Kac-Moody algebra at level 1 along each wire. Here, we review some relevant features of the SO(N)$_1$ algebra, which are well known and can be found in standard texts on conformal field theory (CFT) such as Ref. [56].

The SO(N)$_1$ currents have the free-field representation

$$J^\beta(z) = \frac{i}{2} \boldsymbol{\psi}(z)^T t^\beta \boldsymbol{\psi}(z) = \frac{i}{2} \sum_{ab} \psi^a(z) t^\beta_{ab} \psi^b(z), \tag{2.9}$$

where the t^β's are antisymmetric $N \times N$ matrices that generate the SO(N) Lie algebra (see Appendix A), $z = e^{\tau + ix}$ is the complex space-time parameter, and (2.9) is normal ordered. The coupled Majorana wire model carries currents that propagate in alternating directions (see Fig. 1) so that $J^\beta_y(z)$ are holomorphic for even y and $J^\beta_y(\bar{z})$ are antiholomorphic for odd y. Focusing on an even wire, from the operator product expansion (OPE)

$$\psi^a(z)\psi^b(w) = \frac{\delta^{ab}}{z-w} + \cdots, \tag{2.10}$$

the SO(N)$_1$ currents obey the product expansion

$$J^\beta(z) J^\gamma(w) = \frac{\delta^{\beta\gamma}}{(z-w)^2} + \sum_\delta \frac{i f_{\beta\gamma\delta}}{z-w} J^\delta(w) + \ldots, \tag{2.11}$$

where $f_{\beta\gamma\delta}$ are the structure constants of the SO(N) Lie algebra with $[t^\beta, t^\gamma] = \sum_\delta f_{\beta\gamma\delta} t^\delta$ (see Appendix A). The Sugawara energy-momentum tensor (along a single wire) is equivalent to the free-fermion one [85]

$$T(z) = \frac{1}{2(N-1)} \mathbf{J}(z) \cdot \mathbf{J}(z) = -\frac{1}{2} \boldsymbol{\psi}(z)^T \partial_z \boldsymbol{\psi}(z) \tag{2.12}$$

for $\mathbf{J} = (J^\beta)$ the current vector and $\boldsymbol{\psi} = (\psi^1, \ldots, \psi^N)$ the N-component real fermion. The energy-momentum tensor defines a chiral Virasoro algebra and characterizes a chiral CFT. It satisfies the OPE

$$T(z)T(w) = \frac{c_-/2}{(z-w)^4} + \frac{2T(w)}{(z-w)^2} + \frac{\partial_w T(w)}{z-w} + \cdots, \tag{2.13}$$

where the chiral central charge $c_- = N/2$, loosely speaking, counts the conformal degrees of freedom on the Majorana wires and is proportional to the energy current [62–65] and entanglement entropy [86–88] carried by the wire.

Excitations of the N-component Majorana wire transform according to the SO(N) symmetry. They decompose into *primary fields* and their corresponding descendants. A primary field $\mathbf{V}_\lambda = (V^1, \ldots, V^d)$ is a simple excitation sector that irreducibly represents the SO(N)$_1$ Kac-Moody algebra

$$J^\beta(z) V^r(w) = -\sum_{s=1}^{d} \frac{(t^\beta_\lambda)_{rs}}{z-w} V^s(w) + \cdots, \tag{2.14}$$

where λ labels some d-dimensional irreducible representation of SO(N) and t^β_λ is the $d \times d$ matrix representing the generator t^β of SO(N). For example, it is straightforward to check by using the definition (2.9) and the OPE (2.10) that the Majorana fermion $\boldsymbol{\psi} = (\psi^1, \ldots, \psi^N)$ is primary with respect to the fundamental representation, i.e.,

$$J^\beta(z)\psi^a(w) = -\sum_{b=1}^{N} \frac{t^\beta_{ab}}{z-w} \psi^b(w) + \cdots. \tag{2.15}$$

From (2.12), space-time translation of a primary field $\mathbf{V}_\lambda$ is governed by

$$T(z)\mathbf{V}_\lambda(w) = \frac{h_\lambda}{(z-w)^2} \mathbf{V}_\lambda(w) + \frac{\partial_w \mathbf{V}_\lambda(w)}{z-w} + \cdots, \tag{2.16}$$

where the conformal (scaling) dimension is given by

$$h_\lambda = \frac{\mathcal{Q}_\lambda}{2(N-1)} \tag{2.17}$$

for $-\sum_\beta t^\beta_\lambda t^\beta_\lambda = \mathcal{Q}_\lambda \mathbb{1}_{d\times d}$ the quadratic Casimir operator. For instance, $\mathcal{Q}_\psi$, the quadratic Casmir eigenvalue for the fundamental representation, is $N-1$ (see Appendix A) and therefore the fermion $\boldsymbol{\psi}$ has conformal dimension $h_\psi = \frac{1}{2}$. This agrees with the OPE (2.10) by dimension analysis.

There are extra primary fields other than the trivial vacuum 1 and the fermion ψ. The spinor representations (see Appendix A) σ, for N odd, or s_+ and s_-, for N even, also correspond to primary fields of SO(N)$_1$. Their conformal dimensions can be read off from their quadratic Casmir values (A7), and are

$$h_\sigma = \frac{N}{16}, \quad h_{s\pm} = \frac{N}{16}. \tag{2.18}$$

Unlike the infinite number of irreducible representations of a Lie algebra, the extended affine SO(N)$_1$ algebra only has a truncated set of primary fields $\{1,\sigma,\psi\}$, for N odd, or $\{1,s_+,s_-,\psi\}$, for N even.

These SO(N)$_1$ primary fields take more explicit operator forms after bosonization and can be found in Appendixes B and C.

B. Bosonizing even Majorana cones

In the case when $N = 2r$ is even, the N Majorana (real) fermions on each wire can be paired into r Dirac (complex) fermions and *bosonized* [67,89]

$$c^j_y = \frac{\psi^{2j-1}_y + i\psi^{2j}_y}{\sqrt{2}} \sim \frac{1}{\sqrt{l_0}} \exp\left(i\widetilde{\phi}^j_y\right), \tag{2.19}$$

where $\widetilde{\phi}_y^1, \ldots, \widetilde{\phi}_y^r$ are real bosons on the yth wire, and the vertex operator in Eq. (2.19) is normal ordered. The bosons obey the equal-time commutation relation

$$\left[\widetilde{\phi}_y^j(x), \widetilde{\phi}_{y'}^{j'}(x')\right] = i\pi(-1)^{\max\{y,y'\}}[\delta_{yy'}\delta^{jj'}\mathrm{sgn}(x'-x) + \delta_{yy'}\mathrm{sgn}(j-j') + \mathrm{sgn}(y-y')], \quad (2.20)$$

where $\mathrm{sgn}(s) = s/|s| = \pm 1$ for $s \neq 0$ and $\mathrm{sgn}(0) = 0$. The first line of (2.20) is equivalent to the commutation relation between conjugate fields

$$\left[\widetilde{\phi}_y^j(x), \partial_{x'}\widetilde{\phi}_{y'}^{j'}(x')\right] = 2\pi i(-1)^y \delta_{yy'}\delta^{jj'}\delta(x-x') \quad (2.21)$$

and is set by the "$p\dot{q}$" term of the Lagrangian density

$$\mathcal{L}_0 = \frac{1}{2\pi}\sum_{y=-\infty}^{\infty}\sum_{j=1}^{r}(-1)^y \partial_x \widetilde{\phi}_y^j \partial_t \widetilde{\phi}_y^j. \quad (2.22)$$

The second line of (2.20) guarantees the correct anticommutation relations between Dirac fermions along distinct channels. The alternating signs $(-1)^y$ in Eqs. (2.21) and (2.22) specify the propagating directions along each wire, R (or L) for y even (resp. odd). Equation (2.20) is symmetric under time reversal (2.2), which sends

$$\mathcal{T} c_y^j \mathcal{T}^{-1} = (-1)^y c_y^{j\dagger}, \quad \mathcal{T}\widetilde{\phi}_y^i \mathcal{T}^{-1} = \widetilde{\phi}_{y+1}^i + \pi y. \quad (2.23)$$

We notice time reversal, in this convention, flips the fermion parity as it interchanges between the creation and annihilation operators.

The entire coupled Majorana wire Hamiltonian (2.4), when $N = 2r$ is even, can be turned into a model of coupled boson wires. The total Lagrangian density is a combination

$$\mathcal{L} = \mathcal{L}_0 - \mathcal{H} = \mathcal{L}_0 - (\mathcal{H}_\parallel + \mathcal{H}_\perp), \quad (2.24)$$

where the Hamiltonian density $\mathcal{H} = \mathcal{H}_\parallel + \mathcal{H}_\perp$ consists of the sliding Luttinger liquid [32–36] (SLL) component along each wire

$$\mathcal{H}_\parallel = V_{\mathsf{x}}\sum_{y=-\infty}^{\infty}\sum_{j=1}^{r}\partial_x\widetilde{\phi}_y^j\partial_x\widetilde{\phi}_y^j \quad (2.25)$$

and the backscattering component between wires

$$\mathcal{H}_\perp = -V_{\mathsf{y}}\sum_{y=-\infty}^{\infty}\sum_{j=1}^{r}(-1)^y\cos\left(2\vartheta_{y+1/2}^j\right), \quad (2.26)$$

$$2\vartheta_{y+1/2}^j = \widetilde{\phi}_y^j - \widetilde{\phi}_{y+1}^j. \quad (2.27)$$

The SLL Hamiltonian (2.25) contains the (normal-ordered) kinetic term $i\boldsymbol{\psi}_y^T\partial_x\boldsymbol{\psi}_y = i(c_y^\dagger\partial_x c_y + c_y\partial_x c_y^\dagger)$ in Eq. (2.4) as well as possible forward scattering terms like the density-density coupling $(c_y^\dagger c_y)(c_y^\dagger c_y)$. The interwire backscattering Hamiltonian (2.26) is identical to the second term $i\boldsymbol{\psi}_y^T\boldsymbol{\psi}_{y+1} = i(c_y^\dagger c_{y+1} + c_y c_{y+1}^\dagger)$ in Eq. (2.4). This can be derived directly by applying the bosonization (2.19) and the Baker-Campbell-Hausdorff formula $e^{i\widetilde{\phi}_y}e^{-i\widetilde{\phi}_{y+1}} = e^{i(\widetilde{\phi}_y - \widetilde{\phi}_{y+1}) + [\widetilde{\phi}_y, \widetilde{\phi}_{y+1}]/2}$. The alternating sign $(-1)^y$ in Eq. (2.26) is crucial to preserve time-reversal symmetry (2.23), which relates $\mathcal{T}2\vartheta_{y+1/2}^j\mathcal{T}^{-1} = 2\vartheta_{y+3/2}^j - \pi$.

The r sine-Gordon terms in Eq. (2.26) between the same pair of adjacent wires mutually commute

$$\left[2\vartheta_{y+1/2}^j(x), 2\vartheta_{y+1/2}^{j'}(x')\right] = 0 \quad (2.28)$$

and share simultaneous eigenvalues. If there was a single pair of counterpropagating wires, these potentials would have pinned $\langle 2\vartheta_{y+1/2}^j(x)\rangle = (2n+y)\pi$ between the two wires. However, they compete with the sine-Gordon terms between the next pair of wires due to the noncommuting relation

$$\left[2\vartheta_{y+1/2}^j(x), 2\vartheta_{y+3/2}^{j'}(x')\right] = 2\pi i(-1)^y[\theta(j-j') + \delta^{jj'}\theta(x'-x)], \quad (2.29)$$

where the unit step function $\theta(s) = 0$ when $s \leqslant 0$, or 1 when $s > 0$. In other words, the vertex operators $e^{i2\vartheta_{y+1/2}^j}$ produce fluctuations to adjacent pairs

$$e^{-i2\vartheta_{y+1/2}^j(x)}2\vartheta_{y+3/2}^j(x')e^{i2\vartheta_{y+1/2}^j(x)} = 2\vartheta_{y+3/2}^j(x') + 2\pi(-1)^y\theta(x'-x). \quad (2.30)$$

The uniform backscattering strength V_{y}, as protected by time reversal (2.2), exactly balances the competing potentials so that the Hamiltonian $\mathcal{H} = \mathcal{H}_\parallel + \mathcal{H}_\perp$ remains gapless.

III. GAPPING SURFACE MAJORANA CONES

The previous section describes the gapless surface Majorana fermions of a 3D topological superconductor using a coupled wire model (2.4). It consists of an array of chiral wires, each of which carries N flavors of Majorana fermions copropagating in alternating directions (see Fig. 1). Together with uniform backscattering interactions between adjacent wires, the model captures N surface Majorana cones with linear energy dispersion about zero energy and momentum (see Fig. 2). In this section, we construct explicit fermion interactions that introduce an excitation energy gap to the surface Majorana cones while preserving time-reversal symmetry. Generically, this leaves behind a fermionic surface topological order, which will not be discussed until the next section.

We begin with the simplest case when there are $N = 2$ chiral Majorana channels along each wire and correspond to two surface Majorana cones. As eluded in Sec. II, due to the nonlocal nature of time reversal, the coupled wire model can be gapped by single-body backscattering terms without violating the symmetry. Although this cannot be applied to a conventional topological superconductor with local time reversal, this model demonstrates the idea of *fractionalization*, which can be generalized to the many-body interacting case and subsequently lead to surface topological order. The Hamiltonian $\mathcal{H} = \mathcal{H}_0 + \mathcal{H}_{\mathrm{bc}}$ consists of the original model (2.4) with two fermion flavors $\boldsymbol{\psi}_y = (\psi_y^1, \psi_y^2)$ and the interflavor backscattering

$$\mathcal{H}_{\mathrm{bc}} = iu\sum_{y=-\infty}^{\infty}\psi_y^1\psi_{y+1}^2 \quad (3.1)$$

which is symmetric under the time reversal (2.2), $\mathcal{T}: \psi_y^a \to (-1)^y\psi_{y+1}^a$. The BdG Hamiltonian $H_{\mathrm{BdG}}(\mathbf{k}) = H_{\mathrm{BdG}}^0(\mathbf{k}) +$

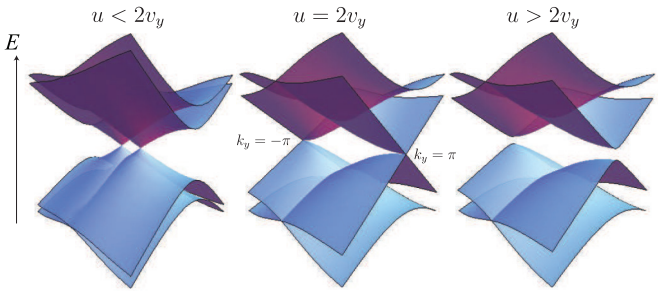

FIG. 4. Energy spectrum of the $N = 2$ coupled Majorana wire model with interflavor mixing.

$H^{\rm bc}_{\rm BdG}(\mathbf{k})$ is the combination of (2.5) and

$$H^{\rm bc}_{\rm BdG}(\mathbf{k}) = \frac{u}{2}[(1-\cos k_y)\sigma_x\tau_z + (1+\cos k_y)\sigma_y\tau_y - \sin k_y(\sigma_y\tau_z + \sigma_x\tau_y)] \tag{3.2}$$

which is symmetric under $T_{\mathbf{k}}$ in Eq. (2.6). The energy spectrum depends on the relative strength between the two interwire couplings $iv_{\rm y}(\psi^1_y\psi^1_{y+1} + \psi^1_y\psi^1_{y+1})$ and $iu\psi^1_y\psi^2_{y+1}$ (see Fig. 4). When $u = 0$, the two Majorana cones coincide at zero momentum. A finite u separates the two until they have traveled across the Brillouin zone and annihilate each other at $k_y = \pi$ when $u > 2v_{\rm y}$. Once an energy gap has opened up, the BdG Hamitonian has a unit Chern invariant

$$\mathrm{Ch} = \frac{i}{2\pi}\int_{-\infty}^{\infty} dk_x \int_{-\pi}^{\pi} dk_y \mathrm{Tr}(\mathcal{F}_{\mathbf{k}}) = 1, \tag{3.3}$$

where $\mathrm{Tr}(\mathcal{F}_{\mathbf{k}}) = \mathrm{Tr}(\langle\partial_{k_y}u^a_{\mathbf{k}}|\partial_{k_x}u^b_{\mathbf{k}}\rangle - \langle\partial_{k_x}u^a_{\mathbf{k}}|\partial_{k_y}u^b_{\mathbf{k}}\rangle)$ is the Berry curvature constructed from the two occupied eigenstates $u^1_{\mathbf{k}}, u^2_{\mathbf{k}}$ below zero energy of $H_{\rm BdG}(\mathbf{k})$. The coupled Majorana wire model thus behaves like a chiral $p+ip$ topological superconductor [4,81]. However the single-body Hamiltonian does not possess a topological order in the sense that it does not support anyonic excitations. For instance, the $\psi \to -\psi$ $\mathbb{Z}_2$ symmetry is global and π vortices are not quantum excitations of the model but rather introduced as classical extrinsic defects.

This example relies on a simple decomposition of the degrees of freedom along each wire, $N = 2 = 1 + 1$. The two Majorana fermions ψ^1_y, ψ^2_y are backscattered independently to adjacent wires in opposite directions. Unlike the intraflavor couplings $iv_{\rm y}(\psi^1_y\psi^1_{y+1} + \psi^1_y\psi^1_{y+1})$, interflavor terms $iu\psi^1_y\psi^2_{y+1}$ freeze independent degrees of freedom and they are not competing with each other. It is useful to notice that the decomposition breaks the $\mathrm{SO}(2)_1$ symmetry described in Sec. II A, and as a result the $\mathrm{SO}(2r)_1$ CFT along each wire splits into a pair of chiral Ising CFTs.

We can now generalize this idea to all N, but with many-body interwire interactions. From now on, unless specified otherwise, we turn off all single-body scattering terms. For instance, the vertical velocity now vanishes, $v_{\rm y} = 0$, in the kinetic part $\mathcal{H}_0$ of the coupled wire model (2.4). First, we seek a decomposition of the $\mathrm{SO}(N)_1$ degrees of freedom along each wire (see Sec. II A) into a pair of identical but independent sectors (also see Fig. 1)

$$\mathrm{SO}(N)_1 \supseteq \mathcal{G}^+_N \times \mathcal{G}^-_N, \tag{3.4}$$

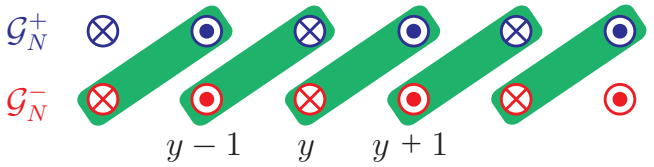

FIG. 5. Interwire gapping terms (3.8) (green rectangular boxes) between chiral fractional $\mathcal{G}^{R,\pm}_N, \mathcal{G}^{L,\pm}_N$ sectors (resp. $\otimes, \odot$) in opposite direction.

where $\mathcal{G}^{\pm}_N$ are the Kac-Moody subalgebras

$$\mathcal{G}^{\pm}_N = \begin{cases} \mathrm{SO}(N/2)_1 & \text{for } N \text{ even,} \\ \mathrm{SO}(3)_3 \times \mathrm{SO}\left(\frac{N-9}{2}\right)_1 & \text{for } N \text{ odd} \end{cases} \tag{3.5}$$

to be discussed below. This fractionalization has to be complete in the sense that the Sugawara energy-momentum tensor exactly splits into

$$T_{\mathrm{SO}(N)_1} = T_{\mathcal{G}^+_N} + T_{\mathcal{G}^-_N}. \tag{3.6}$$

In particular, the central charge divides

$$c_-[\mathrm{SO}(N)_1] = 2c_-(\mathcal{G}_N) = c_-(\mathcal{G}^+_N) + c_-(\mathcal{G}^-_N) \tag{3.7}$$

and there are no degrees of freedom left behind. Using the subalgebra current operators $\mathbf{J}_{\mathcal{G}^{\pm}_N}$, which are quadratic in ψ's, we construct the four-fermion backscattering interaction

$$\mathcal{H}_{\rm int} = u\sum_{y=-\infty}^{\infty} \mathbf{J}^y_{\mathcal{G}^-_N}\cdot\mathbf{J}^{y+1}_{\mathcal{G}^+_N} = u\sum_{y'=-\infty}^{\infty} \mathbf{J}^{2y'-1}_{\mathcal{G}^{L,-}_N}\cdot\mathbf{J}^{2y'}_{\mathcal{G}^{R,+}_N} + \mathbf{J}^{2y'}_{\mathcal{G}^{R,-}_N}\cdot\mathbf{J}^{2y'+1}_{\mathcal{G}^{L,+}_N} \tag{3.8}$$

for u positive, and R, L labels the propagating directions of the currents. This is pictorially presented in Figs. 1 and 5.

In this section, we design the fractionalization (3.4) of $\mathrm{SO}(N)_1$ for all N and show that the backscattering interactions (3.8) open an excitation energy gap without breaking time reversal. In CFT context, (3.4) is also known as a conformal embedding [56,59–61]. When $N = 2r$ is even, there is an obvious decomposition

$$\mathrm{SO}(2r)_1 \supseteq \mathrm{SO}(r)^+_1 \times \mathrm{SO}(r)^-_1, \tag{3.9}$$

where the "+" sector contains $\psi^1, \ldots, \psi^r$ while the "−" one contains the rest $\psi^{r+1}, \ldots, \psi^{2r}$. In Sec. III A, we review how the $\mathbf{J}_{\mathrm{SO}(r)^R_1}\cdot\mathbf{J}_{\mathrm{SO}(r)^L_1}$ interactions contribute an energy gap. This is a direct application of the well-studied $O(N)$ Gross-Neveu problem [73–76] in 1D. In the discrete limit, this is related to the Haldane $O(3)$ antiferromagnetic spin chain [90,91], the Affleck-Kennedy-Lieb-Tasaki (AKLT) spin chains [92,93], and the $\mathrm{SO}(n)$ Heisenberg chain [94–96]. When N is odd, the splitting (3.4) is less trivial. We will make use of the level-rank duality [56–58]

$$\mathrm{SO}(n^2)_1 \supseteq \mathrm{SO}(n)_n \times \mathrm{SO}(n)_n \tag{3.10}$$

which comes from the fact that the tensor product $\mathrm{SO}(n)\otimes\mathrm{SO}(n)$ is a Lie subgroup in $\mathrm{SO}(n^2)$. In particular, we will demonstrate the simplest case in Sec. III B when $n = 3$. The division of $\mathrm{SO}(9)_1$ can subsequently be generalized to $\mathrm{SO}(N)_1$

for all odd N effectively by writing $N = 9 + 2r$. This sets $\mathcal{G}_N^{\pm} = \mathrm{SO}(3)_3 \times \mathrm{SO}(r)_1$ in Eq. (3.4) and the corresponding interwire backscattering interactions (3.8).

A. Gapping even Majorana cones

We begin with the coupled Majorana wire model (2.4) (or Fig. 1) with $N = 2r$ chiral fermion channels per wire and corresponds to the same number of gapless Majorana cones. Similar to the previously shown $N = 2$ case, the gapless modes can be removed using simple single-body backscattering terms. We, however, are interested in finding gapping interactions that would support surface topological order as well. In Sec. II A and Appendixes B and C, we described the $\mathrm{SO}(N)_1$ WZW theory, which along the yth wire is generated by chiral current operators (2.9):

$$J_y^{(a,b)} = (-1)^y i \psi_y^a \psi_y^b. \tag{3.11}$$

We take the alternating sign convention $(-1)^y$ so that under time reversal, $\mathcal{T} J_y^{(a,b)} \mathcal{T}^{-1} = J_{y+1}^{(a,b)}$. We consider two subsets of generators: $\mathrm{SO}(r)_1^+$ containing $J^{(a,b)}$ for $1 \leqslant a < b \leqslant r$, and $\mathrm{SO}(r)_1^-$ containing $J^{(a,b)}$ for $r+1 \leqslant a < b \leqslant 2r$. As they act on independent fermion sectors, the two sets of operators commute or equivalently their operator product expansions (OPE) are trivial up to nonsingular terms. Moreover, the Sugawara energy-momentum tensor (2.12) for $\mathrm{SO}(N)_1$ completely splits into a sum between

$$T_{\mathrm{SO}(r)_1^+} = -\frac{1}{2}\sum_{a=1}^{r} \psi^a \partial \psi^a, \quad T_{\mathrm{SO}(r)_1^-} = -\frac{1}{2}\sum_{a=r+1}^{2r} \psi^a \partial \psi^a. \tag{3.12}$$

This ensures all degrees of freedom in $\mathrm{SO}(2r)_1$ are generated by tensor products between those in the $\mathrm{SO}(r)_1^{\pm}$ sectors. Precisely, this means any $\mathrm{SO}(2r)_1$ primary field is a fusion channel of the OPE of certain primary field pair in $\mathrm{SO}(r)_1^+$ and $\mathrm{SO}(r)_1^-$. Thus, as long as the gapping terms independently freeze both sectors, they remove all gapless degrees of freedom.

The backscattering interactions (3.8) couple the $\mathrm{SO}(r)_1^-$ sector on the yth wire with the $\mathrm{SO}(r)_1^+$ sector on the $(y+1)$th one. They can be explicitly written as

$$\mathcal{H}_{\mathrm{int}} = u \sum_{y=-\infty}^{\infty} \sum_{1 \leqslant a < b \leqslant r} \psi_y^{r+a} \psi_y^{r+b} \psi_{y+1}^a \psi_{y+1}^b. \tag{3.13}$$

First, the interactions are time-reversal symmetric as (3.13) is unchanged by $\psi_y^a \to (-1)^y \psi_{y+1}^a$. Second, it breaks the $O(2r)$ symmetry to $O(r)^+ \times O(r)^-$. The symmetry breaking can be facilitated by forward scattering within wires that renormalize the velocities differently between the $\mathrm{SO}(r)_1^{\pm}$ sectors. Equation (3.13) is also a combination allowed by the chiral $O(r)$ symmetry

$$\psi_y^a \to (\mathcal{O}^{(-1)^y})_b^a \psi_y^b, \quad \psi_y^{r+a} \to (\mathcal{O}^{(-1)^{y+1}})_b^a \psi_y^{r+b}, \tag{3.14}$$

where $\mathcal{O}$ is an $r \times r$ orthogonal transformation matrix. The chiral symmetry only allows cross couplings $\mathbf{J}^y_{\mathrm{SO}(r)_1^{\pm}} \cdot \mathbf{J}^{y+1}_{\mathrm{SO}(r)_1^{\mp}}$ between adjacent wires. Instead of (3.13), another possibility would be its mirror image with summands $\psi_y^a \psi_y^b \psi_{y+1}^{r+a} \psi_{y+1}^{r+b}$. This competes with the original, but as long as mirror symmetry is broken and their strength is asymmetric, an energy gap will open. In the following, we will ignore the mirror image by assuming it is weaker.

Next, we notice that the four-fermion interaction (3.13) is marginally relevant when velocity v_x is uniform. The dimensionless coupling strength u follows the renormalization group (RG) flow equation

$$\frac{du}{d\lambda} = +4\pi(r-2)u^2 \tag{3.15}$$

when length scale renormalizes by $l \to e^{\lambda} l$. This can be verified by applying the RG formula among marginal operators [97]

$$\frac{dg_l}{d\lambda} = -2\pi \sum_{mn} C_l^{mn} g_m g_n, \tag{3.16}$$

where C_l^{mn} is the fusion coefficient of the OPE $\mathcal{O}_m \mathcal{O}_n = C_l^{mn} \mathcal{O}_l + \cdots$ between operators in the perturbative action $\delta S = \int d\tau dx \sum_m g_m \mathcal{O}_m$. In the current case, the fusion coefficient $\mathcal{O}\mathcal{O} = -2(r-2)\mathcal{O} + \cdots$ can be evaluated simply by applying the Wick's theorem of fermions, for $\mathcal{O} = -\sum_{y,a,b} \psi_y^{r+a} \psi_y^{r+b} \psi_{y+1}^a \psi_{y+1}^b$. The plus sign in Eq. (3.15) shows the interacting strength grows at weak coupling. To show that the backscattering (3.13) indeed opens up a gap, we first focus on a single coupled pair of counterpropagating $\mathrm{SO}(r)_1$ channels (see Fig. 5).

1. *O(r) Gross-Neveu model*

Here, we concentrate on a particular set of backscattering terms in Eq. (3.13) at say an even y. We relabel $\psi_y^{r+a} = \psi_R^a$ and $\psi_{y+1}^a = \psi_L^a$, for $a = 1, \ldots, r$. The interaction between the yth and $(y+1)$th wires is identical to that of the $O(r)$ Gross-Neveu (GN) model [73–76]

$$\mathcal{H}_{\mathrm{GN}} = -\frac{u}{2}(\boldsymbol{\psi}_R \cdot \boldsymbol{\psi}_L)^2, \tag{3.17}$$

where the minus sign is from the fermion exchange statistics $\psi_R^a \psi_R^b \psi_L^a \psi_L^b = -\psi_R^a \psi_L^a \psi_R^b \psi_L^b$. This GN model is known to have an excitation energy gap for $r > 2$.

For even $r = 2n > 2$, the Majorana fermions can be paired into Dirac ones and subsequently bosonized (see Sec. II B), $c_{R/L}^j = (\psi_{R/L}^{2j-1} + i\psi_{R/L}^{2j})/\sqrt{2} \sim e^{i\widetilde{\phi}_{R/L}^j}$, for $j = 1, \ldots, n$. Using

$$\boldsymbol{\psi}_R \cdot \boldsymbol{\psi}_L = \sum_{j=1}^{n} c_R^j (c_L^j)^{\dagger} + (c_R^j)^{\dagger} c_L^j \sim \sum_{j=1}^{n} \cos(2\Theta^j) \tag{3.18}$$

for $2\Theta^j = \widetilde{\phi}_R^j - \widetilde{\phi}_L^j$ [also see (2.27)] are mutually commuting variables, the GN interaction (3.17) takes the bosonized form

$$\begin{aligned} \mathcal{H}_{\mathrm{GN}} &\sim u \sum_{j=1}^{n} \partial_x \widetilde{\phi}_R^j \partial_x \widetilde{\phi}_L^j - u \sum_{j_1 \neq j_2} \sum_{\pm} \cos(2\Theta^{j_1} \pm 2\Theta^{j_2}) \\ &= u \sum_{j=1}^{n} \partial_x \widetilde{\phi}_R^j \partial_x \widetilde{\phi}_L^j - u \sum_{\boldsymbol{\alpha} \in \Delta} \cos(\boldsymbol{\alpha} \cdot 2\boldsymbol{\Theta}), \end{aligned} \tag{3.19}$$

where $2\boldsymbol{\Theta} = (2\Theta^1, \ldots, 2\Theta^n)$ and $\boldsymbol{\alpha}$ are roots of $\mathrm{SO}(2n)$ [see (A8)]. The first term renormalizes the velocity V_x in Eq. (2.25) as well as the Luttinger parameter. We assume

$V_x \gg u$ so that the first term can be dropped. The remaining sine-Gordon terms are responsible for gapping out all low-energy degrees of freedom. First, the angle parameters mutually commute and share simultaneous eigenvalues. The ground state minimizes the energy by uniformly pinning the ground-state expectation value (GEV)

$$\langle 2\Theta^j(x)\rangle = \pi m_\psi^j, \quad m_\psi^j \in \mathbb{Z}. \tag{3.20}$$

We notice in passing that the following subset of sine-Gordon terms

$$-u\sum_{I=1}^{n}\cos(\boldsymbol{\alpha}_I\cdot 2\boldsymbol{\Theta}) = -u\sum_{I=1}^{n}\cos\left[\sum_{J=1}^{n}K_{IJ}\left(\phi_R^J-\phi_L^J\right)\right] = -u\sum_{I=1}^{n}\cos\left(\mathbf{n}_I^T\mathbb{K}\boldsymbol{\Phi}\right), \tag{3.21}$$

using the simple roots $\boldsymbol{\alpha}_I$ in Eq. (A9), is already enough to remove all low-energy degrees of freedom. Here, K_{IJ} is the Cartan matrix (A12) of SO($2n$) that appears in the Lagrangian density

$$\mathcal{L}_0 = \frac{1}{2\pi}\partial_x\boldsymbol{\Phi}^T\mathbb{K}\partial_t\boldsymbol{\Phi} \tag{3.22}$$

for $\mathbb{K} = K\oplus(-K)$ and $\boldsymbol{\Phi} = (\boldsymbol{\phi}_R,\boldsymbol{\phi}_L)$, and ϕ is related to $\widetilde{\phi}$ by the basis transformation (B13). For instance, the n vector coefficients $\mathbf{n}_J = (\mathbf{e}_J,\mathbf{e}_J)$ in Eq. (3.21) form a null basis

$$\mathbf{n}_I^T\mathbb{K}\mathbf{n}_J = 0 \tag{3.23}$$

and guarantee an energy gap according to Ref. [98]. The remaining GN terms in Eq. (3.19) are compatible with (3.21) as they share the same minima.

There are constraints on the GEV m_ψ^j in Eq. (3.20). In order to minimize $-\cos(\boldsymbol{\alpha}\cdot 2\boldsymbol{\Theta})$ in Eq. (3.19), $\langle\boldsymbol{\alpha}\cdot 2\boldsymbol{\Theta}\rangle$ must be an integer multiple of 2π. This restricts uniform parity among m_ψ^j so that the sign in the fermion backscattering amplitude

$$\left\langle\psi_R^a(x)\psi_L^a(x)\right\rangle = \left\langle c_R^j(x)c_L^j(x)^\dagger\right\rangle \sim \langle e^{i2\Theta^j(x)}\rangle = (-1)^{m_\psi} \tag{3.24}$$

does not depend on fermion flavor j. This is not the only nonzero GEV as ψ is not the only primary field in SO($2n$)$_1$. The backscattering of spinor fields $V_{s_\pm} = e^{i\boldsymbol{\varepsilon}\cdot\widetilde{\boldsymbol{\phi}}/2}$ [Eq. (B24)] corresponds to the two GEV's

$$\left\langle V_{s_\pm}^R(x)V_{s_\pm}^L(x)^\dagger\right\rangle = \langle e^{i\boldsymbol{\varepsilon}\cdot\boldsymbol{\Theta}(x)}\rangle = e^{i\pi m_{s_\pm}/2}, \tag{3.25}$$

where $\boldsymbol{\varepsilon} = (\varepsilon_1,\ldots,\varepsilon_n)$ for $\varepsilon_j = \pm 1$, and the overall sign $\prod_j\varepsilon_j$ is positive for the even spinor field s_+, or negative for s_-. Here, the GEV (3.25) does not depend on the choice of $\boldsymbol{\varepsilon}$. This is because given $\boldsymbol{\varepsilon}$ and $\boldsymbol{\varepsilon}'$ with the same overall parity $\prod\varepsilon_j = \prod\varepsilon_j'$, $\boldsymbol{\varepsilon}\cdot\boldsymbol{\Theta}$ and $\boldsymbol{\varepsilon}'\cdot\boldsymbol{\Theta}$ differ by some combination of $\boldsymbol{\alpha}\cdot 2\boldsymbol{\Theta}$, which takes expectation value in $2\pi\mathbb{Z}$.

There are extra constraints between m_ψ and $m_{s_\pm}$ from the fusion rules of the primary fields of SO($2n$)$_1$ [see (B25) and (B26)]. First, $s_\pm\times\psi = s_\mp$ requires

$$m_{s_+} \equiv m_{s_-} + 2m_\psi \mod 4\mathbb{Z}. \tag{3.26}$$

Take the highest weights $\boldsymbol{\varepsilon}_+^0 = (1,\ldots,1)$ and $\boldsymbol{\varepsilon}_-^0 = (1,\ldots,-1)$ for instance. $\boldsymbol{\varepsilon}_+^0\cdot\boldsymbol{\Theta} = \boldsymbol{\varepsilon}_-^0\cdot\boldsymbol{\Theta} + 2\Theta^n$ implies $m_{s_+}(\boldsymbol{\varepsilon}_+^0) = m_{s_-}(\boldsymbol{\varepsilon}_+^0) + 2m_\psi^n$. Lastly, the fusion rules

$$s_\pm\times s_\pm\begin{cases}1 & \text{for } n \text{ even},\\ \psi & \text{for } n \text{ odd}\end{cases} \tag{3.27}$$

requires the GEVs to obey

$$\begin{aligned}(-1)^{m_{s_\pm}} &= 1 \quad \text{for } n \text{ even},\\ (-1)^{m_{s_\pm}} &= (-1)^{m_\psi} \quad \text{for } n \text{ odd}\end{aligned} \tag{3.28}$$

for similar reasons.

The GN model therefore has four ground states when $r = 2n > 2$. They are specified by the quantum numbers (i) $m_{s_+} = 0,1,2,3$ modulo 4 when n is odd, or (ii) $m_{s_+} = 0,2$ and $m_{s_-} = 0,2$ modulo 4 when n is even. The rest are fixed by (3.26) and (3.28). Quasiparticle excitations are trapped between domain walls or kinks separating distinct ground states [75,76,99]. For example, the vertex operator $V_{s_+}^R(x_0) = e^{i\boldsymbol{\varepsilon}_+^0\cdot\widetilde{\boldsymbol{\phi}}_R(x_0)/2}$ of an even spinor field creates a jump in the GEV (3.24)

$$\left\langle V_{s_+}^R(x_0)^\dagger e^{i2\Theta^j(x)}V_{s_+}^R(x_0)\right\rangle = (-1)^{m'_\psi+\theta(x_0-x)} \tag{3.29}$$

because of the Baker-Hausdorff-Campbell formula and the commutation relation from (2.20):

$$[2\Theta^j(x),\boldsymbol{\varepsilon}_+^0\cdot\widetilde{\boldsymbol{\phi}}_R(x_0)/2] = i\pi[\theta(x_0-x)-n+j-1] \tag{3.30}$$

for θ the unit step function $\theta(s) = 0$ when $s\leqslant 0$, or 1 when $s > 0$, and $m'_\psi = m_\psi + n - j + 1$. In general, the primary fields $V_{s_\pm}^R = e^{i\boldsymbol{\varepsilon}\cdot\widetilde{\boldsymbol{\phi}}_R}$ and $c_R^j = e^{i\widetilde{\phi}_R^j}$ correspond to the domain walls of $m_{s_\pm}$:

$$\begin{aligned}\left\langle V_{s_\pm}^R(x_0)^\dagger e^{i\boldsymbol{\varepsilon}_\pm^0\cdot\boldsymbol{\Theta}(x)}V_{s_\pm}^R(x_0)\right\rangle &= e^{\frac{i\pi}{2}(m'_{s_\pm}+n\theta(x_0-x))},\\ \left\langle V_{s_\mp}^R(x_0)^\dagger e^{i\boldsymbol{\varepsilon}_\pm^0\cdot\boldsymbol{\Theta}(x)}V_{s_\mp}^R(x_0)\right\rangle &= e^{\frac{i\pi}{2}(m'_{s_\pm}+(n-2)\theta(x_0-x))},\\ \left\langle c_R^j(x_0)^\dagger e^{i\boldsymbol{\varepsilon}_\pm^0\cdot\boldsymbol{\Theta}(x)}c_R^j(x_0)\right\rangle &= e^{\frac{i\pi}{2}(m'_{s_\pm}+2\theta(x_0-x))}.\end{aligned} \tag{3.31}$$

Now, we move on to the odd $r = 2n+1 > 1$ case. First, we pair the first $2n$ Majorana fermions into n Dirac ones and bosonize them similar to the previous even r case. This leaves a single unpaired Majorana fermion $\psi_{R/L}^r$. Dropping terms that only renormalize velocities, the GN model (3.17) takes the partially bosonized form

$$\mathcal{H}_{\rm GN} \sim -u\sum_{\boldsymbol{\alpha}\in\Delta_{\rm SO(2n)}}\cos(\boldsymbol{\alpha}\cdot 2\boldsymbol{\Theta}) - u\left[\sum_{j=1}^{n}\cos(2\Theta^j)\right]i\psi_R^r\psi_L^r, \tag{3.32}$$

where the first line is identical to the even r case (3.32) and is responsible for gapping out first $2n$ Majorana channels. Projecting onto the lowest-energy states and taking the GEV $\langle\cos(2\Theta^j)\rangle = (-1)^{m_\psi}$, the interacting Hamiltonian becomes

$$\mathcal{H}_{\rm GN} \sim -2n(n-1)u - nu(-1)^{m_\psi}i\psi_R^r\psi_L^r \tag{3.33}$$

which is identical to the continuum limit of the quantum Ising model with transverse field after a Jordan-Wigner transformation. The remaining Majorana channel $\psi_{R/L}^r$ is gapped by the single-body backscattering term. The sign of the mass gap $nu(-1)^{m_\psi}$ determines the phase of the Ising model. We take the convention so that a negative (or positive)

mass with $m_\psi \equiv 1$ (resp. $m_\psi \equiv 0$) corresponds to the order (resp. disorder) phase.

Like the previous case, the fermion backscattering amplitude (3.24) is not the only ground-state expectation value. From (C5), the Ising twist field of $\mathrm{SO}(2n+1)_1$ can be written as the product $V_\sigma = e^{i\boldsymbol{\varepsilon}\cdot\tilde{\boldsymbol{\phi}}/2}\sigma^r$, where $\boldsymbol{\varepsilon} = (\varepsilon_1, \ldots, \varepsilon_n)$ for $\varepsilon_j = \pm 1$, and $\sigma^r_{R/L} = \sigma^{2n+1}_{R/L}$ is the twist field along the last Majorana channel. There are three possible GEVs for the backscattering:

$$\left\langle V^R_\sigma(x) V^L_\sigma(x)^\dagger \right\rangle = \left\langle e^{i\boldsymbol{\varepsilon}\cdot\boldsymbol{\Theta}(x)} \sigma^r_R(x)\sigma^r_L(x)\right\rangle \sim \begin{cases} 0 & \text{for the disorder phase,} \\ \pm 1 & \text{for the order phase.} \end{cases} \tag{3.34}$$

Here, we choose the convention so that $\sigma_R\sigma_L$ takes the role of the spin operator $\boldsymbol{\sigma}$ in the Ising model and its nontrivial GEVs in the order phase specify two ground states $|\uparrow\rangle$ and $|\downarrow\rangle$.

Again, quasiparticle excitations are trapped between domain walls separating distinct ground states [75,76,99]. For example, a twist field V^R_σ (or V^L_σ) sits between the order to disorder phase boundary where the quantum number m_ψ flips from 1 to 0 or, equivalently, the fermion mass gap in Eq. (3.33) changes sign. This is because the twist field $V^R_\sigma(x_0)$ introduces a flip in boundary condition $\psi_R(x_0+) = -\psi_R(x_0-)$ and corresponds to a change of sign in front of the fermion backscattering $i\psi_R\psi_L$. Alternatively, this can also be understood by identifying V_σ as a Jackiw-Rebbi soliton [100] or a zero-energy Majorana bound state between a trivial and topological superconductor [22] in 1D.

Next, a $\uparrow - \downarrow$ domain wall of opposite signs of the GEV (3.34) in the order phase traps an excitation in the fermion sector ψ. This can be seen by equating the order Ising phase to a 1D topological superconductor [22], where the two Ising ground states correspond to the even and odd fermion parity states among the pair of boundary Majorana zero modes. Adding (or subtracting) a fermion therefore flips the parity as well as the GEV in Eq. (3.34). We notice this domain-wall interpretation of excitations is consistent with the non-Abelian fusion rule

$$\sigma \times \sigma = 1 + \psi. \tag{3.35}$$

The trivial fusion channel corresponds to the annihilation of a domain-wall pair such as

$$|\underbrace{\ldots\uparrow\uparrow}_{\text{order}}\underbrace{\leftarrow\leftarrow}_{\text{disorder}}\underbrace{\uparrow\uparrow\ldots}_{\text{order}}\rangle \xrightarrow{\text{fusion}} |\ldots\uparrow\uparrow\ldots\rangle \tag{3.36}$$

while the fermion fusion channel corresponds to joining the pair of "order-disorder" domain walls into a kink

$$|\underbrace{\ldots\uparrow\uparrow}_{\text{order}}\underbrace{\leftarrow\leftarrow}_{\text{disorder}}\underbrace{\downarrow\downarrow\ldots}_{\text{order}}\rangle \xrightarrow{\text{fusion}} |\ldots\uparrow\uparrow\downarrow\downarrow\ldots\rangle. \tag{3.37}$$

2. *The special case:* $\mathrm{SO}(4)_1 = \mathrm{SU}(2)_1 \times \mathrm{SU}(2)_1$

The case when $r = 2$ requires special attention. The $O(2)$ GN model (3.17) is a gapless Luttinger liquid because its bosonized form (3.19) contains no sine-Gordon terms and the rest only renormalizes velocities and the Luttinger parameter. As a result, the fractionalization (or conformal embedding) $\mathrm{SO}(4)_1 \supseteq \mathrm{SO}(2)_1 \times \mathrm{SO}(2)_1$ of wires with $N = 4$ Majorana channels does not lead to a gapped theory. Instead, we turn to an alternative fractionalization $\mathrm{SO}(4)_1 = \mathrm{SU}(2)^+_1 \times \mathrm{SU}(2)^-_1$ that only applies for $N = 4$.

The four Majorana ψ^a_y along each wire can be paired into Dirac channels $c^1_y = (\psi^1_y + i\psi^2_y)/\sqrt{2} = e^{i\tilde{\phi}^1_y}$ and $c^2_y = (\psi^3_y + i\psi^4_y)/\sqrt{2} = e^{i\tilde{\phi}^2_y}$. It will be more convenient if we express the bosons in the new basis using the simple roots of SO(4): $\tilde{\phi}^1 = \phi^1 - \phi^2$ and $\tilde{\phi}^2 = \phi^1 + \phi^2$. Unlike when $r > 2$, these bosons decouple in the Lagrangian density (2.22):

$$\mathcal{L}_0 = \frac{1}{2\pi}\sum_{y=-\infty}^{\infty}(-1)^y \sum_{J=1}^{2} 2\partial_x\phi^J_y\partial_t\phi^J_y. \tag{3.38}$$

This is equivalent to the fact that the Cartan matrix $K_{\mathrm{SO}(4)} = \mathrm{diag}(2,2)$ is diagonal so that the Lie algebra splits into the product $\mathrm{SU}(2)^+ \times \mathrm{SU}(2)^-$ of isoclinic rotations, each with Cartan matrix $K_{\mathrm{SU}(2)} = 2$.

The $\mathrm{SU}(2)_1$ current generators are given by $S^I_{\mathsf{z}}(z) = i\sqrt{2}\partial\phi^I(z)$ and $S^I_\pm(z) = (S^I_{\mathsf{x}} \pm iS^I_{\mathsf{y}})/\sqrt{2} = e^{i2\phi^I(z)}$, and they satisfy the OPE

$$S^I_{\mathsf{i}}(z)S^I_{\mathsf{j}}(w) = \frac{\delta_{\mathsf{ij}}}{(z-w)^2} + \frac{i\sqrt{2}\varepsilon_{\mathsf{ijk}}}{z-w}S^I_{\mathsf{k}}(w) + \cdots \tag{3.39}$$

for $I = 1,2 = +,-$. The $\mathrm{SU}(2)^+_1$ sector is completely decoupled from the $\mathrm{SU}(2)^-_1$ one as the OPE $S^1_{\mathsf{i}}(z)S^2_{\mathsf{j}}(w)$ is nonsingular. They completely decompose all low-energy degrees of freedom as the energy-momentum tensor splits into

$$\begin{aligned} T_{\mathrm{SO}(4)_1} &= -\frac{1}{2}\sum_{j=1}^{2}\partial\tilde{\phi}^j(z)\partial\tilde{\phi}^j(z) \\ &= -\sum_{J=1}^{2}\partial\phi^J(z)\partial\phi^J(z) = T_{\mathrm{SU}(2)^+_1} + T_{\mathrm{SU}(2)^-_1}. \end{aligned} \tag{3.40}$$

The gapping Hamiltonian is

$$\begin{aligned} \mathcal{H}_{\mathrm{int}} &= u\sum_{y=-\infty}^{\infty}\mathbf{S}^2_y\cdot\mathbf{S}^1_{y+1} \\ &= 2u\sum_{y=-\infty}^{\infty}\partial_x\phi^2_y\partial_x\phi^1_{y+1} - 2\cos(4\Theta_{y+1/2}), \end{aligned} \tag{3.41}$$

$$\begin{aligned} 4\Theta_{y+1/2} &= 2\phi^1_{y+1} - 2\phi^2_y \\ &= \tilde{\phi}^1_{y+1} + \tilde{\phi}^2_{y+1} + \tilde{\phi}^1_y - \tilde{\phi}^2_y. \end{aligned} \tag{3.42}$$

The first kinetic term of the interacting Hamiltonian only renormalizes velocities and the Luttinger parameter. The second sine-Gordon term involves four-fermion interactions and is responsible for the energy gap as it backscatters the $\mathrm{SU}(2)^-_1$ sector on the yth wire to the $\mathrm{SU}(2)^+_1$ sector on the $(y+1)$th one. It pins the ground-state expectation value (GEV)

$$\langle e^{i2\Theta_{y+1/2}(x)}\rangle = (-1)^{m_s} \tag{3.43}$$

which characterizes the two distinct ground states. Like the previous cases, quasiparticle excitations are kinks in the GEV. The fundamental excitation can be created by the vertex operator $V_s = e^{i\phi^1_{y+1}}$, which is the semionic primary field in the $\mathrm{SU}(2)^+_1$ sector along the $(y+1)$th wire.

B. Gapping odd Majorana cones

We now move on to the case when there are $N = 2r + 1 \geqslant 3$ chiral Majorana channels on each wire in the coupled Majorana wire model (2.4) (of Fig. 1). It corresponds to an odd N number of Majorana cones on the surface of a 3D topological superconductor. The chiral degrees of freedom along each wire are described by a $\mathrm{SO}(N)_1$ WZW theory, which is going to be fractionalized into the pair $\mathcal{G}_N^+ \times \mathcal{G}_N^-$ according to (3.5). The $\mathcal{G}_N^-$ sector along the yth wire will then be backscattered onto the $\mathcal{G}_N^+$ sector along the $(y+1)$th one by the current-current interaction (3.8), which will introduce an energy gap.

Unlike the even N case where $\mathrm{SO}(N)_1$ can simply be split into a pair of $\mathrm{SO}(N/2)_1$'s, here the decomposition is less trivial but leads to more exotic surface topological order. We begin with the particular case where nine Majorana channels can be fractionalized into

$$\mathrm{SO}(9)_1 \supseteq \mathrm{SO}(3)_3 \times \mathrm{SO}(3)_3 \tag{3.44}$$

essentially by noticing that the tensor product $\mathrm{SO}(3) \otimes \mathrm{SO}(3)$ sits inside SO(9). The two $\mathrm{SO}(3)_3$ WZW sectors carry decoupled current generators. They can then be backscattered using the current-current interaction (3.8) onto adjacent wires in opposite directions (also see Figs. 1 and 5).

For a general odd $N \geqslant 9$, one can decompose the Majorana channels into $N = 9 + (N-9)$. The first nine channels can be fractionalized by (3.44), which we will discuss in detail below, and the remaining even number of channels can be split using the previous method, namely, $\mathrm{SO}(N-9)_1 = \mathrm{SO}(\frac{N-9}{2})_1 \times \mathrm{SO}(\frac{N-9}{2})_1$. In the case when N is smaller than 9, one can add $9-N$ number of *nonchiral* Majorana channels to each wire. These additional degrees of freedom can be interpreted as surface reconstruction as they do not violate fermion doubling [79] and are not required to live on the boundary of a topological bulk. Now, each wire consists of 9 right (or left) propagating Majorana channels and $9-N$ left (resp. right) propagating ones. We still refer the remaining even channels by $\mathrm{SO}(N-9)_1$ except now the negative $N-9$ signals the reverse propagating direction of these Majoranas.

The $\mathrm{SO}(9)_1$ and $\mathrm{SO}(N-9)_1$ sectors can then be bipartitioned independently. The fractionalization of a general odd number of Majorana channels is summarized by the sequence

$$\mathrm{SO}(N)_1 \supseteq \mathrm{SO}(9)_1 \times \mathrm{SO}(N-9)_1 \supseteq \mathcal{G}_N^+ \times \mathcal{G}_N^- \tag{3.45}$$

for $\mathcal{G}_N^\pm = \mathrm{SO}(3)_3 \times \mathrm{SO}(\frac{N-9}{2})_1$. The "+" and "−" sectors can now be backscattered independently using (3.8) onto adjacent wires in opposite directions. This removes all low-energy degrees of freedom and opens up an energy gap.

1. *Conformal embedding* $\mathrm{SO}(9)_1 \supseteq \mathrm{SO}(3)_3^+ \times \mathrm{SO}(3)_3^-$

As a matrix Lie algebra, SO(3) is generated by the three antisymmetric matrices $\mathbf{\Sigma} = (\Sigma_\mathsf{x}, \Sigma_\mathsf{y}, \Sigma_\mathsf{z})$:

$$\Sigma_\mathsf{x} = \begin{pmatrix} 0 & 0 & 0 \\ 0 & 0 & 1 \\ 0 & -1 & 0 \end{pmatrix}, \quad \Sigma_\mathsf{y} = \begin{pmatrix} 0 & 0 & 1 \\ 0 & 0 & 0 \\ -1 & 0 & 0 \end{pmatrix},$$
$$\Sigma_\mathsf{z} = \begin{pmatrix} 0 & 1 & 0 \\ -1 & 0 & 0 \\ 0 & 0 & 0 \end{pmatrix}.$$

They can be embedded into SO(9) by tensoring with $\mathbb{1}_3$, the 3×3 identity matrix, on the left or right:

$$\mathbf{\Sigma}^+ = \mathbf{\Sigma} \otimes \mathbb{1}_3, \quad \mathbf{\Sigma}^- = \mathbb{1}_3 \otimes \mathbf{\Sigma}. \tag{3.46}$$

We denote $\mathrm{SO}(3)^\pm = \mathrm{span}\{\Sigma_\mathsf{x}^\pm, \Sigma_\mathsf{y}^\pm, \Sigma_\mathsf{z}^\pm\}$ to be the two mutually commuting subalgebras in SO(9).

Recall the free-field representation (2.9) of the $\mathrm{SO}(9)_1$ WZW current generators $J^\beta = i\psi^a t^\beta_{ab} \psi^b/2$ for t^β an antisymmetric 9×9 matrix, the $\mathrm{SO}(3)_3^\pm$ current generators are given by the substitution of t^β:

$$\mathbf{J}_{\mathrm{SO}(3)_3^\pm}(z) = \frac{i}{2} \psi^a(z) \mathbf{\Sigma}^\pm_{ab} \psi^b(z) \tag{3.47}$$

for $z = e^{\tau + ix}$ and $\mathbf{J} = (J_\mathsf{x}, J_\mathsf{y}, J_\mathsf{z})$. Written explicitly,

$$J_\mathsf{x}^+ = i(\psi^{23} + \psi^{56} + \psi^{89}), \quad J_\mathsf{x}^- = i(\psi^{47} + \psi^{58} + \psi^{69}),$$
$$J_\mathsf{y}^+ = i(\psi^{13} + \psi^{46} + \psi^{79}), \quad J_\mathsf{y}^- = i(\psi^{17} + \psi^{28} + \psi^{39}),$$
$$J_\mathsf{z}^+ = i(\psi^{12} + \psi^{45} + \psi^{78}), \quad J_\mathsf{z}^- = i(\psi^{14} + \psi^{25} + \psi^{36})$$

for $\psi^{ab} = \psi^a \psi^b$. Using Wick's theorem and the OPE $\psi^a(z)\psi^b(w) = \delta^{ab}/(z-w) + \cdots$, it is straightforward to deduce the $\mathrm{SO}(3)_3$ WZW current relations

$$J_\mathsf{i}^\pm(z) J_\mathsf{j}^\pm(w) = \frac{3\delta_{\mathsf{ij}}}{(z-w)^2} + \frac{i\varepsilon_{\mathsf{ijk}}}{z-w} J_\mathsf{k}^\pm(w) + \cdots \tag{3.48}$$

and $J_\mathsf{i}^\pm(z) J_\mathsf{j}^\mp(w)$ is nonsingular, for $\mathsf{i,j} = \mathsf{x,y,z}$ and $\varepsilon_{\mathsf{ijk}}$ the antisymmetric tensor.

The $\mathrm{SO}(3)_3$ current relation (3.48) differs from the $\mathrm{SO}(3)_1$ one (2.11) by the coefficient 3 of the most singular term. This sets the level of the affine Lie algebra. The $\mathrm{SO}(3)_3$ WZW theory is identical to $\mathrm{SU}(2)_6$ by noticing that the structure factor of SU(2) is $f_{\mathsf{ijk}} = \sqrt{2}\varepsilon_{\mathsf{ijk}}$ [see (3.39) and Ref. [56]]. The SU(2) current generators thus need to be normalized by $\mathbf{S}_{\mathrm{SU}(2)_6^\pm} = \sqrt{2}\mathbf{J}_{\mathrm{SO}(3)_3^\pm}$ so that

$$S_\mathsf{i}^\pm(z) S_\mathsf{j}^\pm(w) = \frac{6\delta_{\mathsf{ij}}}{(z-w)^2} + \frac{i\sqrt{2}\varepsilon_{\mathsf{ijk}}}{z-w} S_\mathsf{k}^\pm(w) + \cdots, \tag{3.49}$$

where the coefficient 6 of the most singular term sets the level of the $\mathrm{SU}(2)_6$ affine Lie algebra.

The Sugawara energy-momentum tensors are the normal-ordered product

$$T_{\mathrm{SO}(3)_3^\pm}(z) = \tfrac{1}{8} \mathbf{J}_{\mathrm{SO}(3)_3^\pm}(z) \cdot \mathbf{J}_{\mathrm{SO}(3)_3^\pm}(z). \tag{3.50}$$

Written explicitly in the fermion representation (3.47) and using the normal-ordered product

$$\psi^a(z)\psi^b(z)\psi^a(z)\psi^b(z) = \psi^a(z)\partial\psi^a(z) + \psi^b(z)\partial\psi^b(z), \tag{3.51}$$

the energy-momentum tensor takes the form

$$T_{\mathrm{SO}(3)_3^\pm}(z) = -\frac{1}{4}\sum_{a=1}^{9} \psi^a(z)\partial\psi^a(z) \mp \frac{1}{4}\mathcal{O}_\psi(z), \tag{3.52}$$
$$\mathcal{O}_\psi(z) = \psi^{1245} + \psi^{1278} + \psi^{4578} + \psi^{1346} + \psi^{1379} + \psi^{4679} + \psi^{2356} + \psi^{2389} + \psi^{5689} \tag{3.53}$$

for $\psi^{abcd} = \psi^a(z)\psi^b(z)\psi^c(z)\psi^d(z)$. The four-fermion terms in $\mathcal{O}_\psi$ cancel when combining the "±" sectors, and therefore

TABLE I. The "angular momenta" s, conformal dimensions h_s, and quantum dimensions d_s of primary fields $\mathbf{V}_s$ of $\mathrm{SO}(3)_3 = \mathrm{SU}(2)_6$.

$\mathbf{V}_s$	1	α_+	γ_+	β	γ_-	α_-	f
s	0	1/2	1	3/2	2	5/2	3
h_s	0	3/32	1/4	15/32	3/4	35/32	3/2
d_s	1	$\sqrt{2+\sqrt{2}}$	$1+\sqrt{2}$	$\sqrt{4+2\sqrt{2}}$	$1+\sqrt{2}$	$\sqrt{2+\sqrt{2}}$	1

the energy-momentum tensor (2.12) completely decomposes:

$$T_{\mathrm{SO}(9)_1} = -\frac{1}{2}\sum_{a=1}^{9}\psi^a\partial\psi^a = T_{\mathrm{SO}(3)_3^+} + T_{\mathrm{SO}(3)_3^-}. \tag{3.54}$$

Moreover, as the OPE between $\mathbf{J}_{\mathrm{SO}(3)_3^+}$ and $\mathbf{J}_{\mathrm{SO}(3)_3^-}$ is nonsingular, so is the OPE between $T_{\mathrm{SO}(3)_3^+}$ and $T_{\mathrm{SO}(3)_3^-}$. Each sector carries half the total central charge of nine Majorana channels

$$c_{\mathrm{SO}(3)_3^\pm} = 9/4. \tag{3.55}$$

The primary fields of $\mathrm{SO}(3)_3 = \mathrm{SU}(2)_6$ are characterized by half-integral "angular momenta" $s = 0, 1/2, \ldots, 3$ [56]. Each primary field $\mathbf{V}_s = (V_s^{-s}, V_s^{-s+1}, \ldots, V_s^s)$ irreducibly represents the WZW algebra

$$S_{\mathsf{i}}(z)V_s^m(w) = \frac{1}{z-w}\sum_{m'=-s}^{s}\left(S_{\mathsf{i}}^s\right)_{m'}^{m}V_s^{m'}(w) + \cdots \tag{3.56}$$

for $\mathsf{i} = \mathsf{x},\mathsf{y},\mathsf{z}$ and S_{i}^s the SU(2) generators in the spin-s matrix representation. We label the seven primary fields by greek letters $\mathbf{V}_s = 1, \alpha_\pm, \gamma_\pm, \beta, f$, each has conformal dimension $h_s = s(s+1)/8$ (see Table I). In particular, $1 = \mathbf{V}_0$ is the vacuum and $f = \mathbf{V}_3$ is Abelian and fermionic with spin $\frac{3}{2}$.

The rest of the primary fields are non-Abelian. They obey multichannel fusion rules

$$\mathbf{V}_{s_1} \times \mathbf{V}_{s_2} = \sum_s N_{s_1 s_2}^s \mathbf{V}_s, \tag{3.57}$$

where the fusion matrix element $N_{s_1 s_2}^s = 0, 1$ is determined by the Verlinde formula [101]

$$N_{s_1 s_2}^s = \sum_{s'}\frac{\mathcal{S}_{s_1 s'}\mathcal{S}_{s_2 s'}\mathcal{S}_{s s'}}{\mathcal{S}_{0 s'}} \tag{3.58}$$

and the modular S matrix [56]

$$\mathcal{S}_{s_1 s_2} = \frac{1}{2}\sin\left[\frac{\pi(2s_1+1)(2s_2+1)}{8}\right] \tag{3.59}$$

which is symmetric and orthogonal. Explicitly, the fusion rules are given by

$$\begin{aligned}
&f\times f = 1, \quad f\times\gamma_\pm = \gamma_\mp, \quad f\times\alpha_\pm = \alpha_\mp, \quad f\times\beta = \beta,\\
&\gamma_\pm\times\gamma_\pm = 1+\gamma_+ + \gamma_-, \quad \alpha_\pm\times\alpha_\pm = 1+\gamma_+,\\
&\beta\times\beta = 1+\gamma_+ + \gamma_- + f,\\
&\alpha_\pm\times\gamma_\pm = \alpha_+ + \beta, \quad \beta\times\gamma_\pm = \alpha_+ + \alpha_- + \beta,\\
&\alpha_\pm\times\beta = \gamma_+ + \gamma_-.
\end{aligned} \tag{3.60}$$

The quantum dimension d_s of the primary field $\mathbf{V}_s$ is defined to be the largest eigenvalue of the fusion matrix $N_s = (N_{ss_1}^{s_2})$. It coincides with the modular S matrix element $\mathcal{S}_{0s}/\mathcal{S}_{00}$ and respects fusion rules so that

$$d_{s_1}d_{s_2} = \sum_s N_{s_1 s_2}^s d_s. \tag{3.61}$$

They are listed in Table I.

2. $\mathbb{Z}_6$ parafermions

We first study the simplest odd case when there are nine Majorana cones mimicked by the coupled Majorana wire model (2.4) with nine chiral Majorana channels per wire. Now that we have bipartite the degrees of freedom according to the two $\mathrm{SO}(3)_3^\pm$ WZW current algebras in Eq. (3.47), they can be backscattered independently to adjacent wires in opposite directions [see Eq. (3.8) and Fig. 1]. As the $\mathrm{SO}(3)_3^+$ sector completely decomposes from the $\mathrm{SO}(3)_3^-$ one, the current backscattering $\mathbf{J}_{\mathrm{SO}(3)_3^-}^{y-1}\cdot\mathbf{J}_{\mathrm{SO}(3)_3^+}^{y}$ between the $(y-1)$th and yth wire does not compete with the next pair $\mathbf{J}_{\mathrm{SO}(3)_3^-}^{y}\cdot\mathbf{J}_{\mathrm{SO}(3)_3^+}^{y+1}$.

The current-current interaction consists of four-fermion terms and is marginally relevant. This can be seen from the RG equation (3.16) using the operator product expansion $(\mathbf{J}^y\cdot\mathbf{J}^{y+1})^2 \sim +\mathbf{J}^y\cdot\mathbf{J}^{y+1}$. [Recall the time-reversal-symmetric convention (3.11) and that $\mathbf{J}^y\mathbf{J}^y \sim i(-1)^y\mathbf{J}^y$.] To see that the interaction indeed opens up an excitation energy gap, it suffices to focus on a single pair of wires with the Hamiltonian

$$\mathcal{H}_{\mathrm{int}} = u\mathbf{J}_{\mathrm{SO}(3)_3^-}^R\cdot\mathbf{J}_{\mathrm{SO}(3)_3^+}^L, \tag{3.62}$$

where R/L labels the counterpropagating directions along wire y and $y+1$.

First, we further decompose the $\mathrm{SO}(3)_3$ WZW theory by the coset construction [56]

$$\mathrm{SO}(3)_3 = u(1)_6\times\text{"}\mathbb{Z}_6\text{"}, \quad \text{"}\mathbb{Z}_6\text{"} = \frac{\mathrm{SO}(3)_3}{\mathrm{SO}(2)_3} = \frac{\mathrm{SU}(2)_6}{U(1)_6}, \tag{3.63}$$

where "$\mathbb{Z}_6$" refers to the $\mathbb{Z}_6$ parafermion CFT model by Zamolodchikov and Fateev [77,78]. This is done by noticing that SO(3) [or equivalently SU(2)] contains the Abelian subgroup SO(2) [resp. $U(1)$] of rotations about the z axis, and on the CFT level, the $\mathrm{SO}(2)_3$ WZW subtheory of $\mathrm{SO}(3)_3$ [resp. $U(1)_6 \subseteq \mathrm{SU}(2)_6$] can be bosonized and singled out. To do this, we first group three pairs of Majorana fermions into three Dirac fermions on each chiral sector

$$\begin{aligned}
c_R^1 &= \frac{\psi_R^1 + i\psi_R^4}{\sqrt{2}}, \quad c_R^2 = \frac{\psi_R^2 + i\psi_R^5}{\sqrt{2}}, \quad c_R^3 = \frac{\psi_R^3 + i\psi_R^6}{\sqrt{2}},\\
c_L^1 &= \frac{\psi_L^1 + i\psi_L^2}{\sqrt{2}}, \quad c_L^2 = \frac{\psi_R^4 + i\psi_L^5}{\sqrt{2}}, \quad c_L^3 = \frac{\psi_L^7 + i\psi_L^8}{\sqrt{2}}
\end{aligned}$$

and bosonize

$$c_{R/L}^j \sim \frac{1}{\sqrt{l_0}}\exp\left(i\widetilde{\phi}_{R/L}^j\right) \tag{3.64}$$

for $j = 1,2,3$. The $\mathrm{SO}(2)_3$ subalgebra in the R and L sectors is generated by the J_{z}^- and J_{z}^+ current operators in Eq. (3.47):

$$J_{\mathsf{z}}^R = -3i\partial\phi_R^\rho, \quad J_{\mathsf{z}}^L = 3i\partial\phi_L^\rho, \tag{3.65}$$

where the boson field of the "charge" sector is the average

$$\phi^{\rho}_{R/L} = \frac{\widetilde{\phi}^{1}_{R/L} + \widetilde{\phi}^{2}_{R/L} + \widetilde{\phi}^{3}_{R/L}}{3}. \tag{3.66}$$

The "neutral" sector is carried by the three boson fields

$$\phi^{\sigma,j}_{R/L} = \widetilde{\phi}^{j}_{R/L} - \phi^{\rho}_{R/L} \tag{3.67}$$

which are not independent as $\phi^{\sigma,1} + \phi^{\sigma,2} + \phi^{\sigma,3} = 0$.

It is straightforward to check that the "charge" and the "neutral" sectors completely decouple from each other. For instance, the Lagrangian density decomposes

$$\begin{aligned}\mathcal{L}_{R/L} &= \frac{(-1)^{R/L}}{2\pi}\sum_{j=1}^{3}\partial_x\widetilde{\phi}^{j}_{R/L}\partial_t\widetilde{\phi}^{j}_{R/L} \\ &= \frac{(-1)^{R/L}}{2\pi}\left[3\partial_x\phi^{\rho}_{R/L}\partial_t\phi^{\rho}_{R/L} + \sum_{j=1}^{3}\partial_x\phi^{\sigma,j}_{R/L}\partial_t\phi^{\sigma,j}_{R/L}\right],\end{aligned} \tag{3.68}$$

where the remaining fermions $\psi^{7,8,9}_{R}$, $\psi^{3,6,9}_{L}$ are suppressed, and $(-1)^{R} = 1$, $(-1)^{L} = -1$.

The Lagrangian density (3.68) involves more degrees of freedom in $\mathrm{SO}(9)^{R/L}_{1}$ than just $\mathrm{SO}(3)^{R,-}_{3}$ or $\mathrm{SO}(3)^{L,+}_{3}$. Therefore, *a priori*, it is not obvious that this $\rho - \sigma$ decomposition is a splitting of $\mathrm{SO}(3)_3$, and in fact it is not. Only the charge sector $\phi^{\rho}_{R/L}$ is entirely belonging to $\mathrm{SO}(3)^{R,-}_{3}$ or $\mathrm{SO}(3)^{L,+}_{3}$. To show this, we go back to the energy-momentum tensor $T_{\mathrm{SO}(3)^{\pm}_{3}}$ in Eq. (3.52), say for R movers:

$$T_{\mathrm{SO}(3)^{R,\pm}_{3}}(z) = \tfrac{1}{2}T_{\mathrm{SO}(9)^{R}_{1}}(z) \mp \tfrac{1}{4}\mathcal{O}_{\psi}(z), \tag{3.69}$$

where the total energy-momentum tensor in partially bosonized basis is

$$\begin{aligned}T_{\mathrm{SO}(9)^{R}_{1}} = -\frac{1}{2}\Bigg[&3\partial\phi^{\rho}_{R}\partial\phi^{\rho}_{R} + \sum_{j=1}^{3}\partial\phi^{\sigma,j}_{R}\partial\phi^{\sigma,j}_{R} \\ &+\psi^{7}_{R}\partial\psi^{7}_{R} + \psi^{8}_{R}\partial\psi^{8}_{R} + \psi^{9}_{R}\partial\psi^{9}_{R}\Bigg]\end{aligned} \tag{3.70}$$

and the operator $\mathcal{O}_{\psi}$ defined in Eq. (3.53) is now

$$\begin{aligned}\mathcal{O}_{\psi} = &-3\partial\phi^{\rho}_{R}\partial\phi^{\rho}_{R} + \frac{1}{2}\sum_{j=1}^{3}\partial\phi^{\sigma,j}_{R}\partial\phi^{\sigma,j}_{R} \\ &- 2i\big[\cos\big(\phi^{\sigma,1}_{R} - \phi^{\sigma,2}_{R}\big)\psi^{78}_{R} + \cos\big(\phi^{\sigma,1}_{R} - \phi^{\sigma,3}_{R}\big)\psi^{97}_{R} \\ &+ \cos\big(\phi^{\sigma,2}_{R} - \phi^{\sigma,3}_{R}\big)\psi^{89}_{R}\big].\end{aligned} \tag{3.71}$$

Equation (3.71) is deduced by substituting the fermions by the boson fields (3.64), whose OPE can be found in Eqs. (D1)–(D3) in Appendix D. For instance, the factor of i in Eq. (3.71) is a result of mutually noncommuting $\phi^{\sigma,j}$. More importantly, ϕ^{ρ}, ϕ^{σ}, and $\psi^{7,8,9}$ are completely decoupled. As the "charge" sector ϕ^{ρ}_{R} only appears in $T_{\mathrm{SO}(3)^{R,-}_{3}}$, it belongs entirely in $\mathrm{SO}(3)^{R,-}_{3}$. Similarly, ϕ^{ρ}_{L} belongs entirely in $\mathrm{SO}(3)^{L,+}_{3}$. The "$\mathbb{Z}_6$" energy momentum is defined by subtracting the decoupled "charge" sector from $\mathrm{SO}(3)_3$:

$$T_{\mathrm{SO}(2)^{R}_{3}} = \frac{1}{6}J_{\mathsf{z}}J_{\mathsf{z}} = -\frac{1}{2}3\partial\phi_{\rho}\partial\phi_{\rho}, \tag{3.72}$$

$$\begin{aligned}T^{R}_{\mathbb{Z}_6} &= T_{\mathrm{SO}(3)^{R,-}_{3}} - T_{\mathrm{SO}(2)^{R}_{3}} \\ &= -\frac{1}{4}\sum_{a=7}^{9}\psi^{a}_{R}\partial\psi^{a}_{R} - \frac{1}{8}\sum_{j=1}^{3}\partial\phi^{\sigma,j}_{R}\partial\phi^{\sigma,j}_{R} \\ &\quad - \frac{i}{2}\big[\cos\big(\phi^{\sigma,1}_{R} - \phi^{\sigma,2}_{R}\big)\psi^{78}_{R} + \cos\big(\phi^{\sigma,1}_{R} - \phi^{\sigma,3}_{R}\big)\psi^{97}_{R} \\ &\quad + \cos\big(\phi^{\sigma,2}_{R} - \phi^{\sigma,3}_{R}\big)\psi^{89}_{R}\big]\end{aligned} \tag{3.73}$$

and similarly for the L movers.

The remaining current operators $J_{\pm} = (J_{\mathsf{x}} \pm iJ_{\mathsf{y}})/\sqrt{2}$ of $\mathrm{SO}(3)^{-}_{3}$ in the R sector and $\mathrm{SO}(3)^{+}_{3}$ in the L sector [see Eq. (3.47)] now split into "charge" and 'neutral" parafermion components

$$J^{R/L}_{\pm} = \mp\sqrt{3}e^{\mp i\phi^{\rho}_{R/L}}\Psi^{\mp}_{R/L}, \tag{3.74}$$

where the $\mathbb{Z}_6$ parafermions are given by the combinations

$$\begin{aligned}\Psi_R &= \frac{1}{\sqrt{3}}\big(e^{i\phi^{\sigma,1}_{R}}\psi^{7}_{R} + e^{i\phi^{\sigma,2}_{R}}\psi^{8}_{R} + e^{i\phi^{\sigma,3}_{R}}\psi^{9}_{R}\big), \\ \Psi_L &= \frac{1}{\sqrt{3}}\big(e^{i\phi^{\sigma,1}_{L}}\psi^{3}_{L} + e^{i\phi^{\sigma,2}_{L}}\psi^{6}_{L} + e^{i\phi^{\sigma,3}_{L}}\psi^{9}_{L}\big)\end{aligned} \tag{3.75}$$

for $\Psi^{+}_{R/L} = \Psi_{R/L}$ and $\Psi^{-}_{R/L} = \Psi^{\dagger}_{R/L}$. Unlike the ϕ^{σ}'s, here the "neutral" $\mathbb{Z}_6$ parafermions $\Psi_{R/L}$ belong entirely in $\mathrm{SO}(3)^{R,-}_{3}$ or $\mathrm{SO}(3)^{L,+}_{3}$. This is because $\mathbf{J}^{R/L}$ and $\phi^{\rho}_{R/L}$ both completely sit inside the $\mathrm{SO}(3)_3$'s as seen above. Otherwise, one can verify this by computing the OPE with the energy-momentum tensor (3.70) explicitly:

$$\begin{aligned}T_{\mathrm{SO}(3)^{R,-}_{3}}(z)\Psi_R(w) &= \frac{5/6}{(z-w)^2}\Psi_R(w) + \frac{\partial\Psi_R(w)}{z-w} + \cdots, \\ T_{\mathrm{SO}(3)^{R,-}_{3}}(z)e^{\pm i\phi^{\rho}_{R}(w)} &= \frac{1/6}{(z-w)^2}e^{\pm i\phi^{\rho}_{R}(w)} + \frac{\partial e^{\pm i\phi^{\rho}_{R}(w)}}{z-w} + \cdots,\end{aligned} \tag{3.76}$$

and $T_{\mathrm{SO}(3)^{R,+}_{3}}(z)\Psi_R(w)$ and $T_{\mathrm{SO}(3)^{R,+}_{3}}(z)e^{\pm i\phi^{\rho}_{R}(w)}$ are both nonsingular. Similar OPE hold for the L sector. The primary fields (3.75) generate the rest of the $\mathbb{Z}_6$ parafermions [see (D5) in Appendix D] and they obey the known $\mathbb{Z}_6$ structure by Zamolodchikov and Fateev [78].

3. *Gapping potential*

Now that we have further decomposed the $\mathrm{SO}(3)^{\pm}_{3}$ currents in each wire into $\mathrm{SO}(2)_3 = U(1)_6$ and $\mathbb{Z}_6$ parafermion components [see Eq. (3.74)], the current-current backscattering interaction (3.62) between a pair of wires takes the form of

$$\mathcal{H}_{\mathrm{int}} = 9u\partial_x\phi^{\rho}_{R}\partial_x\phi^{\rho}_{L} + 3u\big[e^{i(\phi^{\rho}_{L} - \phi^{\rho}_{R})}\Psi^{\dagger}_{R}\Psi_{L} + \mathrm{H.c.}\big]. \tag{3.77}$$

The first term only renormalizes the velocity of the boson in the $\mathrm{SO}(2)_3$ sector. The second term is responsible for opening an excitation energy gap. It extracts a $\mathbb{Z}_6$ parafermion Ψ and a quasiparticle $e^{i\phi^{\rho}}$ from the $\mathrm{SO}(3)^{+}_{3}$ sector on the yth wire and backscatter them onto the $\mathrm{SO}(3)^{-}_{3}$ sector along the

$(y+1)$th wire. This freezes all low-energy degrees of freedom and the ground state is characterized by the $\mathbb{Z}_6$ expectation value (GEV)

$$\langle \Psi_R^\dagger(x)\Psi_L(x)\rangle \sim -e^{i\langle\phi_R^\rho(x)-\phi_L^\rho(x)\rangle} = e^{2\pi i m/6} \tag{3.78}$$

for m an integer.

Like the $O(N)$ Gross-Neveu model we discussed in Sec. III A 1, quasiparticle excitations here also manifest as kinks or domain walls between segments with different GEVs. The primary fields $\alpha_\pm, \gamma_\pm, \beta$ of the chiral $SO(3)_3$ WZW theory in Table I decompose into components in the "$\mathbb{Z}_6$" and $SO(2)_3$ sectors:

$$\begin{aligned} \alpha_+ &= [\sigma_1]\times[e^{i\phi^\rho/2}], \quad \alpha_- = [\sigma_5]\times[e^{-i\phi^\rho/2}], \\ \gamma_+ &= [\sigma_2]\times[e^{i\phi^\rho}], \quad \gamma_- = [\sigma_4]\times[e^{-i\phi^\rho}], \\ \beta &= [\sigma_3]\times[e^{i3\phi^\rho/2}], \end{aligned} \tag{3.79}$$

where σ_l are primary fields in the chiral $\mathbb{Z}_6$ parafermion theory so that $\sigma_l^R\sigma_l^L$ take the roles of the order parameters of the $\mathbb{Z}_6$ model [77,78]. They satisfy the exchange relations

$$\Psi(x)\sigma_l(x') = \sigma_l(x')\Psi(x)e^{-2\pi i\frac{l}{6}\theta(x-x')} \tag{3.80}$$

for R sector, and similar relations hold for the L sector with the $\mathbb{Z}_6$ phases conjugated. Therefore, adding the operators $\alpha_\pm(x)$, $\gamma_\pm(x)$, $\beta(x)$ to the ground state create kinks of different heights in the GEV (3.78):

$$\begin{aligned} \langle \alpha_\pm^\dagger(x_0)\Psi_R^\dagger(x)\Psi_L(x)\alpha_\pm(x_0)\rangle &\sim e^{\frac{\pi i}{3}[m\pm\theta(x-x_0)]}, \\ \langle \gamma_\pm^\dagger(x_0)\Psi_R^\dagger(x)\Psi_L(x)\gamma_\pm(x_0)\rangle &\sim e^{\frac{\pi i}{3}[m\pm2\theta(x-x_0)]}, \\ \langle \beta^\dagger(x_0)\Psi_R^\dagger(x)\Psi_L(x)\beta(x_0)\rangle &\sim e^{\frac{\pi i}{3}[m+3\theta(x-x_0)]}, \end{aligned} \tag{3.81}$$

where $\theta(s) = (s/|s|+1)/2$ is the unit step function.

The fermionic supersector f in $SO(3)_3$ (see Table I) consists of operators that admit free-field representations. Again, we focus on the $SO(3)_3^{R,-}$ sector. The operators

$$\begin{aligned} V_f^0 &= \Psi^3, \quad V_f^{\pm1} = e^{\mp i\phi^\rho}\Psi^{\mp2}, \\ V_f^{\pm2} &= e^{\mp2i\phi^\rho}\Psi^{\mp}, \quad V_f^{\pm3} = e^{\mp3i\phi^\rho} \end{aligned}$$

span an $s=3$ representation of the affine $SO(3)_3$ Lie algebra, where $\Psi^{-m} = \Psi^{6-m}$ are the $\mathbb{Z}_6$ parafermions satisfying the OPE $\Psi^m(z)\Psi^{m'}(w) \sim (z-w)^{-mm'/3}\Psi^{m+m'}$ (see Appendix D for explicit definitions). From (3.80), they create a kink to the order parameter $\langle b\rangle = \langle \beta_R(x)\beta_L(x)\rangle$:

$$\left\langle \mathbf{V}_f^R(x_0)^\dagger\beta_R(x)\beta_L(x)\mathbf{V}_f^R(x_0)\right\rangle = \langle b\rangle(-1)^{\theta(x-x_0)} \tag{3.82}$$

in the order phase.

The gapping potential can now be generalized to an arbitrary odd number of Majorana channels per wire. Using the decomposition (3.45), the N Majorana channels are first split into $9+(N-9)$. The first nine channels are fractionalized into $SO(3)_3^+ \times SO(3)_3^-$ while the remaining $N-9$ can be split into $SO(\frac{N-9}{2})_1^+ \times SO(\frac{N-9}{2})_1^-$ because $N-9$ is even. The interwire current backscattering (3.8) takes the form

$$\mathcal{H}_{\text{int}} = u\sum_{y=-\infty}^{\infty} \mathbf{J}^y_{SO(3)_3^-}\cdot\mathbf{J}^{y+1}_{SO(3)_3^+} + \mathbf{J}^y_{SO(\frac{N-9}{2})_1^-}\cdot\mathbf{J}^{y+1}_{SO(\frac{N-9}{2})_1^+}, \tag{3.83}$$

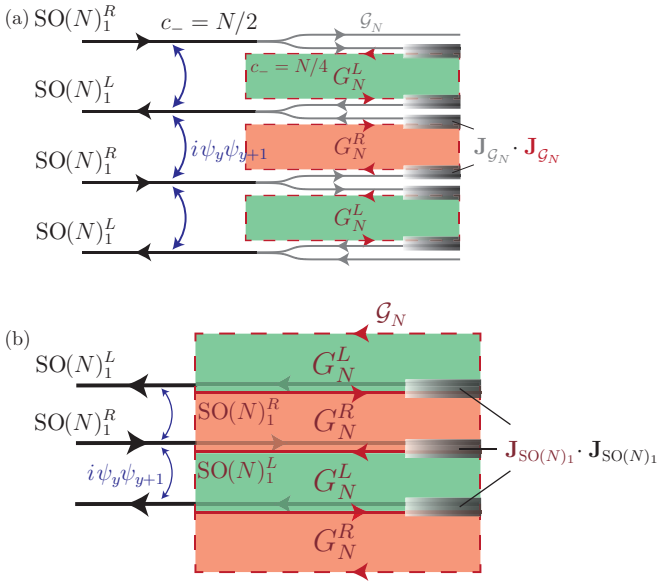

FIG. 6. Gapping N surface Majorana cones by inserting $(2+1)$D G_N stripe state and removing edge modes by current-current backscattering interaction.

where different terms act on completely decoupled degrees of freedom. They also gap out *all* low-energy degrees freedom as the energy-momentum tensor of the CFT along each wire decomposes:

$$\begin{aligned} T_{SO(N)_1} &= T_{SO(9)_1} + T_{SO(N-9)_1} \\ &= T_{SO(3)_3^+} + T_{SO(3)_3^-} + T_{SO(\frac{N-9}{2})_1^+} + T_{SO(\frac{N-9}{2})_1^-} \end{aligned} \tag{3.84}$$

using (3.54) and the fact that

$$T_{SO(m+n)_1} = -\frac{1}{2}\sum_{a=1}^{m+n}\psi^a\partial\psi^a = T_{SO(m)_1} + T_{SO(n)_1}. \tag{3.85}$$

C. Gapping by fractional quantum Hall stripes

Previously, we designed interwire interactions that gap all Majorana modes without breaking time-reversal symmetry. Here, we provide an alternative where each chiral Majorana wire is gapped by backscattering onto the edges of two topological stripes sandwiching the wire (see Fig. 6). The topological stripes could be fractional quantum Hall states, for instance. Similar construction has been proposed to describe surface states of topological insulators [31].

First, we consider inserting between each pairs of Majorana wire a $(2+1)$D topological state. It supports chiral boundary modes which move in a reverse direction to its neighboring Majorana wire. As adjacent wires have opposite propagation directions, the chiralities of the topological states also alternate. This alternating topological stripe state can be regarded as a surface reconstruction of the 3D topological superconductor. It preserves the antiferromagnetic time-reversal symmetry (2.2), which relates adjacent topological stripes by reversing their chirality. Unlike the coupled Majorana wire mode, the topological stripe state itself is a pure $(2+1)$D time-reversal-symmetric system and is not supported by a $(3+1)$D bulk. It has a gapless energy spectrum that is identical to N

surface Majorana cones and is carried by the interface modes between stripes [see Fig. 6(b)]. However, the topological stripe state also carries nontrivial anyonic excitations between wires. This distinguishes it from the coupled Majorana wire model and allows it to exist nonholographically in a pure $(2+1)$D setting.

The Majorana modes along the chiral wires then can be backscattered onto the boundaries or interfaces of the topological stripes by current-current couplings. In order for the boundary or interface modes to exactly cancel the Majorana modes along each wire, the topological stripes must carry specific topological orders. We take a G_N topological state [see Eq. (1.3)] so that its boundary carries a $\mathcal{G}_N$ Kac-Moody current, for $\mathcal{G}_N$ the affine Lie algebra of G_N defined in Eq. (3.5). G_N^R and G_N^L denote stripes with opposite chiralities. The $(2+1)$D G_N topological state itself can be constructed using a coupled wire construction similar to that in Refs. [38,102] and will not be discussed here.

There are two ways the Majorana modes can be backscattered onto the topological stripes. The first is shown in Fig. 6(a). The N Majorana modes along each chiral wire are bipartite into a pair of WZW theories $\mathcal{G}_N^+ \times \mathcal{G}_N^-$ according to (3.4). Each WZW theory is identical to the CFT along the boundary of a neighboring topological stripe but propagates in an opposite direction. It can be then be gapped out by the current-current backscattering

$$\mathcal{H}_{\text{int}} = u \mathbf{J}^{\text{wire}}_{\mathcal{G}_N} \cdot \mathbf{J}^{\text{stripe}}_{\mathcal{G}_N}. \tag{3.86}$$

Alternatively, one could first glue the topological stripes together [see Fig. 6(b)] so that the line interface sandwiched between adjacent G_N^R and G_N^L states hosts a chiral $\text{SO}(N)_1$ CFT. The stripes can then be put on top of the Majorana wire array so that each interface is sitting on top of a wire with opposite chirality. The current-current backscattering

$$\mathcal{H}_{\text{int}} = u \mathbf{J}^{\text{wire}}_{\text{SO}(N)_1} \cdot \mathbf{J}^{\text{interface}}_{\text{SO}(N)_1} \tag{3.87}$$

between each Majorana wire and stripe interface gaps out all low-energy degrees of freedom.

IV. SURFACE TOPOLOGICAL ORDER

In the previous section, we described how a coupled Majorana wire model, which mimics the surface Majorana modes of a 3D bulk topological superconductor (TSC), can be gapped by interwire current-current backscattering interaction without breaking time-reversal (TR) symmetry. In this section, we pay more attention to the topological order and the anyon types [66–68] of gapped excitations. The ground states are time-reversal symmetric and there are no nonvanishing order parameters that break time reversal spontaneously. There is a finite ground-state degeneracy that does not depend on system size. This signifies a nontrivial topological order [103–105].

The surface topological order can be inferred from bulk-boundary correspondence [64,69–71]. There is a one-to-one correspondence between the primary fields of the CFT along the $(1+1)$D gapless boundary and the anyon types in the $(2+1)$D gapped topological bulk. The conformal scaling dimension or spin $h = h_R - h_L$ of a primary field corresponds to the exchange statistical phase $\theta = e^{2\pi i h}$ of the corresponding anyon. The fusion rules of primary fields are identical to those of the anyons. And, the modular S matrix of the CFT at the boundary equals the braiding S matrix [64]

$$\mathcal{S}_{\mathbf{ab}} = \frac{1}{\mathcal{D}} \sum_{\mathbf{c}} d_{\mathbf{c}} N^{\mathbf{c}}_{\mathbf{ab}} \frac{\theta_{\mathbf{c}}}{\theta_{\mathbf{a}}\theta_{\mathbf{b}}} \tag{4.1}$$

in the bulk, where the non-negative integers $N^{\mathbf{c}}_{\mathbf{ab}}$ are the degeneracies of the fusion rules

$$\mathbf{a} \times \mathbf{b} = \sum_{\mathbf{c}} N^{\mathbf{c}}_{\mathbf{ab}} \mathbf{c} \tag{4.2}$$

between anyons, and the total quantum dimension $\mathcal{D} = \sqrt{\sum_{\mathbf{a}} d_{\mathbf{a}}^2}$ quantifies topological entanglement [106] and can be evaluated by knowing the quantum dimensions $d_{\mathbf{a}} \geqslant 1$ of each anyon $\mathbf{a}$ by solving the fusion identities

$$d_{\mathbf{a}} d_{\mathbf{b}} = \sum_{\mathbf{c}} N^{\mathbf{c}}_{\mathbf{ab}} d_{\mathbf{c}}. \tag{4.3}$$

On the surface of a topological superconductor, where there are no boundaries, the $(2+1)$D topological order corresponds to a $(1+1)$D interface that separates the time-reversal-symmetric topologically ordered domain and a time-reversal-breaking domain. This interface hosts chiral gapless modes (see Fig. 7). This geometry can be wrapped onto the surface of a slab where the TR-symmetric and -breaking domains occupy the top and bottom surface of a 3D bulk (see Fig. 8). The quasi-2D system has an energy gap except along its boundary which is previously the interface that carries the $\mathcal{G}_N$ WZW CFT. The bulk-boundary correspondence then determines a bulk G_N topological order on the quasi-2D slab.

Wires in the trivial TR-breaking domain are gapped by nonuniform current backscattering

$$\mathcal{H}_{\text{TR-breaking}} = \sum_y \Delta \mathbf{J}^{2y-1}_{\text{SO}(N)_1} \cdot \mathbf{J}^{2y}_{\text{SO}(N)_1} + \delta \mathbf{J}^{2y}_{\text{SO}(N)_1} \cdot \mathbf{J}^{2y+1}_{\text{SO}(N)_1} \tag{4.4}$$

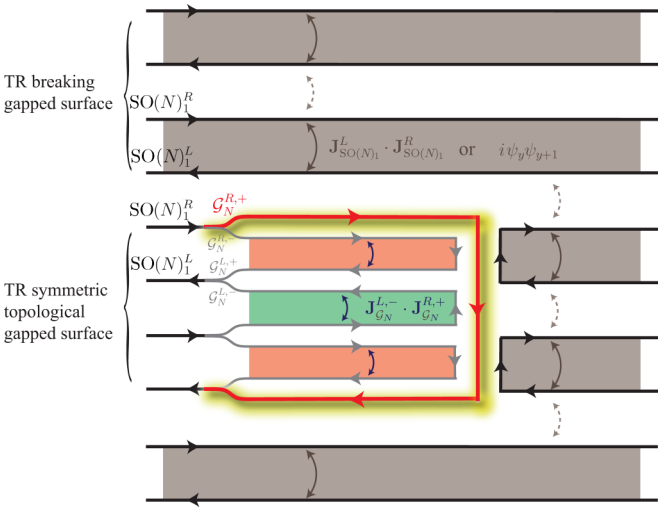

FIG. 7. Chiral interface (highlighted line) between a time-reversal-breaking gapped region and a TR-symmetric topologically ordered gapped region.

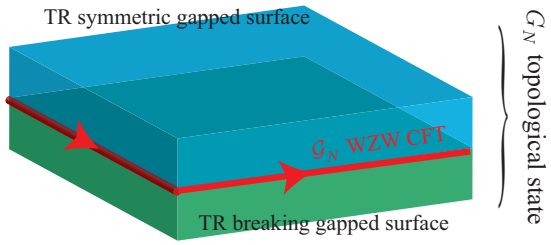

FIG. 8. The G_N topological order of a quasi-2D slab with time-reversal-symmetric gapped top surface and time-reversal-breaking gapped bottom surface

or single-body fermion backscattering perturbation

$$\mathcal{H}_{\text{TR-breaking}} = \sum_y i\Delta \boldsymbol{\psi}^T_{2y-1}\boldsymbol{\psi}_{2y} + i\delta\boldsymbol{\psi}^T_{2y}\boldsymbol{\psi}_{2y+1} \tag{4.5}$$

to the coupled Majorana wire model (2.4), for $\Delta > \delta$ and $\boldsymbol{\psi}_y = (\psi^1_y, \ldots, \psi^N_y)$. This violates the antiferromagnetic time-reversal symmetry (2.2) and leads to a gapped surface with trivial topological order. This TR-breaking half-plane is put side by side against a TR-symmetric gapped half-plane, where the N Majorana channels per wire are *fractionalized* into $\text{SO}(N)_1 \supseteq \mathcal{G}^+_N \times \mathcal{G}^-_N$, for $\mathcal{G}_N$ previously defined in Eq. (3.5). Each $\mathcal{G}_N$ sector is then paired with the adjacent one on the next wire and are gapped by current-current backscattering $\mathbf{J}_{\mathcal{G}^-_N} \cdot \mathbf{J}_{\mathcal{G}^+_N}$. The interface between the TR-symmetric and TR-breaking regions leaves behind one single unpaired fractional $\mathcal{G}_N$ channel. This can be regarded as a 2D analog of the fractional boundary modes in the Haldane integral spin chain [90,91] and the AKLT spin chain [92].

As eluded in the Introduction, when the coupled wire model involves only current-current backscattering interaction, it is a boson model where the bosonic current operators, rather than Majorana fermions, are treated as fundamental local objects. It is therefore more natural for us to use the current backscattering Hamiltonian (4.4) instead of the fermionic single-body one (4.5) to introduce a time-reversal-breaking gap. In this case, π fluxes are deconfined anyonic excitations realized as π kinks along a stripe where there is no energy cost in separating a flux-antiflux pair. If the fermionic TR-breaking Hamiltonian (4.5) were used instead, π fluxes would be confined on the bottom layer and Majorana fermions would become local. We, however, will mostly be focusing on the former bosonic case, although the fermionic scenario may be more realistic in a superconducting medium.

The bulk-interface correspondence depends on the orientation of the time-reversal-breaking order. In Eq. (4.4), if the backscattering tunneling strengths are reversed so that $\delta > \Delta$, Fig. 7 will need to be shifted by $y \to y+1$ and all propagating directions will need to be inverted. As a result, the interface CFT will also be reversed to its time-reversal partner $\mathcal{G}_N \to \overline{\mathcal{G}_N}$. This will flip the spins of all primary fields $h_{\mathbf{a}} \to h_{\bar{\mathbf{a}}} = -h_{\mathbf{a}}$ and conjugate all exchange phases $\theta_{\mathbf{a}} \to \theta_{\bar{\mathbf{a}}} = \theta^*_{\mathbf{a}}$.

An interface with a particular orientation therefore corresponds to a time-reversal-breaking topological order. This is also apparent in the slab geometry in Fig. 8 where the TR-breaking order on the bottom surface can have opposite orientations. Unlike the conventional case on the surface of a topological superconductor where time reversal is local, here time reversal involves a half-translation $y \to y+1$ and relates a stripe gapped by $\mathbf{J}^-_y \cdot \mathbf{J}^+_{y+1}$ to its neighbor $\mathbf{J}^-_{y+1} \cdot \mathbf{J}^+_{y+2}$. As anyonic excitations are realized as kinks or domain walls that separate distinct ground states along a stripe, time reversal nonlocally translates anyons on an even stripe (green) to an odd one (red) or vice versa (see Fig. 7). However, an interface with a particular orientation can only correspond to anyons on stripes with a particular parity. For example, the bulk-interface correspondence in Fig. 7 singles out anyons on even stripes gapped by $\mathbf{J}^-_{2y} \cdot \mathbf{J}^+_{2y+1}$. There is therefore no reason to expect the anyon theory would be closed under time reversal.

TABLE II. The exchange phase $\theta_{\mathbf{x}} = e^{2\pi i h_{\mathbf{x}}}$ and quantum dimensions of anyons $\mathbf{x}$ in a $(2+1)$D $\text{SO}(r)_1$ topological phase.

	r even				r odd		
$\mathbf{x}$	1	ψ	s_+	s_-	1	ψ	σ
$d_{\mathbf{x}}$	1	1	1	1	1	1	$\sqrt{2}$
$\theta_{\mathbf{x}}$	1	-1	$e^{\pi i r/8}$	$e^{\pi i r/8}$	1	-1	$e^{\pi i r/8}$

A. Summary of anyon contents

The interface carries chiral gapless degrees of freedom, which are captured by the $\mathcal{G}_N$ WZW theory whose primary fields correspond to the anyon content of the TR-symmetry gapped surface. For even $N = 2r$, the surface carries a

$$G_N = \text{SO}(r)_1 \tag{4.6}$$

topological order summarized in Table II. Its anyonic excitations obey the Abelian fusion rules

$$\psi \times \psi = 1, \quad s_\pm \times \psi = s_\mp,$$
$$s_\pm \times s_\pm = \begin{cases} 1 & \text{for } r \equiv 0 \bmod 4, \\ \psi & \text{for } r \equiv 2 \bmod 4 \end{cases} \tag{4.7}$$

for r even, or the Ising fusion rules

$$\psi \times \psi = 1, \quad \psi \times \sigma = \sigma, \quad \sigma \times \sigma = 1 + \psi \tag{4.8}$$

for r odd. Equations (4.7) and (4.8) follow directly from the fusion properties of the primary fields in the $\text{SO}(r)_1$ Kac-Moody algebra (see Sec. II A and Appendixes B and C). The exchange phase (also known as topological spin) $\theta_{\mathbf{x}} = e^{2\pi i h_{\mathbf{x}}}$ can be read off from the conformal dimension $h_{\mathbf{x}}$ of the primary field $V_{\mathbf{x}}$ in $\text{SO}(r)_1$ that corresponds to the anyon type $\mathbf{x}$. Again, we extend r to negative integers by defining $\text{SO}(-r)_1 = \overline{\text{SO}(r)_1}$ to be the time-reversal conjugate of the $\text{SO}(r)_1$ topological state.

For odd $N = 9 + 2r$, the $\mathcal{G}_N$ WZW CFT at the interface corresponds the TR-symmetric gapped surface that carries a topological order given by the *relative* tensor product

$$G_N = \text{SO}(3)_3 \boxtimes_b \text{SO}(r)_1, \tag{4.9}$$

where the fermion pair $b = \psi_{\text{SO}(3)_3} \times \psi_{\text{SO}(r)_1}$ is condensed. The concept of anyon condensation [72] will be demonstrated more explicitly later in Sec. IV B. The topological state carries seven types of anyons and is summarized in Table III. For

TABLE III. The exchange phase $\theta_{\mathbf{x}} = e^{2\pi i h_{\mathbf{x}}}$ and quantum dimensions of anyons $\mathbf{x}$ in a $(2+1)$D $SO(3)_3 \boxtimes_b SO(r)_1$ topological phase.

$\mathbf{x}$	1	α_+	γ_+	β	γ_-	α_-	f
$d_{\mathbf{x}}$	1	$\sqrt{2+\sqrt{2}}$	$1+\sqrt{2}$	$\sqrt{4+2\sqrt{2}}$	$1+\sqrt{2}$	$\sqrt{2+\sqrt{2}}$	1
$\theta_{\mathbf{x}}$	1	$e^{\pi i \frac{3+2r}{16}}$	$e^{i\pi/2}$	$e^{\pi i \frac{15+2r}{16}}$	$e^{-i\pi/2}$	$e^{\pi i \frac{3+2r}{16}}$	-1
				r even			
$d_{\mathbf{x}}$	1	$\sqrt{2+\sqrt{2}}$	$1+\sqrt{2}$	$\sqrt{4+2\sqrt{2}}$	$1+\sqrt{2}$	$\sqrt{2+\sqrt{2}}$	1
$\theta_{\mathbf{x}}$	1	$e^{\pi i \frac{15+2r}{16}}$	$e^{i\pi/2}$	$e^{\pi i \frac{3+2r}{16}}$	$e^{-i\pi/2}$	$e^{\pi i \frac{15+2r}{16}}$	-1
				r odd			

instance, the anyon structure matches the primary field content of the $SO(3)_3$ WZW theory (see Table I) when $r = 0$. The quasiparticle fusion rules of G_N are similar to the $SO(3)_3$ ones in Eq. (3.60):

$$\begin{aligned} &f \times f = 1, \quad f \times \gamma_\pm = \gamma_\mp, \quad f \times \alpha_\pm = \alpha_\mp, \quad f \times \beta = \beta, \\ &\gamma_\pm \times \gamma_\pm = 1 + \gamma_+ + \gamma_-, \quad \alpha_\pm \times \beta = \gamma_+ + \gamma_-, \\ &\beta \times \beta = 1 + \gamma_+ + \gamma_- + f, \quad \beta \times \gamma_\pm = \alpha_+ + \alpha_- + \beta \end{aligned} \tag{4.10}$$

except the following modifications that depend on $r = (N-9)/2$:

$$\alpha_\pm \times \alpha_\pm = \begin{cases} 1+\gamma_+ & \text{for } r \equiv 0 \bmod 4, \\ f+\gamma_+ & \text{for } r \equiv 1 \bmod 4, \\ f+\gamma_- & \text{for } r \equiv 2 \bmod 4, \\ 1+\gamma_- & \text{for } r \equiv 3 \bmod 4, \end{cases}$$

$$\alpha_\pm \times \gamma_\pm = \begin{cases} \alpha_+ + \beta & \text{for } r \text{ even}, \\ \alpha_- + \beta & \text{for } r \text{ odd}. \end{cases} \tag{4.11}$$

This quasiparticle spin and fusion structure will be shown later in Sec. IV B. The braiding S matrices of the G_N states are summarized in Appendix E.

The G_N sequence extends the 16-fold periodic anyon structure [64,107,108] $SO(r+16)_1 \cong SO(r)_1$ to a periodic class of 32 topological states

$$G_{N+32} \cong G_N. \tag{4.12}$$

This seemingly contradicts the 16-fold prediction of topologically ordered surface states from Refs. [11–17]. This is due to the nonlocal nature of the antiferromagnetic time-reversal symmetry in the coupled Majorana wire model. On the other hand, in general there are multiple possible gapping potentials that lead to distinct topological order. For instance, we will show in a subsequent section that for $N = 16$, there is an extended E_8 symmetry or an alternative conformal embedding that would allow a different set of gapping terms but would forbid all electronic quasiparticle excitations.

The 32 topological states here follow a $\mathbb{Z}_{32}$ tensor product algebraic structure

$$G_{N_1} \boxtimes_b G_{N_2} \cong G_{N_1+N_2}, \tag{4.13}$$

where certain maximal set of mutually local bosons from G_{N_1} and G_{N_2} are pair condensed in the relative tensor product. We will discuss this in more detail below.

B. The 32-fold tensor product structure

We first explain the relative tensor product that defines the G_N topological state in Eq. (4.9). We begin with the tensor product state $SO(3)_3 \otimes SO(r)_1$ which consists of decoupled $SO(3)_3 = SU(2)_6$ and $SO(r)_1$ topological states. The primary fields of the $SU(2)_6$ WZW CFT are labeled by seven half-integral "spins" $s = \mathbf{0}, \frac{\mathbf{1}}{\mathbf{2}}, \mathbf{1}, \frac{\mathbf{3}}{\mathbf{2}}, \mathbf{2}, \frac{\mathbf{5}}{\mathbf{2}}, \mathbf{3}$ and are summarized in Table I and Eq. (3.60). These correspond to the anyon structure of the $(2+1)$D $SO(3)_3$ topological state. The topological order of $SO(r)_1$ is well known [64] and was summarized earlier in this section. For instance, "spin" $\mathbf{3}$ corresponds to the BdG fermion quasiparticle f, and the half-integral "spins" $\frac{\mathbf{1}}{\mathbf{2}}$, $\frac{\mathbf{3}}{\mathbf{2}}$, and $\frac{\mathbf{5}}{\mathbf{2}}$ are π fluxes that give a -1 monodromy phase of an orbiting fermion.

In the coupled Majorana wire model where there are $N = 9 + 2r$ Majorana channels per wire, the gapping term explicitly separates the first 9 and final $2r$ channels and the current backscattering potential does not mix these two sectors. This model would therefore give a decoupled $SO(3)_3 \otimes SO(r)_1$ topological state. However, there could be additional local time-reversal-symmetric terms, such as intrawire forward scattering $i\psi_a^R \psi_b^R$ and $i\psi_a^L \psi_b^L$, that mix the two sectors and condense the fermion pair $b = f_{SO(3)_3} \otimes \psi_{SO(r)_1}$. In fact, fermion pair condensation is natural in a superconducting medium where the ground state consists of Cooper pairs. The condensation of the bosonic anyon b results in the confinement of certain quasiparticles that have nontrivially monodromy around it [72]. These include all the π fluxes $\frac{\mathbf{1}}{\mathbf{2}}$, $\frac{\mathbf{3}}{\mathbf{2}}$, and $\frac{\mathbf{5}}{\mathbf{2}}$ in the $SO(3)_3$ sector, $s_\pm$ (or σ) in $SO(r)_1$ for r even (resp. odd), as well as the tensor product $\frac{\mathbf{1}}{\mathbf{2}} \otimes \psi$, $\frac{\mathbf{3}}{\mathbf{2}} \otimes \psi$, $\frac{\mathbf{5}}{\mathbf{2}} \otimes \psi$, $\mathbf{1} \otimes s_\pm$, $\mathbf{2} \otimes s_\pm$ and $\mathbf{3} \otimes s_\pm$ (or $\mathbf{1} \otimes \sigma$, $\mathbf{2} \otimes \sigma$ and $\mathbf{3} \otimes \sigma$). The remaining anyons are local with respect to the boson b and survive the condensation, but certain pairs are identified if they differ only by the boson condensate $\mathbf{a} \times b \equiv \mathbf{a}$. This includes $\mathbf{3} \equiv \psi$, $\mathbf{1} \otimes \psi \equiv \mathbf{2}$, $\mathbf{2} \otimes \psi \equiv \mathbf{1}$, $\frac{\mathbf{1}}{\mathbf{2}} \otimes s_\pm \equiv \frac{\mathbf{5}}{\mathbf{2}} \otimes s_\mp$, and $\frac{\mathbf{3}}{\mathbf{2}} \otimes s_+ \equiv \frac{\mathbf{3}}{\mathbf{2}} \otimes s_-$ for even r, or $\frac{\mathbf{1}}{\mathbf{2}} \otimes \sigma \equiv \frac{\mathbf{5}}{\mathbf{2}} \otimes \sigma$ for r odd. Special care has to be taken for the tensor product $\frac{\mathbf{3}}{\mathbf{2}} \otimes \sigma$ when r is odd. After condensation, the fusion rule of a pair of $\frac{\mathbf{3}}{\mathbf{2}} \otimes \sigma$ becomes

$$\begin{aligned} \left(\tfrac{\mathbf{3}}{\mathbf{2}} \otimes \sigma\right) \times \left(\tfrac{\mathbf{3}}{\mathbf{2}} \otimes \sigma\right) &= (\mathbf{0} + \mathbf{1} + \mathbf{2} + \mathbf{3}) \otimes (1 + \psi) \\ &\equiv \mathbf{0} + \mathbf{0} + \mathbf{1} + \mathbf{1} + \mathbf{2} + \mathbf{2} + \mathbf{3} + \mathbf{3} \end{aligned} \tag{4.14}$$

which has two vacuum fusion channels and indicates that $\frac{\mathbf{3}}{\mathbf{2}} \otimes \sigma$ cannot be a simple object. This leads to the decomposition

$$\tfrac{\mathbf{3}}{\mathbf{2}} \otimes \sigma \equiv \alpha_+ + \alpha_-, \tag{4.15}$$

where $\alpha_\pm$ are simple anyons with identical exchange statistics but opposite fermion parity $\alpha_\pm \times f = \alpha_\mp$ and obey the fusion rules (4.11).

We summarize the identification of the seven anyon types in $G_N = SO(3)_3 \boxtimes_b SO(r)_1$ as tensor products in Table IV. This explains the exchange statistics and quantum dimensions of the quasiparticles in Table III:

$$\theta_{\mathbf{a}\otimes\mathbf{b}} = \theta_{\mathbf{a}}\theta_{\mathbf{b}}, \quad d_{\mathbf{a}\otimes\mathbf{b}} = d_{\mathbf{a}} d_{\mathbf{b}} \tag{4.16}$$

with the exception of the nonsimple object $\frac{\mathbf{3}}{\mathbf{2}} \otimes \sigma$ in Eq. (4.15) where each component $\alpha_\pm$ carries half of its dimension. The

TABLE IV. Identification of the seven anyon types in Table III as tensor products.

	1	α_+	γ_+	β	γ_-	α_-	f
r even	**0**	$\mathbf{1/2}\otimes s_+$	**1**	$\mathbf{3/2}\otimes s_\pm$	**2**	$\mathbf{5/2}\otimes s_+$	**3**
r odd	**0**	$(\mathbf{3/2}\otimes\sigma)_+$	**1**	$\mathbf{1/2}\otimes\sigma$	**2**	$(\mathbf{3/2}\otimes\sigma)_-$	**3**

fusion rules in Eqs. (4.10) and (4.11) are explained by the tensor product

$$(\mathbf{a}_1\otimes\mathbf{b}_1)\times(\mathbf{a}_2\otimes\mathbf{b}_2)=(\mathbf{a}_1\times\mathbf{a}_2)\otimes(\mathbf{b}_1\times\mathbf{b}_2) \tag{4.17}$$

except in the odd r cases where again the nonsimple object $\frac{\mathbf{3}}{\mathbf{2}}\otimes\sigma=\alpha_++\alpha_-$ requires special attention.

The fusion rules (4.11) of $\alpha_\pm$ in the odd r cases are fixed by modular invariance. The braiding S matrix (4.1) is determined by fusion rules and quasiparticle exchange statistics. On the other hand, fusion rules can also be determined by the S matrix using the Verlinde formula (3.58) [101]. Moreover, one can define the T matrix according to the quasiparticle exchange statistics

$$T_{\mathbf{ab}}=\delta_{\mathbf{ab}}\theta_{\mathbf{a}} \tag{4.18}$$

which corresponds to the modular T transformation in the CFT along the boundary. As a consequence, they satisfy the SL(2;$\mathbb{Z}$) algebraic relation [64]

$$(\mathcal{S}T^\dagger)^3=e^{-2\pi i c_-/8}\mathcal{S}^2, \tag{4.19}$$

where $c_-=c_R-c_L$ is the chiral central charge of the corresponding CFT along the boundary

$$c_-(G_N)=c_-[\mathrm{SO}(3)_3]+c_-[\mathrm{SO}(r)_1]=\frac{9}{4}+\frac{r}{2}=\frac{N}{4}. \tag{4.20}$$

These put a very restrictive constraint on the allowed topological field theory and fix the fusion rules (4.11) for $\alpha_\pm$ when r is odd. The braiding S matrices can be found in Appendix E.

The relative tensor product structure of the 16-fold $\mathrm{SO}(r)_1$ sequence itself can also be understood using anyon condensation

$$\mathrm{SO}(r_1)_1\boxtimes_b\mathrm{SO}(r_2)_1\cong\mathrm{SO}(r_1+r_2)_1, \tag{4.21}$$

where the fermion pair $\psi_1\otimes\psi_2$ is condensed. This can be verified by a similar condensation procedure as the one presented above. For instance, if r_1 and r_2 are both odd, the tensor product $\sigma_1\otimes\sigma_2$ will become nonsimple after condensation and decompose into a pair of Abelian π fluxes s_++s_-, with identical exchange statistics but opposite fermion parities $s_\pm\times\psi=s_\mp$ and are related by an anyonic symmetry [107,108].

Next, we move on to explaining the general relative tensor product structure (4.13) of the 32-fold G_N states. Equation (4.21) describes the cases when both N_1 and N_2 are even, i.e., $G_{2r_1}\boxtimes_b G_{2r_2}\cong G_{2r_1+2r_2}$. A similar anyon condensation procedure that defined the relative tensor product $\mathrm{SO}(3)_3\boxtimes_b\mathrm{SO}(r)_1$ above would prove that

$$G_N\boxtimes_b\mathrm{SO}(r)_1\cong G_{N+2r} \tag{4.22}$$

for N odd, where the fermion pair $b=f_{G_N}\otimes\psi_{\mathrm{SO}(r)_1}$ is condensed.

When both $N_1=9+2r_1$ and $N_2=9+2r_2$ are odd, each of the two $G_{N_i}=\mathrm{SO}(3)_3\boxtimes_b\mathrm{SO}(r_i)_1$ theories contains seven anyon types 1, $\alpha_\pm^i$, $\gamma_\pm^i$, β^i, f^i. The tensor product state $G_{N_1}\otimes G_{N_2}$ contains three nontrivial bosons

$$b=\{b_0,b_+,b_-\}=\{f^1\otimes f^2,\gamma_+^1\otimes\gamma_-^2,\gamma_-^1\otimes\gamma_+^2\} \tag{4.23}$$

as $\gamma_\pm$ have conjugate exchange phases $\theta_{\gamma_\pm}=\pm i$. Moreover, these bosons are mutually local. First, b_0 have trivial monodromy around $b_\pm$ as $\gamma_\pm$ are local with respect to the fermion f. Second, as there are bosonic fusion channels $b_\pm\times b_\pm=1+b_++b_-+\cdots$ and $b_\pm\times b_\mp=b_0+b_++b_-+\cdots$, $b_\pm$ are local among themselves because their mutual monodromy phases are trivial. We first condensed the Abelian fermion pair $b_0=f^1\otimes f^2$. The resulting theory contains the following set of (nonconfined) anyon types:

$$G_{N_1}\boxtimes_{b_0}G_{N_2}=\left\langle\begin{matrix}1,f,\gamma_\pm^1,\gamma_\pm^2,\gamma_+^1\gamma_+^2,\gamma_+^1\gamma_-^2,\\ \alpha_+^1\alpha_+^2,\alpha_+^1\alpha_-^2,\alpha_+^1\beta^2,\beta^1\alpha_+^2,\beta^1\beta^2\end{matrix}\right\rangle, \tag{4.24}$$

where some anyon types are identified by the b_0 condensate, such as $f\equiv f^1\equiv f^2$ and $\gamma_-^1\gamma_-^2=\gamma_+^1\gamma_+^2\times b_0$, and are therefore not listed. Next, we condense the non-Abelian boson $b_+=\gamma_+^1\gamma_-^2$, which is already equated with $b_-=b_+\times b_0$. The general condensation procedure of a non-Abelian boson was proposed by Bais and Slingerland in Ref. [72]. In the present case, it begins with the fusion theory $\mathcal{F}$ of $G_{N_1}\boxtimes_{b_0}G_{N_2}$ that only encodes the associative fusion content but neglects the braiding structure of the anyons. As the boson b_+ is condensed, it decomposes as $b_+=\gamma_+^1\gamma_-^2=1+\cdots$, which now contains the vacuum channel 1. This reduces the fusion theory $\mathcal{F}$ into a new fusion theory $\mathcal{F}'$, where the certain anyons in Eq. (4.24) become nonsimple objects and decompose into simpler components while others are identified by the boson condensate. This new fusion category $\mathcal{F}'$ contains the nonconfined anyons in the resulting state as well as confined nonpointlike objects.

We start with the first line of anyons in Eq. (4.24), which are all local with respect to the fermion f. The semion γ_+^1 is self-conjugate as $\gamma_+^1\times\gamma_+^1=1+\gamma_+^1+\gamma_-^1$. However, γ_-^2 is now also an antiparticle of γ_+^1 since $\gamma_+^1\times\gamma_-^2=b_+=1+\cdots$ also contains the vacuum channel. The uniqueness of antipartner guarantees the identifications

$$\gamma_+\equiv\gamma_+^1\equiv\gamma_-^2,\quad \gamma_-\equiv\gamma_-^1\equiv\gamma_+^2 \tag{4.25}$$

which obey the usual fusion rules $\gamma_\pm\times\gamma_\pm=1+\gamma_++\gamma_-$ and $f\times\gamma_\pm=\gamma_\mp$. This in turn determines the decomposition of the non-Abelian boson

$$b_+=\gamma_+^1\gamma_-^2\equiv\gamma_+\times\gamma_+=1+\gamma_++\gamma_- \tag{4.26}$$

which is consistent with the boson quantum dimension $d_{b_+}=d_\gamma^2=1+2d_\gamma$. Moreover, the non-Abelian fermion also decomposes:

$$\gamma_+^1\gamma_+^2\equiv\gamma_+\times\gamma_-=f+\gamma_++\gamma_-. \tag{4.27}$$

Next, we move on to the second line of anyons in Eq. (4.24), which are π fluxes with respect to the fermion

f. From the original fusion rules (4.10) and (4.11) and the identifications (4.25)–(4.27), the π fluxes satisfy the fusion rules

$$(\alpha_+^1\alpha_+^2)\times(\alpha_+^1\alpha_+^2) = \begin{cases} 1+f+2\gamma_++2\gamma_- & \text{for } r_1+r_2 \text{ even},\\ 1+1+\gamma_++\gamma_-+2\gamma_\pm & \text{for } r_1+r_2\equiv 3 \bmod 4,\\ f+f+\gamma_++3\gamma_- & \text{for } r_1+r_2\equiv 1 \bmod 4,\end{cases} \tag{4.28}$$

$$(\alpha^1\beta^2)\times(\alpha^1\beta^2) = 1+1+f+f+4\gamma_++4\gamma_-, \tag{4.29}$$

$$(\beta^1\beta^2)\times(\beta^1\beta^2) = 4(1+f+2\gamma_++2\gamma_-), \tag{4.30}$$

$$(\alpha_+^1\alpha_+^2)\times(\alpha_+^1\beta^2) = 1+f+3\gamma_++3\gamma_-, \tag{4.31}$$

$$(\alpha_+^1\alpha_+^2)\times(\beta^1\beta^2) = 1+1+f+f+4\gamma_++4\gamma_- \tag{4.32}$$

for $N_1 = 9+2r_1$ and $N_2 = 9+2r_2$.

These show $\alpha^1\beta^2$ and $\beta^1\beta^2$ must be nonsimple because their corresponding fusion rules contain multiple vacuum channels. The decomposition of $\beta^1\beta^2$ is simplest and applies to all r_1, r_2:

$$\beta^1\beta^2 = \alpha_+^1\alpha_+^2 + \alpha_+^1\alpha_-^2, \tag{4.33}$$

where $\alpha_+^1\alpha_-^2 = \alpha_+^1\alpha_+^2\times f$. For instance, it is straightforward to check that this decomposition is consistent with the fusion rules. $\alpha_+^1\beta^2$ and $\alpha_-^1\beta^2$ are clearly identified as they differ only by the Abelian boson $b_0 = f^1f^2$. We therefore will simply denote them as $\alpha^1\beta^2$. Moreover, one can show that $\alpha^1\beta^2$ and $\beta^1\alpha^2$ are also identified after the condensation of the non-Abelian boson $\gamma_+^1\gamma_-^2 = 1+\gamma_++\gamma_-$ in Eq. (4.26). This can be verified by equating the fusion equations $(\alpha^1\beta^2)\times(\gamma_+^1\gamma_-^2) = (\alpha^1\beta^2)\times(1+\gamma_++\gamma_-)$. The decomposition of $\alpha^1\beta^2\equiv\beta^1\alpha^2$ depends on the parity of r_1+r_2.

When r_1+r_2 is even, the pair fusion rule for $\alpha_+^1\alpha_+^2$ allows it to be simple since there is a unique vacuum channel. Moreover as the pair fusion rule is unaltered by the addition of a fermion f, it is identical to $(\alpha_+^1\alpha_+^2)\times(\alpha_+^1\alpha_-^2)$. This shows $\alpha_\pm^1\alpha_-^2$ conjugates and therefore identifies with $\alpha_\pm^1\alpha_+^2$, which is self-conjugate:

$$\alpha^1\alpha^2 \equiv \alpha_\pm^1\alpha_\pm^2 \equiv \alpha_\pm^1\alpha_\mp^2. \tag{4.34}$$

In this case, $\alpha^1\beta^2$ is decomposed into

$$\alpha^1\beta^2 = \sigma + \alpha^1\alpha^2, \tag{4.35}$$

where we introduce the Ising anyon σ that obeys

$$\begin{aligned} &\sigma\times\sigma = 1+f, \quad \sigma\times f = \sigma,\\ &\sigma\times\alpha^1\alpha^2 = \gamma_++\gamma_-, \quad \sigma\times\gamma_\pm = \alpha^1\alpha^2. \end{aligned} \tag{4.36}$$

The decomposition (4.35) is consistent with the fusion rules (4.31) and (4.29). The reduced fusion category after condensing the boson (4.26) is therefore generated by the following simple objects:

$$\mathcal{F}'_{\text{even}} = \langle 1, f, \sigma, \gamma_\pm, \alpha^1\alpha^2\rangle \tag{4.37}$$

when r_1+r_2 is even. It has the fusion rules (4.36) together with $\gamma_\pm\times\alpha^1\alpha^2 = \sigma+2\alpha^1\alpha^2$.

When r_1+r_2 is odd, we need to further separate into two cases. When $r_1+r_2\equiv 3 \bmod 4$, the fusion rule of a pair of $\alpha_+^1\alpha_+^2$ in Eq. (4.28) forbids it to be simple. It decomposes into

$$\alpha_+^1\alpha_+^2 = s_+ + \gamma_+ \quad \text{or} \quad s_+ + \gamma_-, \tag{4.38}$$

where $s_\pm$ are Abelian anyons that satisfy the fusion rules

$$s_\pm\times s_\pm = 1, \quad s_\pm\times f = s_\mp, \quad s_+\times\gamma_\pm = \gamma_\pm \tag{4.39}$$

and the fermion parity $\gamma_\pm$ in Eq. (4.38) depends on $(r_1,r_2)\equiv(0,3)$ or $(1,2)$ mod 4 but is unimportant for the current discussion. The decomposition (4.38) is consistent with the fusion rule (4.28). In this case, the fusion rules $(\alpha_+^1\alpha_+^2)\times(\alpha^1\beta^2)$ in Eq. (4.31) require a different decomposition of $\alpha^1\beta^2$ than (4.35):

$$\alpha^1\beta^2 = \gamma_+ + \gamma_-. \tag{4.40}$$

The reduced fusion category after condensing the boson (4.26) is therefore generated by the following simple objects:

$$\mathcal{F}'_3 = \langle 1, f, s_\pm, \gamma_\pm\rangle \tag{4.41}$$

when $r_1+r_2\equiv 3 \bmod 4$.

When $r_1+r_2\equiv 1 \bmod 4$, the fusion rule (4.28) again forbids $\alpha_+^1\alpha_+^2$ to be simple. Moreover, as the vacuum channel is absent, it is no longer self-conjugate but instead is conjugate with $\alpha_+^1\alpha_-^2$ since it has opposite fermion parity and $(\alpha_+^1\alpha_+^2)\times(\alpha_+^1\alpha_-^2) = 1+1+3\gamma_++\gamma_-$. We decompose

$$\alpha_+^1\alpha_+^2 = s_+ + g_+, \tag{4.42}$$

where $s_\pm$ are Abelian anyons and $g_\pm$ are non-Abelian objects that satisfy

$$s_\pm\times s_\pm = f, \quad s_\pm\times f = s_\mp, \quad g_\pm = \gamma_+\times s_\pm. \tag{4.43}$$

The decomposition of $\alpha^1\beta^2$ also needs to be modified:

$$\alpha^1\beta^2 = g_+ + g_-. \tag{4.44}$$

One can check that these decompositions are consistent with the original fusion rules. The reduced fusion category after condensing the boson (4.26) is therefore generated by the following simple objects:

$$\mathcal{F}'_1 = \langle 1, f, s_\pm, \gamma_\pm, g_\pm\rangle \tag{4.45}$$

when $r_1+r_2\equiv 1 \bmod 4$.

Not all objects in the reduced fusion theories $\mathcal{F}'_{\text{even}}$, $\mathcal{F}'_1$, and $\mathcal{F}'_3$ in Eqs. (4.37), (4.45), and (4.41) are nonconfined anyons in the new topological states. Some may be nonlocal with respect to the boson b_+ [Eq. (4.26)] and are therefore not pointlike objects when b_+ is condensed. They are equipped with a physical string or branch cut that extends. The anyon theory, which encodes both fusion and braiding information, after condensation excludes these confined extended objects. To determine which objects in the reduced fusion categories $\mathcal{F}'$ are nonconfined anyons, we look at the possible monodromy around the condensed boson b_+. Suppose $\mathbf{a}_1\otimes\mathbf{a}_2$ and $\mathbf{b}_1\otimes\mathbf{b}_2$ are anyons in the tensor product state $G_{N_1}\boxtimes_{b_0} G_{N_2}$ [Eq. (4.24)]

that are related by the fusion rule $b_+ \times (\mathbf{a}_1 \otimes \mathbf{a}_2) = \mathbf{b}_1 \otimes \mathbf{b}_2 + \ldots$, the monodromy under this fixed fusion channel is [72]

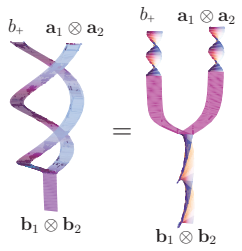

$$= \frac{\theta_{\mathbf{b}_1\otimes\mathbf{b}_2}}{\theta_{b_+}\theta_{\mathbf{a}_1\otimes\mathbf{a}_2}} = \frac{\theta_{\mathbf{b}_1\otimes\mathbf{b}_2}}{\theta_{\mathbf{a}_1\otimes\mathbf{a}_2}} \tag{4.46}$$

as b_+ is a boson with $\theta_{b_+} = 1$. In other words, trivial monodromy simply requires the invariance of exchange statistics upon an addition of the boson.

Given any simple object $\mathbf{x}$ in the reduced fusion category $\mathcal{F}'$ in Eqs. (4.37), (4.45), or (4.41), it may be *lifted* to multiple anyons in the tensor product state $G_{N_1} \boxtimes_{b_0} G_{N_2}$ in Eq. (4.24) in the sense that it belongs in distinct decompositions $\mathbf{a}_1 \otimes \mathbf{a}_2 = \mathbf{x} + \cdots$ and $\mathbf{b}_1 \otimes \mathbf{b}_2 = \mathbf{x} + \cdots$. For instance, $\gamma_\pm$ are components of the boson $\gamma_+^1\gamma_-^2 = 1 + \gamma_+ + \gamma_-$ as well as the fermion $\gamma_+^1\gamma_+^2 = f + \gamma_+ + \gamma_-$ [see (4.26) and (4.27)]. If $\mathbf{x}$ is an object not confined by the boson condensation, then its exchange statistics should be independent from the choices of lift

$$\theta_{\mathbf{x}} = \theta_{\mathbf{a}_1\otimes\mathbf{a}_2} = \theta_{\mathbf{b}_1\otimes\mathbf{b}_2} \tag{4.47}$$

since the monodromy (4.46) should be trivial. Otherwise, the object $\mathbf{x}$ has to be nonpointlike and extended as it does not have well-defined statistics. For example, since $\gamma_\pm$ belongs to the decomposition of a non-Abelian boson and fermion, they have to be confined objects after condensation.

The relative tensor product $G_{N_1} \boxtimes_b G_{N_2}$ with the condensation of the set of bosons b [Eq. (4.23)] contains nonconfined anyons in the reduced fusion categories $\mathcal{F}'_{\text{even}}$, $\mathcal{F}'_1$, and $\mathcal{F}'_3$ in Eqs. (4.37), (4.45), and (4.41). For example, when $r_1 + r_2$ is even, the simple object $\alpha^1\alpha^2$ in Eq. (4.37) is confined and is not an anyon because it can be lifted into $\alpha^1\beta^2$ and $\beta^1\beta^2$, which have distinct statistics, in Eqs. (4.35) and (4.33). When $r_1 + r_2 \equiv 1 \bmod 4$, the simple objects $g_\pm$ are also confined because they belong in $\alpha^1\beta^2$ and $\alpha_+^1\alpha_\pm^2$, which have different spins, in Eqs. (4.44) and (4.42). This shows $G_{N_1} \boxtimes_b G_{N_2}$ is generated by the nonconfined anyons

$$G_{N_1} \boxtimes_b G_{N_2} = \begin{cases} \langle 1, f, \sigma \rangle & \text{for } r_1 + r_2 \text{ even}, \\ \langle 1, f, s_\pm \rangle & \text{for } r_1 + r_2 \text{ odd}. \end{cases} \tag{4.48}$$

The exchange statistics of σ and $s_\pm$ are determined by that of their lifts. For instance,

$$\theta_\sigma = \theta_{\alpha^1\beta^2} = \theta_\alpha\theta_\beta = e^{\pi i \frac{9+r_1+r_2}{8}} = e^{\pi i (N_1+N_2)/16} \tag{4.49}$$

using Table III when $r_1 + r_2$ is even. This shows

$$G_{N_1} \boxtimes_b G_{N_2} = \mathrm{SO}\left(\frac{N_1 + N_2}{2}\right)_1 \tag{4.50}$$

when both N_1 and N_2 are odd and conclude the 32-fold tensor product algebraic structure of the G_N series.

V. OTHER POSSIBILITIES

In the previous sections, we proposed time-reversal-symmetric interactions that gap the coupled Majorana wire model and lead to a G_N topological order [see Eqs. (4.6) and (4.9)]. The interwire current-current backscattering interactions depend on a particular fractionalization $\mathrm{SO}(N)_1 \supseteq \mathcal{G}_N \times \mathcal{G}_N$ of the N Majorana channels per wire. However, in special cases, we have already seen that alternative decompositions exist and correspond to different gapping interactions and topological orders. For example, at the beginning of Sec. III, we showed when there are even Majorana channels per wire, the model could simply be gapped by a single-body backscattering potential [see (3.1)] and have trivial topological order. This is consistent with the $\mathbb{Z}_2$ classification of gapless Majorana modes protected by the antiferromagnetic time-reversal symmetry (2.2). Another example was given in Sec. III A 2 for the special case when there are $N = 4$ Majorana channels per wire where the decomposition needs to be changed into $\mathrm{SO}(4)_1 \supseteq \mathrm{SU}(2)_1 \times \mathrm{SU}(2)_1$. The resulting gapped state carries the $\mathrm{SU}(2)_1$ semion topological order instead of $G_4 = \mathrm{SO}(2)_1$.

Moreover, the 16-fold classification of topological superconductors (TSC) with the presence of interaction [11–17] suggests the 32-fold G_N series could have redundancies. On the other hand, the $\mathbb{Z}_{16}$ classification of TSC is based on the canonical local time-reversal symmetry, which is fundamentally different from the nonlocal antiferromagnetic time reversal considered in this paper. The $\mathbb{Z}_{32}$ structure of surface topological order could be an artifact of such unconventional time-reversal symmetry. Nonetheless, here in Secs. V A and V B, we discuss alternative gapping interactions when $N = 16$ that removes all electronic quasiparticles.

A. Consequence of the emergent E_8 when $N = 16$

We design alternative interwire backscattering terms in the coupled wire model (2.4) with $N = 16$ Majorana channels per wire. They open a time-reversal-symmetric energy gap among 16 surface Majorana cones with the same chirality. In general, these terms can also apply when the number of chiral Majorana channels per wire is larger than 16 by acting on a subset of channels. We begin with the bosonized description presented previously in Sec. II B, where each wire consists of an eight-component chiral $U(1)$ boson $\tilde{\boldsymbol{\phi}} = (\tilde{\phi}^1, \ldots, \tilde{\phi}^8)$ that bosonizes the complex fermions $c_j = (\psi_{2j-1} + i\psi_{2j})/\sqrt{2} = \exp(i\tilde{\phi}^j)$. This theory is special because it carries nontrivial bosonic primary fields, which can condense. For example, the two spinor representations $s_\pm$ correspond to *bosonic* primary fields of $\mathrm{SO}(16)_1$ with conformal dimension $h_{s_\pm} = 1$ [see Eq. (2.18)]. In particular, we will focus on the even sector s_+. It consists of vertex operators

$$V_{s_+}^{\boldsymbol{\varepsilon}} = e^{i\boldsymbol{\varepsilon}\cdot\tilde{\boldsymbol{\phi}}/2}, \quad \boldsymbol{\varepsilon} = (\varepsilon_1, \ldots, \varepsilon_8) \tag{5.1}$$

[see Eq. (B24)] for $\varepsilon_j = \pm 1$ with $\varepsilon_1 \ldots \varepsilon_8 = +1$. The $128 = 2^7$ number of combinations naturally matches with the dimension of the even spinor representation of SO(16) (see Appendix A). These $V_{s_+}^{\boldsymbol{\varepsilon}}$ are related to each other through the OPE with the raising and lowering operators $E^{\boldsymbol{\alpha}} = e^{i\boldsymbol{\alpha}\cdot\tilde{\boldsymbol{\phi}}} = e^{i(\pm\tilde{\phi}^i \pm \tilde{\phi}^j)}$ of $\mathrm{SO}(16)_1$ [see (B8) in Appendix B]. The 128 lattice

vectors $\boldsymbol{\varepsilon}/2$ extend the 112 roots $\boldsymbol{\alpha}$ of SO(16) to the root lattice of the exceptional simple Lie algebra E_8 with size 240 [56]. The unit dimensional vertex operators $V^{\boldsymbol{\varepsilon}}_{s_+}$ themselves can be regarded as raising and lowering operators that enlarge the $\mathrm{SO}(16)_1$ current algebra to E_8 at level 1. This extends the current algebra of each wire

$$\mathrm{SO}(16)_1 \subseteq (E_8)_1 \tag{5.2}$$

and is intimately related to the fact that the surface state can be gapped out without leaving electronic quasiparticles which are nonlocal with respect to the boson s_+.

The gapping strategy is to condense primary fields in the bosonic sector s_+ between adjacent wires. This is facilitated by interwire backscattering interactions that bipartite the emergent E_8 symmetry:

$$E_8 \supseteq \widetilde{\mathrm{SO}(8)}^{+}_1 \times \widetilde{\mathrm{SO}(8)}^{-}_1. \tag{5.3}$$

However, these $\widetilde{\mathrm{SO}(8)}_1$ subalgebras are distinct from the ones in the decomposition $\mathrm{SO}(16)_1 \supseteq \mathrm{SO}(8)_1 \times \mathrm{SO}(8)_1$. In particular, we will see that they do not support electronic primary fields $c_j = e^{i\tilde{\phi}^j}$. Out of 128 $\boldsymbol{\varepsilon}$ lattice vectors in (5.1), there is a (nonunique) maximal set of eight orthonormal vectors $\boldsymbol{\varepsilon}_{(1)},\ldots,\boldsymbol{\varepsilon}_{(8)}$:

$$\tfrac{1}{2}\boldsymbol{\varepsilon}_{(m)} \cdot \tfrac{1}{2}\boldsymbol{\varepsilon}_{(n)} = 2\delta_{mn}. \tag{5.4}$$

We choose the set containing the highest weight vector $\boldsymbol{\varepsilon}_{(1)} = (1,1,1,1,1,1,1,1)$:

$$\begin{pmatrix} | & & | \\ \boldsymbol{\varepsilon}_{(1)} & \cdots & \boldsymbol{\varepsilon}_{(8)} \\ | & & | \end{pmatrix} = \begin{pmatrix} 1 & 1 & 1 & 1 & 1 & 1 & 1 & 1 \\ 1 & 1 & 1 & 1 & -1 & -1 & -1 & -1 \\ 1 & 1 & -1 & -1 & 1 & 1 & -1 & -1 \\ 1 & 1 & -1 & -1 & -1 & -1 & 1 & 1 \\ 1 & -1 & 1 & -1 & 1 & -1 & 1 & -1 \\ 1 & -1 & 1 & -1 & -1 & 1 & -1 & 1 \\ 1 & -1 & -1 & 1 & 1 & -1 & -1 & 1 \\ 1 & -1 & -1 & 1 & -1 & 1 & 1 & -1 \end{pmatrix}. \tag{5.5}$$

From (2.20), they give eight mutually commuting bosons $\boldsymbol{\varepsilon}_{(n)} \cdot \boldsymbol{\phi}_y/2$ per wire

$$\begin{aligned} &\left[\tfrac{1}{2}\boldsymbol{\varepsilon}_{(m)} \cdot \boldsymbol{\phi}_y(x,t), \tfrac{1}{2}\boldsymbol{\varepsilon}_{(n)} \cdot \boldsymbol{\phi}_{y'}(x',t)\right] \\ &\quad = 2\pi i \delta_{mn}(-1)^y \delta_{yy'} \mathrm{sgn}(x'-x) \end{aligned} \tag{5.6}$$

up to a constant integral multiple of $2\pi i$.

We separate the eight vectors into two groups $\mathcal{S}^+ = \{\boldsymbol{\varepsilon}_{(1)},\boldsymbol{\varepsilon}_{(2)},\boldsymbol{\varepsilon}_{(3)},\boldsymbol{\varepsilon}_{(4)}\}$ and $\mathcal{S}^- = \{\boldsymbol{\varepsilon}_{(5)},\boldsymbol{\varepsilon}_{(6)},\boldsymbol{\varepsilon}_{(7)},\boldsymbol{\varepsilon}_{(8)}\}$. They define the two $\widetilde{\mathrm{SO}(8)}^{\pm}_1$ subalgebras in E_8, whose roots lie in the root lattice of E_8 orthogonal to $\mathcal{S}^{\mp}$, respectively. One could pick the simple roots

$$\begin{aligned} &\widetilde{\boldsymbol{\alpha}}^+_1 = \boldsymbol{\varepsilon}_{(1)}/2, \quad \widetilde{\boldsymbol{\alpha}}^+_2 = \mathbf{e}_1 + \mathbf{e}_2, \quad \widetilde{\boldsymbol{\alpha}}^+_2 = \mathbf{e}_3 + \mathbf{e}_4, \quad \widetilde{\boldsymbol{\alpha}}^+_4 = \mathbf{e}_5 + \mathbf{e}_6, \\ &\widetilde{\boldsymbol{\alpha}}^-_1 = \boldsymbol{\varepsilon}_{(5)}/2, \quad \widetilde{\boldsymbol{\alpha}}^-_2 = \mathbf{e}_2 - \mathbf{e}_1, \quad \widetilde{\boldsymbol{\alpha}}^-_2 = \mathbf{e}_4 - \mathbf{e}_3, \quad \widetilde{\boldsymbol{\alpha}}^-_4 = \mathbf{e}_6 - \mathbf{e}_5 \end{aligned}$$

so that their inner product recovers the Cartan matrix of SO(8):

$$\widetilde{\boldsymbol{\alpha}}^{\pm}_I \cdot \widetilde{\boldsymbol{\alpha}}^{\pm}_J = K_{IJ}, \quad K = \begin{pmatrix} 2 & -1 & -1 & -1 \\ -1 & 2 & 0 & 0 \\ -1 & 0 & 2 & 0 \\ -1 & 0 & 0 & 2 \end{pmatrix} \tag{5.7}$$

while opposite sectors decouple $\widetilde{\boldsymbol{\alpha}}^{\pm}_I \cdot \widetilde{\boldsymbol{\alpha}}^{\mp}_J = 0$.

The new gapping potential is constructed by backscattering the two decoupled $\widetilde{\mathrm{SO}(8)}^{\pm}_1$ currents to adjacent wires in opposite directions:

$$\mathcal{H}_{\mathrm{int}} = u \sum_{y=-\infty}^{\infty} \mathbf{J}^{y}_{\widetilde{\mathrm{SO}(8)}^{-}_1} \cdot \mathbf{J}^{y+1}_{\widetilde{\mathrm{SO}(8)}^{+}_1}. \tag{5.8}$$

However, not every term can be written as four-fermion interactions. In particular, $\mathcal{H}_{\mathrm{int}}$ contains interwire s_+ quasiparticle backscattering

$$V^{\boldsymbol{\varepsilon}}_y V^{-\boldsymbol{\varepsilon}'}_{y+1} + \mathrm{H.c.} \sim \cos\left(\sum_{j=1}^{8} \frac{\varepsilon_j}{2}\tilde{\phi}^j_y - \frac{\varepsilon'_j}{2}\tilde{\phi}^j_{y+1}\right) \tag{5.9}$$

for $\varepsilon_j,\varepsilon'_j = \pm 1$ that condenses pairs of s_+'s along adjacent wires and confines all electronic excitations. The $\widetilde{\mathrm{SO}(8)}^{\pm}_1$ WZW CFT carries three emergent fermionic primary fields

$$\widetilde{c}^{\pm}_p = \exp\left[\frac{i}{2}(\tilde{\phi}^{2p-1} \pm \tilde{\phi}^{2p} - \tilde{\phi}^7 \mp \tilde{\phi}^8)\right] \tag{5.10}$$

for $p = 1,2,3$, all of which have neutral electric charge and even fermion parity with respect to the original electronic operators $c_j = e^{i\tilde{\phi}^j}$. This is because the $\widetilde{c}^{\pm}_p$'s are invariant under the $U(1)$ gauge transformation $\tilde{\phi}^j \to \tilde{\phi}^j + \varphi$. As a result, the interaction (5.8) corresponds to a gapped $\widetilde{\mathrm{SO}(8)}_1$ topological order but contains no electronlike anyon excitations. Lastly, we notice that this matches with the surface topological order of a type-II topological paramagnet [14,109].

B. Alternative conformal embeddings

The fractionalization $\mathrm{SO}(9)_1 \supseteq \mathrm{SO}(3)_3 \otimes \mathrm{SO}(3)_3$ in Sec. III B 1 is the cornerstone for the construction of symmetric gapping interactions when there are an odd number of Majorana species. However, this is not the unique decomposition. In general, when the number of Majorana channels is a whole square, the wire can be bipartitioned into $\mathrm{SO}(n^2)_1 \supseteq \mathrm{SO}(n)_n \otimes \mathrm{SO}(n)_n$ [56,59–61].

For instance, this provides yet another alternative when $N = 16$ where each wire is fractionalized into a pair of $\mathrm{SO}(4)_4 = \mathrm{SU}(2)_4 \times \mathrm{SU}(2)_4$. The $\mathrm{SO}(4)^{\pm}_4$ current operators can be constructed in a similar fashion as those in the $\mathrm{SO}(3)^{\pm}_3$ case, $\mathbf{J} = \frac{i}{2}\boldsymbol{\Sigma}^{\pm}_{ab}\psi^a\psi^b$ for $\boldsymbol{\Sigma}^+ = \boldsymbol{\Sigma} \otimes \mathbb{1}_4$ and $\boldsymbol{\Sigma}^- = \mathbb{1}_4 \otimes \boldsymbol{\Sigma}$ where $\boldsymbol{\Sigma}$ are antisymmetric 4×4 matrices generating SO(4). After introducing the current-current backscattering interactions $\mathbf{J}^{y}_{\mathrm{SO}(4)^-_4} \cdot \mathbf{J}^{y+1}_{\mathrm{SO}(4)^+_4}$, the surface would carry a $\mathrm{SO}(4)_4 = \mathrm{SU}(2)_4 \times \mathrm{SU}(2)_4$ topological order. Each $\mathrm{SU}(2)_4$ theory contains five anyon types $j = \mathbf{0},\frac{\mathbf{1}}{\mathbf{2}},\mathbf{1},\frac{\mathbf{3}}{\mathbf{2}},\mathbf{2}$ with spins $h_j = j(j+1)/6$. The $\mathrm{SO}(4)_4$ topological state does not carry fermionic excitations and, therefore, like the previous example

in Sec. V A, this gapping potential also removes all electronic quasiparticle excitations.

The gapped symmetric states for N odd are not unique either. For example, the decomposition $\mathrm{SO}(25)_1 \supseteq \mathrm{SO}(5)_5 \otimes \mathrm{SO}(5)_5$ leads to a surface $\mathrm{SO}(5)_5$ topological order which is inequivalent to $G_{25} = \mathrm{SO}(3)_3 \boxtimes_b \mathrm{SO}(8)_1$.

VI. CONCLUSION AND DISCUSSION

We constructed a coupled Majorana wire model in $(2+1)$D that imitates the massless Majorana modes on the surface of a topological superconductor. This model had a nonlocal antiferromagnetic time-reversal symmetry and consequently was $\mathbb{Z}_2$ classified, rather than $\mathbb{Z}$ in the class DIII TSC case, under the single-body framework. Despite the difference, this model adequately described the surface behavior of a TSC when the number N of Majorana species was odd, and it was worth studying and interesting in and of itself.

We introduced the four-fermion gapping potentials in Sec. III. They relied on the fractionalization or bipartition of the $\mathrm{SO}(N)_1$ current along each wire into a pair of $\mathcal{G}_N$ channels [see Eqs. (3.4) and (3.5)]. The two fractional channels then were backscattered onto adjacent wires in opposite directions. This froze all low-energy degrees of freedom and opened an excitation energy gap without breaking time-reversal symmetry. When $N = 2r$ was even, each wire could simply be split into a pair of $\mathcal{G}_N = \mathrm{SO}(r)_1$ channels. The fractionalization was not as obvious when N was odd. We first made use of the conformal embedding that decomposed nine Majoranas into two subsectors: $\mathrm{SO}(9)_1 \supseteq \mathrm{SO}(3)_3 \otimes \mathrm{SO}(3)_3$ (see Sec. III B 1). This division could be generalized by all odd cases by splitting a subset of nine Majoranas into a pair of $\mathrm{SO}(3)_3$ and the remaining even number of Majoranas into a pair of $\mathrm{SO}(r)_1$. This could even be applied when N is less then 9 because each wire could be reconstructed by adding an arbitrary number of helical Majorana modes with the same number of right and left movers.

The surface G_N topological ordered was inferred from the bulk-boundary correspondence [see Eq. (1.3)]. These topological states followed a 32-fold periodicity $G_N \cong G_{N+32}$ and a relative tensor product structure $G_{N_1} \boxtimes_b G_{N_2} \cong G_{N_1+N_2}$. We presented the quasiparticle types as well as their fusion and braiding statistics properties. We explained the relative tensor product structure using the notion of anyon condensation [72]. On a more fundamental level, one should be able to deduce the topological order without the knowledge of the boundary by studying the modular properties of the degenerate bulk ground states under a compact torus geometry [68], or by directly looking at exchange and braiding behaviors of bulk excitations. In fact, the coupled wire construction provided a fitting model for this purpose. Being an exactly solvable model, a ground state could be explicitly expressed as entangled superposition of tensor product ground states between each pair of wires. In the simplest case when the model is bosonizable, a ground state could be specified by the pinned angle variables of a collection of sine-Gordon potentials. The bulk excitations could be realized as kinks between a pair of wires and could be created by vertex operators. The virtue of a bulk description is that the action of time reversal on quasiparticle excitations could be examined explicitly, which we have not performed or addressed here. These issues are beyond the scope of this paper and we refer a more detailed discussion to subsequent works.

We noticed that there were alternative ways of fractionalization that led to different gapping interactions and consequently different topological orders. We saw in Sec. III A 2 that $N = 4$ was an exceptional case that requires the special bipartition $\mathrm{SO}(4)_1 \supseteq \mathrm{SU}(2)_1 \times \mathrm{SU}(2)_1$ instead of two copies of $\mathrm{SO}(2)_1$. We also saw in Sec. V that when $N = 16$, the surface could be gapped by alternative interactions that corresponded to a $\widetilde{\mathrm{SO}(8)}_1$ or $\mathrm{SO}(4)_4$ topological order, none of which contained electronic quasiparticle excitations. Other conformal embeddings $\mathrm{SO}(n^2)_1 \supseteq \mathrm{SO}(n)_n \otimes \mathrm{SO}(n)_n$ could give rise to multiple possibilities. Our 32-fold topological states, which only utilized $\mathrm{SO}(9)_1 \supseteq \mathrm{SO}(3)_3 \otimes \mathrm{SO}(3)_3$, therefore should belong into a wider universal framework. These should be addressed in future works.

APPENDIX A: SO(N) LIE ALGEBRA AND ITS REPRESENTATIONS

The $\mathrm{SO}(N)$ Lie algebra is generated by real antisymmetric matrices $t^{(rs)} = (t^{(rs)}_{ab})_{N\times N}$ with entries

$$t^{(rs)}_{ab} = \delta^r_a \delta^s_b - \delta^r_b \delta^s_a \tag{A1}$$

for $r,s = 1,\ldots,N$. There are $N(N-1)/2$ linearly independent generators since $t^{(rs)} = -t^{(sr)}$ and $t^{(rr)} = 0$. In the main text, we write the basis labels as $\beta = (rs)$, for $r < s$, for conciseness. The generators obey the commutator relation

$$[t^{(rs)}, t^{(pq)}] = \sum_{m<n} f_{(rs)(pq)(mn)} t^{(mn)}, \tag{A2}$$

where the structure constant is

$$\begin{aligned} f_{(rs)(pq)(mn)} = {} & \delta_{mr}\delta_{nq}\delta_{sp} - \delta_{mr}\delta_{np}\delta_{sq} \\ & + \delta_{ms}\delta_{rq}\delta_{np} - \delta_{ms}\delta_{nq}\delta_{rp}. \end{aligned} \tag{A3}$$

The matrix representation (A1) is referred as the fundamental representation of $\mathrm{SO}(N)$ and is labeled by ψ. In general, the generators of $\mathrm{SO}(N)$ can have different irreducible matrix representations $t^{(rs)}_\lambda = t^\beta_\lambda$ labeled by λ. Since the quadratic Casmir operator

$$\hat{\mathcal{Q}}_\lambda = -\sum_\beta t^\beta_\lambda t^\beta_\lambda \tag{A4}$$

commutes with all the generators, it must have a fixed eigenvalue $\mathcal{Q}_\lambda$ that (incompletely) characterizes the irreducible representation λ. For instance, the fundamental representation in Eq. (A1), denoted by ψ, has quadratic Casmir value $\mathcal{Q}_\psi = N-1$.

The spinor representation σ of $\mathrm{SO}(N)$ makes use of the Clifford algebra [110] $\{\gamma_a,\gamma_b\} = \gamma_a\gamma_b + \gamma_b\gamma_a = 2\delta_{ab}$ where $\gamma_1,\ldots,\gamma_N$ are Hermitian matrices of dimension $d = 2^{N/2}$ for N even or $d = 2^{(N-1)/2}$ for N odd. The $\mathrm{SO}(N)$ generators are represented as the quadratic combination

$$t^{(rs)}_\sigma = \frac{1}{4}\sum_{ab} \gamma_a t^{(rs)}_{ab} \gamma_b = \frac{1}{2}\gamma_r\gamma_s \tag{A5}$$

and satisfy (A2). When N is even, the parity operator $(-1)^F = i^{N/2}\gamma_1 \ldots \gamma_N$ commutes with all $t_\sigma^{(rs)}$ and the representation is decomposable into $\sigma = s_+ \oplus s_-$, where $s_\pm$ are $2^{N/2-1}$-dimensional sectors with $(-1)^F = \pm 1$. The SO(N) generators are then irreducibly represented by

$$t_{s_\pm}^{(rs)} = P_\pm t_\sigma^{(rs)} P_\pm^\dagger, \tag{A6}$$

where $P_\pm$ are the projection operators onto the fixed parity subspaces. As $t_\sigma^{(rs)} t_\sigma^{(rs)} = -(1/4)\mathbb{1}$, the quadratic Casmir values (A4) of spinor representations are

$$\mathcal{Q}_\sigma = \frac{N(N-1)}{8}, \quad \mathcal{Q}_{s_\pm} = \frac{N(N-1)}{8}. \tag{A7}$$

The complexified SO(N) Lie algebra has an alternative set of *Cartan-Weyl* generators. It consists of a maximal set of commuting Hermitian generators $H^1, \ldots, H^r$, and a finite set of raising or lowering operators $E^{\boldsymbol{\alpha}} = (E^{-\boldsymbol{\alpha}})^\dagger$, labeled by integral vectors $\boldsymbol{\alpha} = (\alpha^1, \ldots, \alpha^r) \in \Delta$ called roots. The root lattice is given by the set

$$\begin{aligned} \Delta_{\mathrm{SO}(2r)} &= \{\pm \mathbf{e}_I \pm \mathbf{e}_J : 1 \leqslant I < J \leqslant r\}, \\ \Delta_{\mathrm{SO}(2r+1)} &= \Delta_{\mathrm{SO}(2r)} \cup \{\pm \mathbf{e}_I : 1 \leqslant I \leqslant r\}, \end{aligned} \tag{A8}$$

where $\mathbf{e}_I$ are unit basis vectors of $\mathbb{R}^r$. In particular, there are r simple roots $\boldsymbol{\alpha}_1, \ldots, \boldsymbol{\alpha}_r$ that form a basis for the root lattice. For SO(N) they can be chosen to be

$$\boldsymbol{\alpha}_I = \begin{cases} \mathbf{e_I} - \mathbf{e_{I+1}} & \text{for } I = 1, \ldots, r-1, \\ \mathbf{e}_r & \text{for } I = r \text{ and } N \text{ odd}, \\ \mathbf{e}_{r-1} + \mathbf{e}_r & \text{for } I = r \text{ and } N \text{ even}. \end{cases} \tag{A9}$$

The set of roots Δ consists of integral combinations of the simple roots $\boldsymbol{\alpha} = \sum_{J=1}^r b^J \boldsymbol{\alpha}_J$ so that its length is $|\boldsymbol{\alpha}| = \sqrt{2}$, for even N, or $|\boldsymbol{\alpha}| = 1$ or $\sqrt{2}$, for odd N.

The integer r is the rank of the SO(N) Lie algebra and is determined by $N = 2r$ for N even or $N = 2r+1$ for N odd. These generators satisfy

$$\begin{aligned} &[H^i, E^{\boldsymbol{\alpha}}] = \alpha^i E^{\boldsymbol{\alpha}}, \quad [E^{\boldsymbol{\alpha}}, E^{-\boldsymbol{\alpha}}] = \frac{2}{|\boldsymbol{\alpha}|^2} \sum_{i=1}^r \alpha^i H^i, \\ &[E^{\boldsymbol{\alpha}}, E^{\boldsymbol{\beta}}] \propto \begin{cases} E^{\boldsymbol{\alpha}+\boldsymbol{\beta}} & \text{if } \boldsymbol{\alpha}+\boldsymbol{\beta} \in \Delta, \\ 0 & \text{if otherwise} \end{cases} \quad \text{for } \boldsymbol{\alpha} \neq \boldsymbol{\beta}. \end{aligned} \tag{A10}$$

The Cartan matrix $K = (K_{IJ})_{r\times r}$ of the algebra is defined by the scalar product

$$K_{IJ} = \frac{2\boldsymbol{\alpha}_I^T \boldsymbol{\alpha}_J}{|\boldsymbol{\alpha}_J|^2} = \sum_{i=1}^r \frac{2\alpha_I^i \alpha_J^i}{|\boldsymbol{\alpha}_J|^2}. \tag{A11}$$

SO($2r$) is *simply laced* in the sense that all roots have identical length and the Cartan matrix is therefore symmetric:

$$K_{\mathrm{SO}(2r)} = \begin{pmatrix} 2 & -1 & 0 & \ldots & 0 \\ -1 & 2 & \ddots & & \vdots \\ 0 & \ddots & 2 & -1 & -1 \\ \vdots & & -1 & 2 & 0 \\ 0 & \ldots & -1 & 0 & 2 \end{pmatrix}. \tag{A12}$$

Sometimes it would be convenient to use the *Chevalley* basis so that the commuting generators are redefined

$$h^I = \frac{2}{|\boldsymbol{\alpha}_I|^2} \sum_{i=1}^r \alpha_I^i H^i \tag{A13}$$

so that the commutator relations (A10) become

$$[h^I, E^{\pm\boldsymbol{\alpha}_J}] = \pm K_{IJ} E^{\pm\boldsymbol{\alpha}_J}, \quad [E^{\boldsymbol{\alpha}_J}, E^{-\boldsymbol{\alpha}_J}] = \delta^{IJ} h^J. \tag{A14}$$

APPENDIX B: BOSONIZING THE SO($2r$)$_1$ CURRENT ALGEBRA

Here, we review the bosonization [56,67,89] of a chiral wire with $N = 2r$ Majorana fermions, and express the SO($2r$)$_1$ current operators in bosonized form. The $2r$ Majorana (real) fermions can be paired into r Dirac (complex) fermions and bosonized into the normal-ordered vertex operators

$$c^j(z) = \frac{\psi^{2j-1}(z) + i\psi^{2j}(z)}{\sqrt{2}} \sim \exp(i\widetilde{\phi}^j(z)). \tag{B1}$$

Here, we focus on a single wire, say at an even y, so that all fields depend on the holomorphic parameter $z = e^{\tau+ix}$. The r-component boson $\widetilde{\boldsymbol{\phi}} = (\widetilde{\phi}^1, \ldots, \widetilde{\phi}^r)$ is governed by the Lagrangian density

$$\mathcal{L}_0 = \frac{1}{2\pi} \sum_{j=1}^r \partial_x \widetilde{\phi}^j \partial_t \widetilde{\phi}^j = \frac{1}{2\pi} \partial_x \widetilde{\boldsymbol{\phi}} \partial_t \widetilde{\boldsymbol{\phi}} \tag{B2}$$

and follows the algebraic relations

$$[\widetilde{\phi}^j(x,t), \widetilde{\phi}^{j'}(x',t)] = i\pi[\delta^{jj'} \operatorname{sgn}(x'-x) + \operatorname{sgn}(j-j')] \tag{B3}$$

or, equivalently, the time-ordered correlation function

$$\langle \widetilde{\phi}^j(z) \widetilde{\phi}^{j'}(w) \rangle = -\delta^{jj'} \log(z-w) + \frac{i\pi}{2} \operatorname{sgn}(j-j') \tag{B4}$$

for $\operatorname{sgn}(s) = s/|s|$ when $s \neq 0$ and $\operatorname{sgn}(0) = 0$. Operator product expansions between unordered vertex operators can be evaluated by $e^{A(z)} e^{B(w)} = e^{A(z)+B(w)+\langle A(z)B(w)\rangle}$, for A, B linear combination of the bosons $\widetilde{\phi}^j$. For instance, the vertex operators in Eq. (B1) reproduce the product expansion of a pair of identical Dirac fermions

$$c^j(z)[c^j(w)]^\dagger = \frac{1}{z-w} + i\partial\widetilde{\phi}^j(w) + \cdots \tag{B5}$$

and the singular piece is dropped when the product is normal ordered in the limit $z \to w$. The nonsingular sign factor $i\pi \operatorname{sgn}(j-j')$ ensures fermions with distinct flavors anticommute:

$$c^j(z) c^{j'}(w) = -c^{j'}(w) c^j(z). \tag{B6}$$

The SO($2r$)$_1$ currents in the Cartan-Weyl basis can now be bosonized:

$$\begin{aligned} H^j(z) &= c^j(z) c^j(z)^\dagger = i\partial_z \widetilde{\phi}^j(z), \\ E^{\boldsymbol{\alpha}}(z) &= \prod_{j=1}^r c^j(z)^{\alpha^j} = \exp(i\boldsymbol{\alpha} \cdot \widetilde{\boldsymbol{\phi}}(z)), \end{aligned} \tag{B7}$$

where $\boldsymbol{\alpha} = (\alpha^1, \ldots, \alpha^r) \in \Delta$ are roots of SO($2r$) [see (A8)] and the fermion products are normal ordered. For instance, $\boldsymbol{\alpha}$ has two and only two nonzero entries and $E^{\boldsymbol{\alpha}}$ must be of the form

$$E^{\boldsymbol{\alpha}}(z) = c^i(z)^{\pm} c^j(z)^{\pm} = e^{i[\pm\widetilde{\phi}^i(z) \pm \widetilde{\phi}^j(z)]}. \tag{B8}$$

Combining raising or lowering operators gives

$$E^{\boldsymbol{\alpha}}(z) E^{\boldsymbol{\beta}}(w) = i^{-\boldsymbol{\alpha}\cdot\boldsymbol{\beta}} \epsilon(\boldsymbol{\alpha},\boldsymbol{\beta}) \frac{e^{i[\boldsymbol{\alpha}\cdot\widetilde{\boldsymbol{\phi}}(z) + \boldsymbol{\beta}\cdot\widetilde{\boldsymbol{\phi}}(w)]}}{(z-w)^{-\boldsymbol{\alpha}\cdot\boldsymbol{\beta}}}, \tag{B9}$$

where the vertex operator here is again normal ordered and the 2-cocycle is given by the star product

$$\epsilon(\boldsymbol{\alpha},\boldsymbol{\beta}) = (-1)^{\boldsymbol{\alpha}*\boldsymbol{\beta}} = (-1)^{\sum_{i>j} \alpha^i \beta^j}. \tag{B10}$$

As $\sum_{i=1}^r \alpha^i$ is even for all roots, we have the following simplification when interchanging $\boldsymbol{\alpha} \leftrightarrow \boldsymbol{\beta}$:

$$\epsilon(\boldsymbol{\alpha},\boldsymbol{\beta})\epsilon(\boldsymbol{\beta},\boldsymbol{\alpha}) = (-1)^{\boldsymbol{\alpha}\cdot\boldsymbol{\beta}}. \tag{B11}$$

Using the boson OPE (B4), the product of the two vertex operators above is singular only when (i) $\boldsymbol{\alpha} = -\boldsymbol{\beta}$ or (ii) $\boldsymbol{\alpha}\cdot\boldsymbol{\beta} = -1$ in other words $\boldsymbol{\alpha} + \boldsymbol{\beta} \in \Delta$. To summarize, the Cartan-Weyl generators satisfy the product expansion

$$\begin{aligned}
H^i(z)H^j(w) &= \frac{\delta^{ij}}{(z-w)^2} - \partial\widetilde{\phi}^i(w)\partial\widetilde{\phi}^j(w) + \cdots, \\
H^i(z)E^{\boldsymbol{\alpha}}(w) &= \frac{\alpha^i}{z-w} E^{\boldsymbol{\alpha}}(w) + \cdots, \\
E^{\boldsymbol{\alpha}}(z)E^{-\boldsymbol{\alpha}}(w) &= \frac{1}{(z-w)^2} + \sum_{i=1}^r \frac{\alpha^i}{z-w} H^i(w) \\
&\quad - \frac{1}{2}(\boldsymbol{\alpha}\cdot\partial\widetilde{\boldsymbol{\phi}}(w))^2 + \cdots, \\
E^{\boldsymbol{\alpha}}(z)E^{\boldsymbol{\beta}}(w) &= \frac{i\epsilon(\boldsymbol{\alpha},\boldsymbol{\beta})}{z-w} E^{\boldsymbol{\alpha}+\boldsymbol{\beta}}(w) + \cdots, \quad \text{if } \boldsymbol{\alpha}\cdot\boldsymbol{\beta} = -1.
\end{aligned} \tag{B12}$$

For instance, the 2-cocycle coefficient $\epsilon(\boldsymbol{\alpha},\boldsymbol{\beta})$ ensures the OPE between $E^{\boldsymbol{\alpha}}(z)$ and $E^{\boldsymbol{\beta}}(w)$ commute as the sign in Eq. (B11) when exchanging $\boldsymbol{\alpha} \leftrightarrow \boldsymbol{\beta}$ cancels that in $1/(z-w)$ when switching $z \leftrightarrow w$.

In certain derivations, especially when involving quasiparticle excitations, it may be more convenient to use the Chevalley basis. Here, fields are expressed in terms of nonlocal bosons $\boldsymbol{\phi} = (\phi^1, \ldots, \phi^r)$, which are related to the original ones by the (nonunimodular) basis transformation

$$\widetilde{\phi}^i = \sum_{I=1}^r \alpha_I^i \phi^I \tag{B13}$$

using the simple roots $\boldsymbol{\alpha}_I = (\alpha_I^1, \ldots, \alpha_I^r) \in \mathbb{Z}^r$ [see (A9) in Appendix A]. The Lagrangian density (B2) now becomes

$$\mathcal{L}_0 = \frac{1}{2\pi} \sum_{I,J=1}^r K_{IJ} \partial_x \phi^I \partial_t \phi^J, \tag{B14}$$

where $K = (K_{IJ})_{r\times r} = \boldsymbol{\alpha}_I \cdot \boldsymbol{\alpha}_J$ is the Cartan matrix of SO($2r$)$_1$ [see Eq. (A12)].

The current generators are rewritten in the Chevalley basis by

$$\begin{aligned}
h_I(z) &= \sum_{i=1}^r \alpha_I^i H^i(z) = i \sum_{J=1}^r K_{IJ} \partial_z \phi^J(z), \\
E^{\mathbf{b}}(z) &= E^{\boldsymbol{\beta}}(z) = \exp(i\mathbf{b}^T K \boldsymbol{\phi}^J(z)),
\end{aligned} \tag{B15}$$

where $\boldsymbol{\beta} = \sum_J b^J \boldsymbol{\alpha}_J$ are roots expressed in integral combinations of the simple ones, for $\mathbf{b} = (b^1, \ldots, b^r) \in \mathbb{Z}^r$. The Chevalley generators satisfy the modified current relations from (B12):

$$\begin{aligned}
h_I(z)h_J(w) &= \frac{K_{IJ}}{(z-w)^2} + \cdots, \\
h_I(z)E^{\mathbf{b}}(w) &= \frac{K_{IJ}b^J}{z-w} E^{\mathbf{b}}(w) + \cdots, \\
E^{\mathbf{b}}(z)E^{-\mathbf{b}}(w) &= \frac{1}{(z-w)^2} + \sum_{I=1}^r \frac{b^I}{z-w} h_I(w) + \cdots, \\
E^{\mathbf{b}_1}(z)E^{\mathbf{b}_2}(w) &= \frac{i\epsilon(\boldsymbol{\beta}_1,\boldsymbol{\beta}_2)}{z-w} E^{\mathbf{b}_1+\mathbf{b}_2}(w) + \cdots
\end{aligned} \tag{B16}$$

if $\mathbf{b}_1^T K \mathbf{b}_2 = -1$.

The (normal-ordered) energy-momentum tensor can be turned from the Sugawara form (2.12) to the usual bosonic one

$$\begin{aligned}
T(z) &= \frac{1}{2(N-1)} \left[\sum_{i=1}^r H^i(z)H^i(z) + \sum_{\boldsymbol{\alpha}\in\Delta} E^{\boldsymbol{\alpha}}(z)E^{-\boldsymbol{\alpha}}(z) \right] \\
&= -\frac{1}{2}\partial\widetilde{\boldsymbol{\phi}}(z)\cdot\partial\widetilde{\boldsymbol{\phi}}(z) = -\frac{1}{2}\partial\boldsymbol{\phi}(z)\cdot K\,\partial\boldsymbol{\phi}(z).
\end{aligned} \tag{B17}$$

Excitations in the CFT can be easily represented by vertex operators

$$V^{\mathbf{a}}(z) = \exp[i\mathbf{a}\cdot\boldsymbol{\phi}(z)] = \exp(i\mathbf{a}_\vee\cdot\widetilde{\boldsymbol{\phi}}(z)) \tag{B18}$$

labeled by integral lattice vectors $\mathbf{a} = (a_1, \ldots, a_r)$ or, equivalently, dual root lattice vectors $\mathbf{a}_\vee = (a_\vee^1, \ldots, a_\vee^r)$ with rational entries

$$a_\vee^j = \sum_{IJ} a_I (K^{-1})^{IJ} \alpha_J^j. \tag{B19}$$

The conformal dimension of $V^{\mathbf{a}}$ can be read off by the inner product

$$\begin{aligned}
h_{\mathbf{a}} &= \tfrac{1}{2}\mathbf{a}^T K^{-1}\mathbf{a} = \tfrac{1}{2}(K^{-1})^{IJ} a_I a_J \\
&= \tfrac{1}{2}\mathbf{a}_\vee^T\mathbf{a}_\vee = \tfrac{1}{2}\delta_{ij} a_\vee^i a_\vee^j.
\end{aligned} \tag{B20}$$

This can be evaluated from definition (2.16) using the energy-momentum tensor (B17) and the OPE

$$\partial_z\phi_I(z)\phi_J(w) = -(K^{-1})^{IJ}\log(z-w) + \cdots \tag{B21}$$

which is equivalent to (B4).

Most vertex operators (B18), however, are not WZW primary and do not represent the SO($2r$)$_1$ Kac-Moody algebra. The OPE with the current generators

$$\begin{aligned}
h_I(z)V^{\mathbf{a}}(w) &= \frac{a_I}{z-w} V^{\mathbf{a}}(w) + \cdots, \\
E^{\mathbf{b}}(z)V^{\mathbf{a}}(w) &= c_{\mathbf{a}}^{\mathbf{b}} (z-w)^{\mathbf{a}\cdot\mathbf{b}} V^{\mathbf{a}+K\mathbf{b}}(w) + \cdots
\end{aligned} \tag{B22}$$

would match the requirement (2.14) for a primary field only when the exponent of the singular term is bounded below, i.e., $\mathbf{a}\cdot\mathbf{b}\geqslant -1$ for all roots $\boldsymbol{\beta}=\sum_I b^I\boldsymbol{\alpha}_I$. Such lattice vectors $\mathbf{a}$ are called weights or *Dynkin labels* of SO($2r$) at level 1. When the exponenet $\mathbf{a}\cdot\mathbf{b}$ in Eq. (B22) is -1, the vertex operators $V^{\mathbf{a}}$ and $V^{\mathbf{a}+K\mathbf{b}}$ are related by the SO($2r$)$_1$ symmetry and belong to the same primary field sector. For example, the unit vector $\mathbf{a}=\mathbf{e}_1$ is the highest weight that generates the fermion sector ψ. Applying lowering operators $E^{-\mathbf{b}}$ to $V^{\mathbf{e}_1}=c^1$ gives all $2r$ Dirac fermions

$$\mathbf{V}_\psi=\text{span}\{(c^j)^\pm=e^{\pm i\widetilde{\phi}^j}:j=1,\ldots,r\} \tag{B23}$$

which in turn irreducibly represent the SO($2r$)$_1$ algebra [see (2.14)] according to the fundamental vector representation.

The unit vectors $\mathbf{a}=\mathbf{e}_{r-1}$ and $\mathbf{e}_r$ generate the two spinor sectors s_- and s_+, respectively. Each of them consists of 2^{r-1} twist fields

$$\begin{aligned}\mathbf{V}_{s_\pm}&=\sigma^1\ldots\sigma^{2r}\\&=\text{span}\left\{\exp\left(i\sum_{j=1}^r\frac{(-1)^{s_j}}{2}\widetilde{\phi}^j\right):\prod_{j=1}^r(-1)^{s_j}=\pm1\right\}.\end{aligned} \tag{B24}$$

They irreducibly represent the SO($2r$)$_1$ algebra according to the even and odd spinor representations. These are the only primary fields of SO($2r$)$_1$ and their conformal dimensions are given by $h_\psi=\frac{1}{2}$ and $h_{s_\pm}=r/8$.

The four primary fields 1, ψ, $s_\pm$ obey a set of fusion rules, which are OPE keeping only primary fields:

$$s_\pm\times\psi=s_\mp, \tag{B25}$$

$$s_\pm\times s_\pm\begin{cases}1 & \text{for } r \text{ even},\\ \psi & \text{for } r \text{ odd},\end{cases}\qquad s_\pm\times s_\mp\begin{cases}\psi & \text{for } r \text{ even},\\ 1 & \text{for } r \text{ odd}.\end{cases} \tag{B26}$$

For instance, the OPE

$$\begin{aligned}V_{s_+}(z)c^r(w)^\dagger&=e^{i\frac{\widetilde{\phi}^1(z)+\ldots+\widetilde{\phi}^r(z)}{2}}e^{-i\widetilde{\phi}^r(w)}\\&\propto(z-w)^{-\frac{1}{2}}e^{i\frac{\widetilde{\phi}^1(w)+\ldots+\widetilde{\phi}^r(w)-\widetilde{\phi}^r(w)}{2}}+\cdots\\&=(z-w)^{-\frac{1}{2}}V_{s_-}(w)+\cdots\end{aligned} \tag{B27}$$

shows $s_+\times\psi=s_-$, and

$$e^{i\sum_j\widetilde{\phi}^j(z)/2}e^{-i\sum_j\widetilde{\phi}^j(w)/2}\propto(z-w)^{-\frac{r}{4}}+\cdots \tag{B28}$$

shows $s_+\times s_+=1$ for r even, or $s_+\times s_-=1$ for r odd.

APPENDIX C: BOSONIZING THE SO($2r+1$)$_1$ CURRENT ALGEBRA

A chiral wire with $N=2r+1$ Majorana fermions can be partially bosonized by grouping $\psi^1,\ldots,\psi^{2r}$ in pairs to form r Dirac fermions [see (B1)]. This leaves a single Majorana ψ^{2r+1} behind. In order for the fermions to obey the correct anticommutation relations, the bosonized complex fermions (B1) have to be modified by a Klein factor

$$c^j(z)=(-1)^\Pi e^{i\widetilde{\phi}^j(z)}=e^{i\widetilde{\phi}^j(z)+i\pi\Pi}, \tag{C1}$$

where $(-1)^\Pi$ is the fermion parity operator that anticommutes with ψ^{2r+1}, and both Π and ψ_{2r+1} commute with the rest of the bosons $\widetilde{\phi}^j$. In a nonchiral system, $(-1)^\Pi$ can be chosen to be the combination $i\gamma_L\gamma_R$, for $\gamma_{L/R}$ the zero mode of $\psi_{L/R}^{2r+1}$. In the chiral case, it can be defined by $i\gamma\gamma_\infty$ using an additional Majorana zero mode γ_∞ that completes the Clifford algebra $\{\gamma,\gamma_\infty\}=0$.

The SO($2r+1$)$_1$ current algebra extends the SO($2r$)$_1$ algebra by the short roots with length 1 [see (A8)]. It contains the SO($2r$)$_1$ generators $H^j=i\partial\widetilde{\phi}^j$ and $E^{\boldsymbol{\alpha}}=e^{i\boldsymbol{\alpha}\cdot\widetilde{\boldsymbol{\phi}}}$ [see (B7) in Appendix B], for $\boldsymbol{\alpha}\in\Delta_{\text{SO}(2r)}$ the long roots with length $|\boldsymbol{\alpha}|=\sqrt{2}$. The remaining raising and lowering operators with the short roots are represented by the normal-ordered products

$$E^{\pm\mathbf{e}_j}(z)=e^{\pm i\widetilde{\phi}^j(z)}\psi^{2r+1}(z). \tag{C2}$$

In addition to (B12), the Cartan-Weyl generators satisfy the current relations

$$\begin{aligned}H^i(z)E^{\pm\mathbf{e}_j}(w)&=\frac{\pm\delta^{ij}}{z-w}E^{\pm\mathbf{e}_j}(w)+\cdots,\\E^{\mathbf{e}_j}(z)E^{-\mathbf{e}_j}(w)&=\frac{1}{(z-w)^2}+\frac{1}{z-w}H^j(w)\\&\quad-\frac{1}{2}\partial\widetilde{\phi}^j(w)\partial\widetilde{\phi}^j(w)\\&\quad-\psi^{2r+1}(w)\partial\psi^{2r+1}(w)+\cdots,\\E^{s_1\mathbf{e}_{j_1}}(z)E^{s_2\mathbf{e}_{j_2}}(w)&=\frac{i^{-s_1s_2}\epsilon(\mathbf{e}_{j_1},\mathbf{e}_{j_2})}{z-w}E^{s_1\mathbf{e}_{j_1}+s_2\mathbf{e}_{j_2}}(w)+\cdots\end{aligned} \tag{C3}$$

for $j_1\neq j_2$ and $s_1,s_2=\pm1$. Moreover, when $\boldsymbol{\alpha}\cdot(\pm\mathbf{e}_j)=-1$, i.e., $\boldsymbol{\alpha}\pm\mathbf{e}_j\in\Delta_{\text{SO}(2r+1)}$,

$$E^{\boldsymbol{\alpha}}(z)E^{\pm\mathbf{e}_j}(w)=\frac{i\epsilon(\boldsymbol{\alpha},\mathbf{e}_j)(-1)^{\sum_j\alpha^j/2}}{z-w}E^{\boldsymbol{\alpha}\pm\mathbf{e}_j}(w)+\cdots,$$

where $\epsilon(\mathbf{m},\mathbf{n})=(-1)^{\mathbf{m}*\mathbf{n}}$ is defined in Eq. (B10).

The (normal-ordered) energy-momentum tensor can be turned from the Sugawara form (2.12) to the usual bosonic and fermionic one

$$\begin{aligned}T(z)&=\frac{1}{2(N-1)}\left[\sum_{i=1}^r H^i(z)H^i(z)+\sum_{\boldsymbol{\alpha}\in\Delta}E^{\boldsymbol{\alpha}}(z)E^{-\boldsymbol{\alpha}}(z)\right.\\&\quad\left.+\sum_{j=1}^r E^{\mathbf{e}_j}(z)E^{-\mathbf{e}_j}(z)+E^{-\mathbf{e}_j}(z)E^{\mathbf{e}_j}(z)\right]\\&=-\frac{1}{2}\partial\widetilde{\boldsymbol{\phi}}(z)\cdot\partial\widetilde{\boldsymbol{\phi}}(z)-\frac{1}{2}\psi^{2r+1}(z)\partial\psi^{2r+1}(z).\end{aligned} \tag{C4}$$

There are only two nontrivial primary fields ψ and σ. The fermion sector ψ consists of the $2r$ Dirac fermions c^j, $(c^j)^\dagger$ in Eq. (B23) as well as the remaining Majorana fermion ψ^{2r+1}. The σ sector consists of 2^r twist fields

$$\begin{aligned}\mathbf{V}_\sigma&=\sigma^1\ldots\sigma^{2r+1}\\&=\text{span}\left\{\exp\left(i\sum_{j=1}^r\frac{(-1)^{s_j}}{2}\widetilde{\phi}^j\right)\sigma^{2r+1}:s_j=0,1\right\}\end{aligned} \tag{C5}$$

which represents $\mathrm{SO}(2r+1)_1$ according to the spinor representation. Their conformal dimensions are given by $h_\psi = \frac{1}{2}$ and $h_\sigma = (2r+1)/16$.

APPENDIX D: $\mathbb{Z}_6$ PARAFERMION MODEL

Here, we represent the $\mathbb{Z}_6$ parafermions using bosonized fields and Majorana fermions in the $\mathrm{SO}(9)_1$ CFT. We focus on a single Majorana wire containing nine right-moving real fermions. The CFT is fractionalized using the conformal embedding into $\mathrm{SO}(9)_1 \supseteq \mathrm{SO}(3)_3^+ \times \mathrm{SO}(3)_3^-$ (see Sec. III B 1). Each $\mathrm{SO}(3)_3$ sector is then further decomposed into $\mathrm{SO}(2)_3 \times$ "$\mathbb{Z}_6$" using the coset construction "$\mathbb{Z}_6$" $= \mathrm{SO}(3)_3/\mathrm{SO}(2)_3$ (see Sec. III B 2). We now provide a more detailed description of the $\mathbb{Z}_6$ parafermion sector. We will focus on the one in $\mathrm{SO}(3)_3^-$.

First, we pair six Majorana channels into three Dirac fermions and bosonize $c^1 = (\psi^1 + i\psi^4)/\sqrt{2} = e^{i\widetilde{\phi}^1}$, $c^2 = (\psi^2 + i\psi^5)/\sqrt{2} = e^{i\widetilde{\phi}^2}$, and $c^3 = (\psi^3 + i\psi^6)/\sqrt{2} = e^{i\widetilde{\phi}^3}$. The Lagrangian density of the boson fields is given in Eq. (3.68). Like the $\mathrm{SO}(N)_1$ case, extra care is required so that the Dirac fermions c^j satisfy the appropriate mutual anticommutation relations. Here, we use a slightly different but more convenient convention

$$\langle \widetilde{\phi}^i(z)\widetilde{\phi}^j(w)\rangle = -\delta^{ij}\log(z-w) + \frac{i\pi}{2}S^{ij},$$
$$S^{ij} = \begin{cases} 0 & \text{if } i=j, \\ 1 & \text{if } i-j \equiv 1 \bmod 3, \\ -1 & \text{if } i-j \equiv -1 \bmod 3 \end{cases} \tag{D1}$$

so that the constant phases S^{ij} have a threefold cyclic symmetry. The $\mathrm{SO}(2)_3$ subtheory is generated by the "charged" boson $\phi_\rho = (\widetilde{\phi}^1 + \widetilde{\phi}^2 + \widetilde{\phi}^3)/3$. It satisfies

$$\langle \phi_\rho(z)\phi_\rho(w)\rangle = -\tfrac{1}{3}\log(z-w). \tag{D2}$$

The remaining "neutral" bosons $\phi_\sigma^j = \widetilde{\phi}^j - \phi_\rho$ are linearly dependent $\phi_\sigma^1 + \phi_\sigma^2 + \phi_\sigma^3 = 0$ and obey the OPE

$$\langle \phi_\sigma^i(z)\phi_\sigma^j(w)\rangle = -\left(\delta^{ij} - \frac{1}{3}\right)\log(z-w) + \frac{i\pi}{2}S^{ij}. \tag{D3}$$

The "charge" and "neutral" sectors completely decoupled so that $\langle \phi_\rho(z)\phi_\sigma^j(w)\rangle = 0$. Lastly, there are three remaining Majorana fermions $\psi^{7,8,9}$ in the $\mathrm{SO}(9)_1$ theory. They completely decouple with ϕ_σ and ϕ_ρ. Although the vertex $e^{i\phi_\rho}$ anticommutes with $\psi^{7,8,9}$, this has no effect on any of our derivations. More importantly, the "neutral" vertices $e^{i\phi_\sigma^j}$ commute with the remaining fermions.

In Sec. III B 2, we defined the $\mathbb{Z}_6$ parafermion (3.75):

$$\Psi = \frac{1}{\sqrt{3}}\left(e^{i\phi_\sigma^1}\psi^7 + e^{i\phi_\sigma^2}\psi^8 + e^{i\phi_\sigma^3}\psi^9\right) \tag{D4}$$

which is part of the $\mathrm{SO}(3)_3^-$ current [see (3.74)]. It generates the rest of the $\mathbb{Z}_6$ parafermions

$$\Psi^2 = \frac{1}{\sqrt{15}}\left[\sum_{j=1}^{3} e^{i2\phi_\sigma^j} + 2i\left(e^{-i\phi_\sigma^1}\psi^{89} + e^{-i\phi_\sigma^2}\psi^{97} + e^{-i\phi_\sigma^3}\psi^{78}\right)\right],$$
$$\Psi^3 = \sqrt{\frac{2}{5}}\left[i\psi^{789} - \cos\left(\phi_\sigma^1 - \phi_\sigma^2\right)\psi^9 - \cos\left(\phi_\sigma^2 - \phi_\sigma^3\right)\psi^7 - \cos\left(\phi_\sigma^3 - \phi_\sigma^1\right)\psi^8\right],$$
$$\Psi^4 = (\Psi^2)^\dagger, \quad \Psi^5 = (\Psi_1)^\dagger, \quad \Psi^0 = \Psi^6 = 1, \tag{D5}$$

where $\psi^{ab} = \psi^a\psi^b$ and $\psi^{abc} = \psi^a\psi^b\psi^c$. Their conformal dimensions

$$h_{\Psi^m} = \frac{m(6-m)}{6} \tag{D6}$$

as well as the fusion rules

$$\Psi^m(z)\Psi^{m'}(w) = \frac{c^{mm'}}{(z-w)^{mm'/3}}\Psi^{m+m'}(w) + \cdots,$$
$$\Psi^m(z)\Psi^{6-m}(w) = \frac{1}{(z-w)^{2h_{\Psi^m}}}\left[1 + \frac{2h_{\Psi^m}}{c_{\mathbb{Z}_6}}(z-w)^2 T_{\mathbb{Z}_6} + \cdots\right] \tag{D7}$$

match with the known result by Zamolodchikov and Fateev [78], for $T_{\mathbb{Z}_6}$ the energy-momentum tensor (3.73) with central charge $c_{\mathbb{Z}_6} = \frac{5}{4}$, and

$$c^{mm'} = \sqrt{\frac{(m+m')!(6-m)!(6-m')!}{m!m'!(6-m-m')!6!}}. \tag{D8}$$

APPENDIX E: S MATRICES OF THE G_N STATE

The surface topological orders of the time-reversal-symmetric gapped coupled wire model are described in Sec. IV. There are 32 distinct topological states defined in Eqs. (4.6) and (4.9), which we repeat here:

$$G_N = \begin{cases} \mathrm{SO}(r)_1 & \text{for } N = 2r, \\ \mathrm{SO}(3)_3 \boxtimes_b \mathrm{SO}(r)_1 & \text{for } N = 9 + 2r. \end{cases} \tag{E1}$$

In this Appendix, we summarize the modular properties of these states. In particular, we present there braiding S matrices (4.1):

$$\mathcal{S}_{\mathbf{ab}} = \frac{1}{\mathcal{D}}\sum_{\mathbf{c}} d_{\mathbf{c}} N_{\mathbf{ab}}^{\mathbf{c}} \frac{\theta_{\mathbf{c}}}{\theta_{\mathbf{a}}\theta_{\mathbf{b}}} \tag{E2}$$

which are identical to the modular S matrix [56] of the $\mathcal{G}_N$ WZW CFT. The fusion matrices $N_{\mathbf{ab}}^{\mathbf{c}}$ that characterize fusion rules $\mathbf{a} \times \mathbf{b} = \sum_{\mathbf{c}} N_{\mathbf{ab}}^{\mathbf{c}}\mathbf{c}$ can in turn be determined by S matrix through the Verlinde formula [101] (3.58):

$$N_{s_1 s_2}^{s} = \sum_{s'} \frac{\mathcal{S}_{s_1 s'}\mathcal{S}_{s_2 s'}\mathcal{S}_{s s'}}{\mathcal{S}_{0 s'}}. \tag{E3}$$

The G_N state is Abelian and carries four anyon types 1, ψ, s_+, s_- when N is a multiple of four. It is non-Abelian otherwise and carries three anyon types 1, ψ, σ when N is 2 mod 4, or seven anyon types 1, $\alpha_+\gamma_+$, β, γ_-, α_-, f when N is odd. The quasiparticle exchange statistics $\theta_{\mathbf{x}}$ and quantum dimensions $d_{\mathbf{x}}$ are summarized in Tables II and III. The total quantum dimensions $\mathcal{D} = \sqrt{\sum_{\mathbf{x}} d_{\mathbf{x}}^2}$ are given by

$$\mathcal{D}_{G_N} = \begin{cases} 2 & \text{for } N \text{ even}, \\ 2\csc(\pi/8) & \text{for } N \text{ odd}, \end{cases} \tag{E4}$$

where $\csc(\pi/8) = \sqrt{4+2\sqrt{2}}$.

The S matrices of G_N for $N = 2r$ even are well known and are given by those of the $\mathrm{SO}(r)_1$ states [64,107]

$$\mathcal{S}_{G_N} = \frac{1}{\mathcal{D}_{G_N}} \begin{pmatrix} 1 & 1 & 1 & 1 \\ 1 & 1 & -1 & -1 \\ 1 & -1 & i^n & -i^n \\ 1 & -1 & -i^n & i^n \end{pmatrix} \quad \text{for } N = 4n, \tag{E5}$$

$$\mathcal{S}_{G_N} = \frac{1}{\mathcal{D}_{G_N}} \begin{pmatrix} 1 & 1 & \sqrt{2} \\ 1 & 1 & -\sqrt{2} \\ \sqrt{2} & -\sqrt{2} & 0 \end{pmatrix} \quad \text{for } N = 4n+2. \tag{E6}$$

The S matrices for the odd N cases are modification of the $G_9 = \mathrm{SO}(3)_3$ prototype (3.59):

$$\mathcal{S}^{\mathrm{SO}(3)_3}_{s_1 s_2} = \frac{1}{2} \sin\left[\frac{\pi(2s_1+1)(2s_2+1)}{8}\right], \tag{E7}$$

where $s_j = 0, \frac{1}{2}, 1, \frac{3}{2}, 2, \frac{5}{2}, 3$ label the seven anyon types 1, α_+, γ_+, β, γ_-, α_-, f (see Table I). For $N = 9 + 2r$ mod 32, the S matrix of G_N is given by

$$\mathcal{S}_{G_N} = \mathcal{F}^r \, S^e(\lceil r/2 \rceil) \mathcal{F}^{-r}, \tag{E8}$$

where $\lceil r/2 \rceil \geqslant r/2$ is the smallest integral ceiling of $r/2$, $\mathcal{S}^e(n)$ is the S matrix when $r = 2n$ is even

$$\mathcal{S}^e(n)_{s_1 s_2} = i^{n(4s_1 s_2)^2} \mathcal{S}^{\mathrm{SO}(3)_3}_{s_1 s_2}, \tag{E9}$$

and $\mathcal{F}$ is the operator that flips the fermion parity of $\alpha_+ \leftrightarrow \alpha_-$ and $\gamma_+ \leftrightarrow \gamma_-$:

$$\mathcal{F} = \begin{pmatrix} 1 & & & & & & \\ & & & & & & 1 \\ & & & & & 1 & \\ & & & & 1 & & \\ & & & 1 & & & \\ & & 1 & & & & \\ & & & & & & 1 \end{pmatrix}. \tag{E10}$$

[1] A. P. Schnyder, S. Ryu, A. Furusaki, and A. W. W. Ludwig, Phys. Rev. B **78**, 195125 (2008).
[2] A. Kitaev, AIP Conf. Proc. **1134**, 22 (2009).
[3] X.-L. Qi, T. L. Hughes, S. Raghu, and S.-C. Zhang, Phys. Rev. Lett. **102**, 187001 (2009).
[4] G. E. Volovik, *Universe in a Helium Droplet* (Oxford University Press, Oxford, UK, 2003).
[5] Y. Aoki, Y. Wada, M. Saitoh, R. Nomura, Y. Okuda, Y. Nagato, M. Yamamoto, S. Higashitani, and K. Nagai, Phys. Rev. Lett. **95**, 075301 (2005).
[6] H. Choi, J. P. Davis, J. Pollanen, and W. P. Halperin, Phys. Rev. Lett. **96**, 125301 (2006).
[7] S. Murakawa, Y. Tamura, Y. Wada, M. Wasai, M. Saitoh, Y. Aoki, R. Nomura, Y. Okuda, Y. Nagato, M. Yamamoto, S. Higashitani, and K. Nagai, Phys. Rev. Lett. **103**, 155301 (2009).
[8] L. Fu and E. Berg, Phys. Rev. Lett. **105**, 097001 (2010).
[9] S. Sasaki, M. Kriener, K. Segawa, K. Yada, Y. Tanaka, M. Sato, and Y. Ando, Phys. Rev. Lett. **107**, 217001 (2011).
[10] A. Altland and M. R. Zirnbauer, Phys. Rev. B **55**, 1142 (1997).
[11] L. Fidkowski, X. Chen, and A. Vishwanath, Phys. Rev. X **3**, 041016 (2013).
[12] M. A. Metlitski, L. Fidkowski, X. Chen, and A. Vishwanath, arXiv:1406.3032.
[13] C. Wang and T. Senthil, Phys. Rev. B **89**, 195124 (2014).
[14] T. Senthil, Annu. Rev. Condens. Matter Phys. **6**, 299 (2015).
[15] A. Kapustin, R. Thorngren, A. Turzillo, and Z. Wang, J. High Energy Phys. 12 (2015) 052.
[16] X.-L. Qi, E. Witten, and S.-C. Zhang, Phys. Rev. B **87**, 134519 (2013).
[17] E. Witten, Rev. Mod. Phys. **88**, 035001 (2016).
[18] L. Fu, C. L. Kane, and E. J. Mele, Phys. Rev. Lett. **98**, 106803 (2007).
[19] R. Roy, Phys. Rev. B **79**, 195322 (2009).
[20] J. E. Moore and L. Balents, Phys. Rev. B **75**, 121306(R) (2007).
[21] X.-L. Qi, T. L. Hughes, and S.-C. Zhang, Phys. Rev. B **78**, 195424 (2008).
[22] A. Y. Kitaev, Phys. Usp. **44**, 131 (2001).
[23] C. Wang, A. C. Potter, and T. Senthil, Phys. Rev. B **88**, 115137 (2013).
[24] M. A. Metlitski, C. L. Kane, and M. P. A. Fisher, Phys. Rev. B **92**, 125111 (2015).
[25] X. Chen, L. Fidkowski, and A. Vishwanath, Phys. Rev. B **89**, 165132 (2014).
[26] P. Bonderson, C. Nayak, and X.-L. Qi, J. Stat. Mech. (2013) P09016.
[27] L. Fidkowski and A. Kitaev, Phys. Rev. B **81**, 134509 (2010).
[28] L. Fidkowski and A. Kitaev, Phys. Rev. B **83**, 075103 (2011).
[29] A. M. Turner, F. Pollmann, and E. Berg, Phys. Rev. B **83**, 075102 (2011).
[30] X. Chen, Z.-C. Gu, and X.-G. Wen, Phys. Rev. B **83**, 035107 (2011).
[31] D. F. Mross, A. Essin, and J. Alicea, Phys. Rev. X **5**, 011011 (2015).
[32] C. S. O'Hern, T. C. Lubensky, and J. Toner, Phys. Rev. Lett. **83**, 2745 (1999).
[33] V. J. Emery, E. Fradkin, S. A. Kivelson, and T. C. Lubensky, Phys. Rev. Lett. **85**, 2160 (2000).
[34] A. Vishwanath and D. Carpentier, Phys. Rev. Lett. **86**, 676 (2001).
[35] S. L. Sondhi and K. Yang, Phys. Rev. B **63**, 054430 (2001).
[36] R. Mukhopadhyay, C. L. Kane, and T. C. Lubensky, Phys. Rev. B **63**, 081103 (2001).
[37] C. L. Kane, R. Mukhopadhyay, and T. C. Lubensky, Phys. Rev. Lett. **88**, 036401 (2002).
[38] J. C. Y. Teo and C. L. Kane, Phys. Rev. B **89**, 085101 (2014).
[39] J. Klinovaja and D. Loss, Eur. Phys. J. B **87**, 171 (2014).
[40] T. Meng, P. Stano, J. Klinovaja, and D. Loss, Eur. Phys. J. B **87**, 203 (2014).
[41] E. Sagi, Y. Oreg, A. Stern, and B. I. Halperin, Phys. Rev. B **91**, 245144 (2015).
[42] Y. Oreg, E. Sela, and A. Stern, Phys. Rev. B **89**, 115402 (2014).

[43] E. M. Stoudenmire, D. J. Clarke, R. S. K. Mong, and J. Alicea, Phys. Rev. B **91**, 235112 (2015).
[44] T. Meng, T. Neupert, M. Greiter, and R. Thomale, Phys. Rev. B **91**, 241106 (2015).
[45] G. Gorohovsky, R. G. Pereira, and E. Sela, Phys. Rev. B **91**, 245139 (2015).
[46] P. H. Huang, J. H. Chen, P. R. S. Gomes, T. Neupert, C. Chamon and C. Mudry, Phys. Rev. B **93**, 205123 (2016).
[47] T. Neupert, C. Chamon, C. Mudry, and R. Thomale, Phys. Rev. B **90**, 205101 (2014).
[48] J. Klinovaja and Y. Tserkovnyak, Phys. Rev. B **90**, 115426 (2014).
[49] E. Sagi and Y. Oreg, Phys. Rev. B **90**, 201102 (2014).
[50] E. Sagi and Y. Oreg, Phys. Rev. B **92**, 195137 (2015).
[51] T. Meng and E. Sela, Phys. Rev. B **90**, 235425 (2014).
[52] T. Meng, Phys. Rev. B **92**, 115152 (2015).
[53] R. A. Santos, C.-W. Huang, Y. Gefen, and D. B. Gutman, Phys. Rev. B **91**, 205141 (2015).
[54] R. S. K. Mong, D. J. Clarke, J. Alicea, N. H. Lindner, P. Fendley, C. Nayak, Y. Oreg, A. Stern, E. Berg, K. Shtengel, and M. P. A. Fisher, Phys. Rev. X **4**, 011036 (2014).
[55] I. Seroussi, E. Berg, and Y. Oreg, Phys. Rev. B **89**, 104523 (2014).
[56] P. Di Francesco, P. Mathieu, and D. Senechal, *Conformal Field Theory* (Springer, Berlin, 1999).
[57] S. Naculich, H. Riggs, and H. Schnitzer, Phys. Lett. B **246**, 417 (1990).
[58] E. J. Mlawer, S. G. Naculich, H. A. Riggs, and H. J. Schnitzer, Nucl. Phys. B **352**, 863 (1991).
[59] F. Bais, F. Englert, A. Taormina, and P. Zizzi, Nucl. Phys. B **279**, 529 (1987).
[60] A. N. Schellekens and N. P. Warner, Phys. Rev. D **34**, 3092 (1986).
[61] F. A. Bais and P. G. Bouwknegt, Nucl. Phys. B **279**, 561 (1987).
[62] C. L. Kane and M. P. A. Fisher, Phys. Rev. B **55**, 15832 (1997).
[63] A. Cappelli, M. Huerta, and G. R. Zemba, Nucl. Phys. B **636**, 568 (2002).
[64] A. Kitaev, Ann. Phys. (NY) **321**, 2 (2006).
[65] J. M. Luttinger, Phys. Rev. **135**, A1505 (1964).
[66] F. Wilczek, *Fractional Statistics and Anyon Superconductivity* (World Scientific, Singapore, 1990).
[67] E. Fradkin, *Field Theories of Condensed Matter Physics*, 2nd ed. (Cambridge University Press, Cambridge, UK, 2013).
[68] X.-G. Wen, *Quantum Field Theory of Many Body Systems* (Oxford University Press, Oxford, UK, 2004).
[69] X.-G. Wen, Adv. Phys. **44**, 405 (1995).
[70] N. Read and G. Moore, Nucl. Phys. B **360**, 362 (1991).
[71] N. Read and G. Moore, Prog. Theor. Phys. Suppl. **107**, 157 (1992).
[72] F. A. Bais and J. K. Slingerland, Phys. Rev. B **79**, 045316 (2009).
[73] D. J. Gross and A. Neveu, Phys. Rev. D **10**, 3235 (1974).
[74] A. B. Zamolodchikov and A. B. Zamolodchikov, Phys. Lett. B **72**, 481 (1978).
[75] E. Witten, Nucl. Phys. B **142**, 285 (1978).
[76] R. Shankar and E. Witten, Nucl. Phys. B **141**, 349 (1978).
[77] V. Fateev and A. Zamolodchikov, Phys. Lett. A **92**, 37 (1982).
[78] A. B. Zamolodchikov and V. A. Fateev, Zh. Eksp. Teor. Fiz. **89**, 380 (1985) [Sov. Phys.–JETP **62**, 215 (1985)].
[79] H. Nielsen and M. Ninomiya, Phys. Lett. B **130**, 389 (1983).
[80] G. E. Volovik, Pis'ma Zh. Eksp. Teor. Fiz. **55**, 363 (1992) [JETP Lett. **55**, 368 (1992)].
[81] N. Read and D. Green, Phys. Rev. B **61**, 10267 (2000).
[82] J. C. Y. Teo and C. L. Kane, Phys. Rev. B **82**, 115120 (2010).
[83] J. Wess and B. Zumino, Phys. Lett. B **37**, 95 (1971).
[84] E. Witten, Nucl. Phys. B **223**, 422 (1983).
[85] P. Goddard, W. Nahm, and D. Olive, Phys. Lett. B **160**, 111 (1985).
[86] I. Affleck and A. W. W. Ludwig, Phys. Rev. Lett. **67**, 161 (1991).
[87] C. Holzhey, F. Larsen, and F. Wilczek, Nucl. Phys. B **424**, 443 (1994).
[88] P. Calabrese and J. Cardy, J. Stat. Mech.: Theory Exper. (2004) P06002.
[89] E. Witten, Commun. Math. Phys. **92**, 455 (1984).
[90] F. D. M. Haldane, Phys. Lett. A **93**, 464 (1983).
[91] F. D. M. Haldane, Phys. Rev. Lett. **50**, 1153 (1983).
[92] I. Affleck, T. Kennedy, E. H. Lieb, and H. Tasaki, Phys. Rev. Lett. **59**, 799 (1987).
[93] I. Affleck, T. Kennedy, E. H. Lieb, and H. Tasaki, Commun. Math. Phys. **115**, 477 (1988).
[94] H.-H. Tu, G.-M. Zhang, and T. Xiang, Phys. Rev. B **78**, 094404 (2008).
[95] H.-H. Tu and R. Orús, Phys. Rev. Lett. **107**, 077204 (2011).
[96] F. Alet, S. Capponi, H. Nonne, P. Lecheminant, and I. P. McCulloch, Phys. Rev. B **83**, 060407 (2011).
[97] J. Cardy, *Scaling and Renormalization in Statistical Physics* (Cambridge University Press, Cambridge, UK, 1996).
[98] F. D. M. Haldane, Phys. Rev. Lett. **74**, 2090 (1995).
[99] P. Fendley and H. Saleur, Phys. Rev. D **65**, 025001 (2001).
[100] R. Jackiw and C. Rebbi, Phys. Rev. D **13**, 3398 (1976).
[101] E. Verlinde, Nucl. Phys. B **300**, 360 (1988).
[102] M. N. Khan, J. C. Y. Teo, and T. L. Hughes (unpublished).
[103] X.-G. Wen, Phys. Rev. B **40**, 7387 (1989).
[104] X.-G. Wen, Int. J. Mod. Phys. B **04**, 239 (1990).
[105] X.-G. Wen and Q. Niu, Phys. Rev. B **41**, 9377 (1990).
[106] A. Kitaev and J. Preskill, Phys. Rev. Lett. **96**, 110404 (2006).
[107] M. N. Khan, J. C. Y. Teo, and T. L. Hughes, Phys. Rev. B **90**, 235149 (2014).
[108] J. C. Teo, T. L. Hughes, and E. Fradkin, Ann. Phys. (NY) **360**, 349 (2015).
[109] C. Wang, A. C. Potter, and T. Senthil, Science **343**, 629 (2014).
[110] H. B. Lawson and M.-L. Michelsohn, *Spin Geometry* (Princeton University Press, Princeton, NJ, 1990).